Enquiries should be addressed to: Karen Wild Allen (karen.wild-allen@csiro.au) or Jenny Skerratt (jennifer.skerratt@csiro.au)

Copyright and Disclaimer

Karen Wild-Allen, Jennifer Skerratt, Farhan Rizwi, John Parslow
Derwent Estuary Biogeochemical Model: Technical Report.
CSIRO Marine and Atmospheric Research October 2009
ISBN 978 0 643 09833 6

Important Disclaimer

Contents

List of Figures

List of Tables

List of Appendices

1. EXECUTIVE SUMMARY

The hydrodynamics of the Derwent Estuary conform to a wave dominated system with generally weak currents and a strongly stratified salt wedge in the upper reaches. In the past it has had significant inputs of organic matter, wood fibre, nutrients and heavy metals, many of which remain at elevated concentrations in the sediments and biota. Current nutrient inputs to the estuary include exchange with coastal marine waters, catchment, river and stormwater loads, industry and sewerage treatment plant (STP) effluents. Nutrients fuel phytoplankton growth and elevated chlorophyll concentrations have been observed along with depleted bottom water dissolved oxygen concentrations at stations throughout the estuary.

The objective of this project was to implement a high resolution 3D biogeochemical model of the estuary, calibrate the model against observations taken throughout the region and better characterise the cycling of carbon, nitrogen, phosphorus and dissolved oxygen in the estuary to inform managers and stakeholders. The calibrated biogeochemical model would also be available for scenario simulation of alternative management strategies and to reconstruct former conditions in the estuary prior to urbanisation.

The CSIRO EMS (Environmental Monitoring Suite) includes a 3D coupled hydrodynamic, sediment and biogeochemical model. In 2005 the hydrodynamic and sediment models were implemented for the Derwent Estuary and calibrated against observations made in 2003 to simulate a seasonal cycle of hydrodynamics, sediment transport and absorption/desorption of zinc. In this project we augment the existing models with the biogeochemical model in EMS to simulate the cycling of carbon, nitrogen, phosphorus and associated dissolved oxygen, through dissolved and particulate organic and inorganic phases. The model includes 4 types of phytoplankton, 2 types of macrophytes, 2 types of zooplankton and 4 types of particulate detritus; dissolved organic and inorganic nutrients and carbon are also included.

Model parameters were derived from observations, literature values and previous model simulations. The model ran from January 2003 for 14 months with tracer concentrations initialised from observations of nutrients, phytoplankton and dissolved oxygen; other model variables were initialised with uniform low concentration. The hydrodynamical model was forced with Derwent River flow, local meteorology and incident irradiation. For the biogeochemical model, boundaries at New Norfolk and across the estuary at Iron Pot were implemented with an upstream condition for inflowing concentrations of model tracers specified from time series derived from observations. Point source nutrient loads into the estuary in 2003 from industry and STPs were estimated from data supplied by the Derwent Estuary Program (DEP), local industry and local councils. Stormwater loads were derived from catchment model results (DEP) and observations. After marine influx and river load, STPs supplied the largest quantity of nitrogen and phosphorus into the estuary whilst industry effluent provided most carbon.

The model was validated against observations made throughout the estuary in 2003 obtained from the DEP database. Observations of nitrate, ammonia, dissolved inorganic phosphorus (DIP), chlorophyll and dissolved oxygen, in surface and bottom waters were directly comparable with model output. There were no observations of macrophytes, phytoplankton group assemblages or zooplankton for 2003, although some information on broad patterns was gathered. Validation criteria were set for the conservation of mass and reproduction of the observed timing and amplitude of the seasonal cycle in dissolved nutrients, chlorophyll and dissolved oxygen. Poorly constrained parameters were varied within known ranges during calibration to optimise the simulation of observed

biogeochemical substances. The model achieved all validation criteria and simulated the observed biogeochemical dynamics of nitrate, ammonia, DIP, chlorophyll, DOC and dissolved oxygen in most parts of the estuary very well. In the upper estuary, complex channel bathymetry was not well resolved by the relatively coarse model grid and model results should be treated with more caution. In some side bays with very high nutrient loads (e.g. Prince of Wales Bay) the model was not able to reproduce the full range of observed values possibly due to sub-grid scale gradients in observed concentrations and/or under-estimation of actual nutrient input. The modelled succession of plankton species, zooplankton abundance and distribution of macrophytes broadly agreed with ancillary data except that favourable conditions for seagrass growth were simulated in Ralphs Bay, where none is currently found.

Model results show a persistent salt wedge structure in the upper estuary which intersects the sea bed upstream of Elwick Bay (near DEP station U7). Modelled nutrient concentrations were greatest in the bottom waters of the mid-estuary adjacent to the salt wedge front. Nutrients appear to accumulate in this area from point source loads and remineralisation of organic material which re-circulates in the estuarine currents. Simulated nutrient concentrations were elevated in winter and reduced in surface waters in other seasons due to phytoplankton assimilation. DIP concentrations exceed Redfield ratio in summer indicating that modelled primary production in the estuary is controlled by access to nitrogen and irradiance for photosynthesis. During 2003 the model simulated a number of high rainfall events. In March model results show the formation and dispersal of long plumes of nitrate originating from STP and stormwater discharge into Elwick Bay over a 10 day period.

Modelled chlorophyll concentrations were highest in the mid-estuary and along the shoreline in regions of elevated nutrient supply. Sustained periods of high chlorophyll occur in all seasons in sub-regions of the estuary depending on the modelled availability of light and nutrients. In the upper estuary coloured dissolved organic matter (CDOM) and opaque industry effluent limit the propagation of light and photosynthesis through the water column and modelled chlorophyll concentrations are generally low. Simulated phytoplankton biomass showed seasonal succession with dinoflagellates dominating in summer and autumn, large phytoplankton in winter and mixed populations in spring, throughout much of the estuary. In the model grazing by small zooplankton was tightly coupled with production by small phytoplankton whilst large zooplankton grazing responded more slowly to increases in large phytoplankton and dinoflagellates. In some areas modelled spring and autumn peak chlorophyll concentrations persisted longer than observed possibly due to under representation of large zooplankton growth rate. Modelled dissolved oxygen levels were reduced in bottom waters in the upper estuary and the mid and lower reaches of the estuary, particularly in autumn. Regions of low dissolved oxygen saturation were simulated adjacent to the salt wedge front, similar to the distribution of elevated nutrient concentration and likely associated with local remineralisation of organic material.

Modelled photosynthetically active radiation reaching the epi-benthos was greatest in the shallow waters of the lower estuary and Ralphs Bay, Elwick Bay and in shallow waters of the upper estuary. The model favoured macrophyte growth in these areas, however it does not resolve gradients in substrate type, disturbance or recruitment and results should be interpreted as potential rather than actual areas of macrophyte growth. The model simulated potentially favourable conditions for seagrass growth in Ralphs Bay whilst there was the potential for epiphytic macroalgae to dominate in the mid and upper estuary due to elevated water column nutrients. With access to more detailed observations of species present, typical biomass levels, substrate type, growth, disturbance and recruitment rates, the model could be improved to resolve macrophyte dynamics better.

Modelled surface sediment dissolved oxygen concentrations were lowest in the mid and lower reaches with 10 percentile monthly concentrations falling below 40% saturation in autumn and spring.

In March 2003 simulated surface sediment dissolved oxygen concentrations fell to 20% saturation for 3 days in a small area close to the Tasman Bridge. Modelled denitrification flux was highest in the upper estuary and mid-estuary corresponding to regions with high sediment ammonia and low dissolved oxygen saturation. In the vicinity of Bridgewater Bridge and Ralphs Bay the simulated denitrification flux was low due to higher dissolved oxygen saturation resulting in part from the shallow bathymetry and in part from simulated photosynthesis of local macrophytes. There were no observations of sediment properties in 2003-4 to validate the simulated sediment biogeochemistry and these results should be treated only as a hypothesis of possible conditions. Recent observations in 2008 have shown high spatial and temporal variability in local sediment conditions due in part to bio-turbation and bio-irrigation of sediment by in-fauna. The impact of sediment in-fauna on pore water biogeochemistry is poorly constrained in the model, due to lack of local observations and parameterisation of these processes, and is a priority area for future model improvement.

The modelled nitrogen budget for the estuary showed that in 2003 the depth-integrated daily flux of nitrogen across the marine boundary was the largest flux into the region (44%), followed by the Derwent River (29%), STP inputs (18%), stormwater (6%) and industrial loads (3%). The largest loss term from the estuary was denitrification (59%) with depth-integrated daily flux of nitrogen across the marine boundary accounting for 41% of export. During 2003 the net accumulation of nitrogen in the estuary was a minor ~44 tN/y which suggests the estuary was in near steady state.

Modelled annual mean chlorophyll concentrations in the top 0-11 m were used to classify the estuary by area as 18.3% mesotrophic and 81.7% eutrophic. The modelled mesotrophic areas (with annual mean chlorophyll 1-3 mg m^{-3}) include the upper estuary where light limits phytoplankton growth, and the lower estuary and southern Ralphs Bay, where near-surface nutrient concentrations were depleted for much of the year. The modelled eutrophic region (with annual mean chlorophyll >3 mg m^{-3}) included the mid- and lower estuary and the remainder of Ralphs Bay.

Recommendations for future work include utilising modern instrumentation in the estuary to collect biogeochemical observations over a greater diversity of time and space scales. In addition, observations of phytoplankton, zooplankton and macrophyte properties would allow these aspects of the model to be better constrained. This study suggests denitrification plays a key role in maintaining the ‘health’ of the ecosystem and it would be good to validate the algorithms and parameterisations included in the model with detailed observations of these (as yet unvalidated) processes. The current modelling study is limited to a specific year and set of environmental conditions, it would be wise to extend the simulated period to place it in the context of natural inter-annual variability. This could be efficiently achieved through the implementation of a near real time operational biogeochemical model which is routinely updated with the most recent advances in science understanding.

2. INTRODUCTION

The Derwent Estuary is a drowned river valley, with a strongly stratified (salt wedge) water column at the upper reaches moving to partially mixed at the mouth. The salt wedge can extend upstream as far as New Norfolk with further incursion limited by the Derwent River flow (minimum flow maintained above 25 cumecs). The estuary conforms to a wave dominated system, currents are generally weak (≤ 0.2 ms^{-1}), and weaker in subsurface waters (Butler 2005, Herzfeld et al.,2005a). Characteristics of the estuary are shown in Table 1.

Table 1 Characteristics of the Derwent Estuary and catchment (adapted from Butler 2005)

Catchment	
Total estuarine catchment area (km^2)	9076
River length (km, source to sea)	215
Topographic relief (m)	0–1449
Catchment land use (%) [a]	
- conservation management	21
- production forests	16
- plantation forests	1
- urban/industry	8
- agriculture	1
- grazing	36
- mining	<1
- other minimal use	13
- lakes/waterbody	3
Human population	190,000
Hydrology [b]	
Mean annual rainfall (mm)	1014
Minimum annual rainfall (mm)	445
Maximum annual rainfall (mm)	2801
Mean run-off coefficient	0.41
Mean annual run-off (mm)	4179
Estuary	
Length (km)	52
Area (km^2)	191
Mean depth (m)	14.7
Volume (m^3 ×106)	2815
Mean tidal amplitude (m)	0.8

[a] DPIWE 2003 & Hydro Tasmania Consulting 2008
[b] Rainfall data derived from Bureau of Meteorology; flow data derived from DPIWE stream gauging.

The Derwent Estuary has had significant inputs of organic matter, suspended solids (wood fibre), nutrients, heavy metals and other toxicants and high levels of heavy metals and toxicants have been found in sediments and biota (Green & Coughanowr 2003). In the past nutrient inputs from river catchments, sewerage treatment plants and industry were not thought to threaten eutrophication, because the estuary flushed rapidly (~ 10 days), and phytoplankton appeared to be light-limited in the middle estuary, where most nutrients entered (Butler 2005). However, elevated chlorophyll concentration and phytoplankton biomass have been observed more recently, in the lower estuary and in some side bays where flushing times are longer (DEP observations). Low dissolved oxygen concentrations have also been observed in bottom waters particularly in the upper estuary, although the spatial and temporal extent of these depleted oxygen events has been difficult to characterise with the monthly monitoring program. Should bottom water oxygen or surface sediment oxygen concentrations fall (< 2000 mg O m-^{3}) then sediment-bound nutrients and heavy metals could be released in more bio-available and toxic forms to marine biota (Jo Banks pers. com.).

High resolution 3D biogeochemical models can now be implemented in coastal and estuarine systems (e.g., Wild-Allen et al., 2005; Robson et al., 2006) to simulate the seasonal dynamics of nutrients, phytoplankton and dissolved oxygen concentrations. Models validated against observations can be used to interpolate between observations and give unprecedented insight into the biogeochemical dynamics of coastal waters, including quantification of nutrient fluxes and simulated budgets. In addition, scenario simulations can be used to explore alternative possible futures, or past events to inform resource managers.

In this project we aimed to implement a high resolution 3D biogeochemical model of the Derwent Estuary from New Norfolk to Iron Pot lighthouse, off Cape Direction, to hind-cast the year 2003. The biogeochemical model was dynamically coupled to an existing calibrated hydrodynamic model (Herzfeld et al., 2005a) and sediment transport model (Margvelashvili 2005). The model was calibrated against water quality observations taken throughout the estuary by the DEP monthly monitoring program and once validated, model results showed the sources, transformation and fate of dissolved and particulate nitrogen, phosphorus and carbon throughout the estuary. Results also characterised, in very high resolution, the spatial and temporal distribution of dissolved oxygen in the water column and surface sediments. Scenario simulations were completed to explore alternative management practices and to reconstruct 'near pristine' estuary conditions and these are documented in a further report (Wild-Allen et al., 2009).

3. BIOGEOCHEMICAL MODEL DESCRIPTION

3.1 Introduction

The biogeochemical model applied in the Derwent Estuary has evolved through a series of case studies including the Port Phillip Bay environmental study (Harris et al., 1996; Murray & Parslow 1997, 1999), the national land and water audit estuaries theme, the Gippsland Lakes environmental study (Webster et al., 2001), the Derwent Estuary ERA (Parslow et al., 2001), the Ord-Bonaparte study (Parslow et al., 2003) the Aquafin CRC study of the D'Entrecasteaux Channel (Wild-Allen et al., 2005) and the Huon Estuary study (CSIRO Huon Estuary Study Team 2000). Each study addressed specific environments and ecological questions resulting in the development, implementation and testing of a diverse range of model components which have been synthesised into the CSIRO environmental modelling suite (EMS).

In most of these previous studies the biogeochemical model was linked to a box model which represented physical transport with relatively low vertical and horizontal resolution (Walker, 1996). In the Aquafin CRC study of the D'Entrecasteaux Channel EMS was directly coupled for the first time, in an estuarine application, to a 3D hydrodynamical model (SHOC; Herzfeld et al., 2005b) and multilayer sediment model (MECOSED; Margvelashvili 2003). This study is the second time the biogeochemical model has been directly coupled to a 3D hydrodynamic model in an estuarine application and the first time where sewage treatment plant and stormwater sources have been included in the model.

The Derwent Estuary model is similar in design to the D'Entrecasteaux model (Wild-Allen et al., 2005) and has a modular form with a software core linked to a central library of ecological processes. With this structure the biogeochemical model is dynamically coupled to the high resolution 3D hydrodynamic model SHOC and multilayer sediment model (Margvelashvili et al., 2005). The grid used for the model is shown in Figure 3-1. The SHOC model parameter file, as used by Herzfeld et al., (2005a) and Margvelashvili (2005) was augmented with biogeochemical model tracers, initial and

boundary conditions, rivers and point source loads from industry, sewerage and stormwater sources. Additional biogeochemical model parameters were sourced from observations, previous modelling studies and literature studies appropriate for the estuary. During model calibration poorly constrained biogeochemical model parameter values (such as phytoplankton mean cell size, growth rate and proportion of each functional group) were varied within known ranges to determine an optimal parameter set which produced model results consistent with observations (model input file 'bio_derwent.prm' is included in Appendix 10-1).

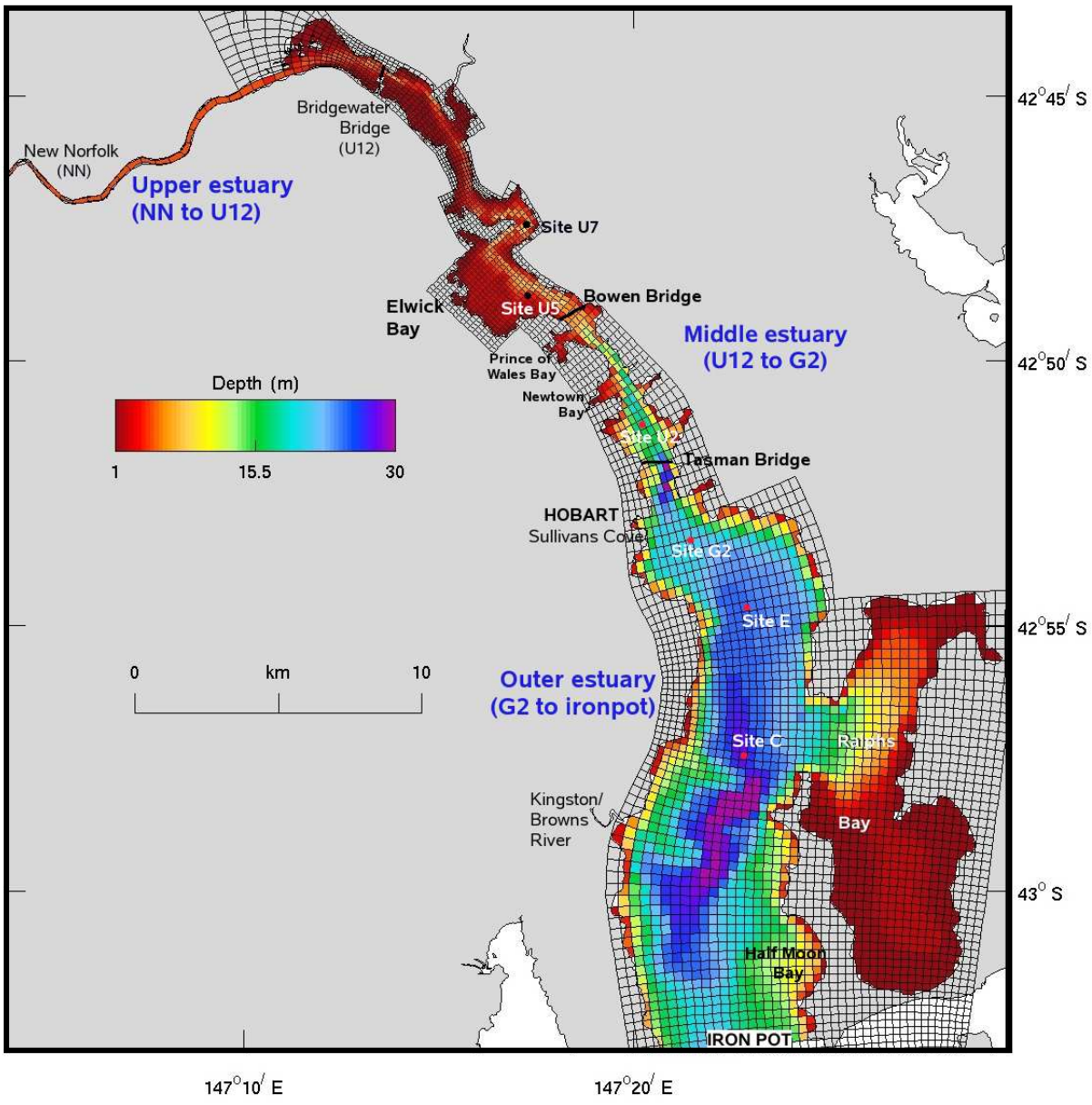

Figure 3-1 Model grid and bathymetry of the Derwent Estuary

3.2 Hydrodynamical Model and Grid

The hydrodynamical model has been implemented on a curvi-linear grid [described in (Herzfeld et al., 2005a)] extending south from New Norfolk to Iron Pot lighthouse off Cape Direction (Figure 3-1). Horizontal grid resolution varies from < 100 m to 500m and there are 25 vertical layers ranging from 0.5 m thick at the surface to 5.0 m thick at 30 m in the deeper reaches of the estuary. Above the

Bridgewater Bridge the model is coarsely resolved relative to the convoluted channel bathymetry and has limited capacity to simulate the complex hydrodynamics, sediment dynamics and biogeochemistry of the upper reaches of the estuary.

The hydrodynamic model is nested in regional and intermediate scale physical models, forced with Derwent river flow and local meteorology and calibrated against mooring data (Herzfeld et al., 2005a). The hydrodynamical model is calculated with a 2D time step of 5 seconds and a 3D time step of 40 seconds for accurate representation of physical processes. Biogeochemical model tracers are advected and diffused through the 3D flow field in an analogous fashion to temperature and salinity, and particulate substances sink and are resuspended similar to sediment particles. Biological processes are evaluated on a 2 hour time step with a 5th order adaptive integration scheme that checks for conservation of mass.

3.2.1 Hydrodynamics of the Estuary (Herzfeld et al., 2005a)

The Derwent Estuary is a salt wedge estuary which typically features a layer of fresher river sourced water overlying an intrusion of more saline marine water. The formation of strongly stratified layers in an estuary restricts vertical exchange and mixing resulting in strong gradients in water properties which support a wide range of biogeochemical conditions. In the Derwent Estuary there is high variability in the salinity structure over a tidal cycle, including the formation of internal waves along the halocline in the mid-estuary which could augment vertical exchange in some situations.

The ebb tide is shorter and stronger than flood (form factor ~1.5) and the instantaneous flow is generally downstream on ebb, upstream on flood with the mean flow upstream in bottom, downstream in surface layers (Figure 3-2). The whole estuary flushing time is approximately 10 days (depending on flow) with flushing time for most embayments ~ half a day and Ralphs Bay 2 to 3 days (Table 2).

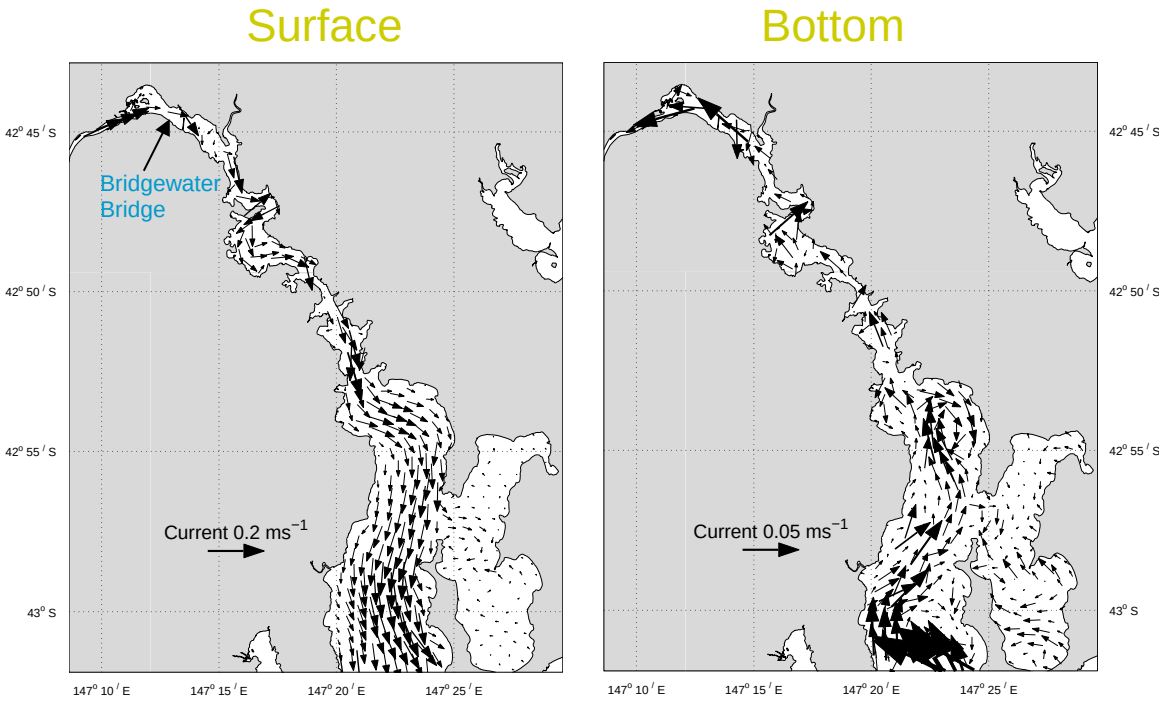

Figure 3-2 Surface and bottom residual circulation (14 day mean flow) in the Derwent Estuary (Herzfeld et al., 2005a).

Table 2 Flushing characteristics under steady moderate (16 Jan - mean flow 56 m^3s^{-1}) and fluctuating high (5 Feb - mean flow 78 m^3s^{-1}) flow conditions in 2003 (Herzfeld et al., 2005a).

Run	Region	Date	Flushing (days)
1	Whole estuary	16 Jan	11.1
2	Whole estuary	5 Feb	9.3
3	Upper + middle	16 Jan	4.0
4	Upper + middle	5 Feb	3.4
5	Elwick Bay	16 Jan	0.78
6	Elwick Bay	5 Feb	0.64
7	Cornelian Bay	16 Jan	0.48
8	Cornelian Bay	5 Feb	0.38
9	Geilston Bay	16 Jan	0.55
10	Geilston Bay	5 Feb	0.32
11	Prince of Wales Bay	16 Jan	0.88
12	Prince of Wales Bay	5 Feb	0.68
13	New Town Bay	16 Jan	0.40
14	New Town Bay	5 Feb	0.17
15	Ralphs Bay	16 Jan	3.42
16	Ralphs Bay	5 Feb	2.14

3.3 Biogeochemical Model Components

Biogeochemical dissolved tracers are advected and diffused in an identical fashion to physical tracers such as temperature and salinity and ecological particulate tracers sink and are resuspended by the same formulation as surface sediment particles. At each ecological time step, non-conservative ecological rate processes such as growth, nutrient uptake, grazing and mortality are integrated within the ecological module which returns updated tracer concentrations to the hydrodynamic and sediment models via an interface routine.

The ecological model water column is organised as 3 ‘zones’: pelagic, epibenthic and sediment. The epibenthic zone overlaps with the lowest pelagic layer and shares the same dissolved and suspended particulate material fields. The sediment is modelled in 3 layers with a thin layer of easily resuspendable material overlying thicker layers of more consolidated sediment.

Ecological processes are organised into the 3 zones with pelagic processes including phytoplankton and zooplankton growth and mortality, detritus remineralisation and fluxes of dissolved oxygen, nitrogen and phosphorus. Macroalgae and seagrass growth and mortality are included in the epibenthic zone whilst further phytoplankton mortality, microphytobenthos (benthic diatom) growth, detrital remineralisation and fluxes of dissolved substances are included in the sediment layer (Figure 3-3).

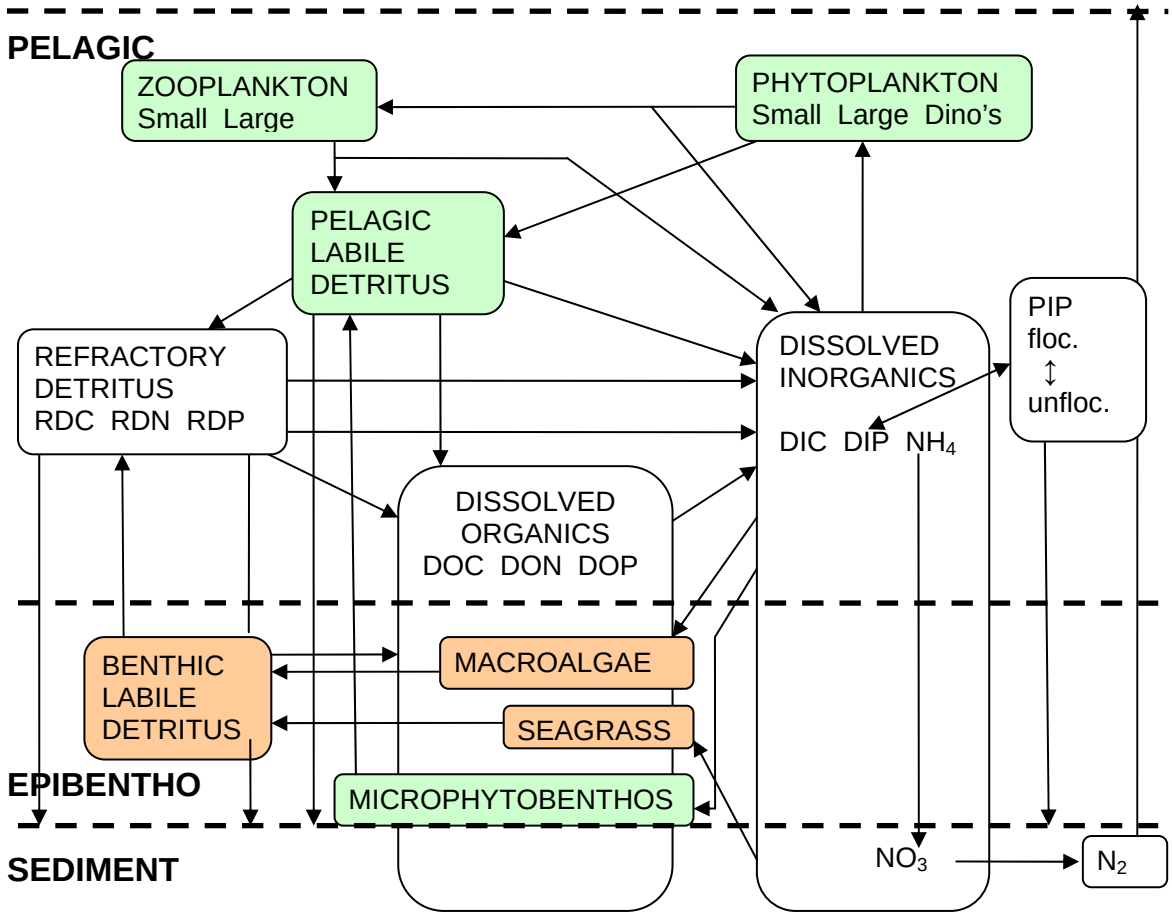

Figure 3-3 Schematic diagram of the biogeochemical model compartments, links and vertical layers. Green compartments have fixed nutrient content at Redfield ratio (106C:16N:1P); brown compartments are fixed at Atkinson ratio (550C:30N:1P).

3.3.1 Primary Production

There are 4 'groups' of microalgae and 2 macrophytes included in the model:

1)'Small phytoplankton' representing small flagellates, and photoautotrophic pico- and nano-plankton. These organisms are small, with relatively high growth rates and are typically neutrally buoyant. Their high surface area to volume ratio enables them to take up nutrients efficiently, even at low concentration, which makes this group of phytoplankton ubiquitous throughout aquatic systems (Fogg 1991). Small phytoplankton are modelled with a fixed nutrient ratio of 106C:16N:1P (Redfield Ratio). The biomass of small phytoplankton is heavily constrained by grazing by tightly coupled small zooplankton. Natural mortality occurs when cells drift into the sediment layer.

2)'Large phytoplankton' represent diatoms with opportunistic ecological characteristics. They have a high growth rate which allows them to respond rapidly when nutrients and light are available, despite having lower nutrient uptake efficiency and a tendency to sink out of the euphotic layer. Modelled large phytoplankton have a fixed nutrient ratio of 106C:16N:1P (Redfield Ratio). Large zooplankton graze on large phytoplankton but their slower growth rate results in a lag in response time allowing bloom events to occur. Large phytoplankton which sink into the sediment layer are assumed to die.

3) ‘Dinoflagellates’ represent large dinoflagellates with much slower growth rates than the large phytoplankton group. They are neutrally buoyant and have some capacity for ‘luxury’ uptake and storage of nutrient, as they are modelled with independent carbon and nitrogen pools. Large zooplankton graze on dinoflagellates and cells which sink or drift into the sediment layer are presumed to die.

4)‘Microphytobenthos’ are large cells representative of benthic diatoms. They have a high sinking rate and grow in the pelagic and sediment layers where there is sufficient light. In the sediment layer they have access to enhanced concentrations of regenerated nutrients. They are modelled with a fixed nutrient ratio of 106C:16N:1P (Redfield Ratio) and are grazed by large zooplankton when suspended.

4) Seagrass grow in the epibenthic layer where there is sufficient light. They have a fixed carbon to nutrient ratio of 550C:30N:1P (Atkinson Ratio) and utilize nutrients directly from the sediment layer by uptake through their root system. Seagrass mortality occurs when there is insufficient light and/or nutrients to sustain growth for metabolic/respiration requirements.

6) Macroalgae in the model represent both macro- and epiphytic- algal groups that might co-exist with seagrass communities. They have a fixed nutrient ratio of 550N:30N:1P (Atkinson Ratio) and utilize nutrients from the pelagic water column by absorption across the frond surface. Macroalgae mortality occurs when there is insufficient light and/or nutrients to sustain growth for metabolic/respiration requirements.

Modelled autotroph growth is determined by access to essential nutrients (nitrogen and phosphate) and photosynthetically active radiation (PAR) by the chemical reaction model of Baird (1999). Dissolved nitrogen is present as ammonium and nitrate and autotrophs take up both equally. Phosphate and dissolved inorganic carbon are also taken up by phytoplankton at Redfield ratio (106C:16N:1P) and by macrophytes at Atkinson ratio (550C:30N:1P) (autotroph parameters are shown in Table 3). Phytoplankton chlorophyll concentration is calculated by assuming a fixed nitrogen to chlorophyll ratio of 7 mgN/mgChl.

Ambient photosynthetically active radiation (PAR) is calculated from incident surface 24 hour mean PAR which is derived from the short wave light-field computed for the hydrodynamical model (including reduction of clear sky irradiance by cloud cover as observed at Hobart airport). Surface PAR is attenuated by seawater, coloured dissolved organic substances (CDOM), organic and inorganic particles and coloured effluent in the proximity of the Norske Skog paper mill (optical parameters are shown in Table 4; mill effluent attenuation and optical degradation half life are shown in Table 7).

Table 3 Characteristics of primary producers included in the model.

Parameter	Large Phyto-plankton	Small Phyto-plankton	Dino flagellates	Micro-phyto-benthos	Sea Grass	Macro-algae
Radius (m)	1.0E-5	2.5E-6	1.0E-5	1.0E-5	N/A	N/A
Max growth rate (μ) (d^{-1})	1.25	1.25	0.2	0.35	0.1	0.02
Respired fraction of μ max (-)	0.025	0.025	0.025	0.025	0.025	0.025
Absorption (m^{-1})	50000	50000	30000	50000	1.0E-5 m^2mgN^{-1}	0.001 m^2mgN^{-1}
Stoichiometry coefficient of phosphorus	N/A	N/A	N/A	N/A	2.4E-6	2.4E-6
Mortality term (d^{-1})	0.14	0.14	0.14	0.0001 (d^{-1}(mgN m^{-3})$^{-1}$)	0.00275	0.01
Half saturation constant for N uptake in sediment (mgN m^{-3})	N/A	N/A	N/A	N/A	15.0	N/A
Half saturation constant for P uptake in sediment (mgP m^{-3})	N/A	N/A	N/A	N/A	15.0	N/A

Table 4 Optical parameters included in the model

Parameter	**Value**
Background attenuation of sea water	0.1
CDOM attenuation coefficient of fresh water (m^{-1})	1.0
Detrital specific attenuation coefficient (m^{-1})	0.0038
TSS specific attenuation coefficient ($m^{-1}kg^{-1}$ m^{-3})	30
Dissolved organic nitrogen specific attenuation coefficient ($m^{-1}mgN^{-1}m^{-3}$)	0.0009

3.3.2 Secondary Production

There are 2 groups of zooplankton included in the model (Table 5):

1) 'Small zooplankton' represent microzooplankton less than 200 μm in size such as zooflagellates, tintinnids, ciliates, rotifers, small copepod nauplii and polychaete larvae. They are mobile, feed on small phytoplankton and have rapid turnover rates. They are modelled with a fixed nutrient ratio of 106C:16N:1P (Redfield Ratio) and grow as a function of maximum specific growth rate and grazing rate. Grazing success depends on the food encounter rate which in turn is based on zooplankton swimming speed, food size and density. Inefficient feeding and excretion returns dissolved and particulate material to the water column at Redfield ratio. A quadratic mortality term is applied to account for both natural mortality and predation and is the closure term for the model's biogeochemical cycling.

2) 'Large zooplankton' represents mesozooplankton such as copepods and small fish larvae. They are mobile, feed on large phytoplankton, microphytobenthos and dinoflagellates They are modelled with a fixed carbon to nutrient ratio of 106C:16N:1P (Redfield Ratio) and have a lower maximum specific growth rate compared with the small zooplankton which results in a lag between enhanced primary and secondary production. Grazing success is a function of food encounter rate and inefficient feeding and excretion returns dissolved and particulate material to the water column at Redfield ratio. Natural mortality and predation of large zooplankton are represented by a quadratic mortality term which is the closure term for the model's biogeochemical cycling.

Table 5 Characteristics of secondary producers included in the model.

Parameter	Small Zooplankton	Large Zooplankton
Radius (m)	$12.5E^{-6}$	$5.0E-^{4}$
Growth efficiency (-)	0.38	0.38
Maximum growth rate at 15˚C (d^{-1})	3.0	0.1
Swimming velocity (m)	$2.0E^{-4}$	$1.5E^{-3}$
Fraction of growth inefficiency lost to detritus (-)	0.5	0.5
Mortality (quadratic) rate ($d^{-1}(mgN\ m^{-3})^{-1}$)	0.02	0.016
Fraction of mortality lost to detritus (-)	0.5	0.5

3.3.3 Detritus and Nutrient Pools

There are 4 types of particulate detritus and 3 pools of dissolved substances included in the model:

'Pelagic labile detritus' represents fresh detritus which is rapidly broken down by bacteria, viruses and fungi into refractory detritus, dissolved organic and dissolved inorganic substances on the timescale of about a week. It is modelled with a fixed carbon to nutrient ratio of 106C:16N:1P (Redfield Ratio) and generated by inefficient feeding and excretion by large and small zooplankton, and by mortality of phytoplankton and zooplankton. Detrital particles contribute to the attenuation of light, sink and enter the sediment layer where remineralisation processes continue.

'Benthic labile detritus' is similar to pelagic labile detritus but has a fixed carbon to nutrient ratio of 550N:30N:1P (Atkinson Ratio). It is generated by mortality of seagrass and macrophytes. Particles contribute to the attenuation of light, sink and enter the sediment layer where remineralisation processes continue.

Refractory detritus represents older detrital material with lower nutrient to carbon content and slower remineralisation time scales of about a year. Refractory material is generated by the breakdown of pelagic and benthic labile detritus (with contrasting carbon to nutrient ratios) which necessitates modelling the carbon, nitrogen and phosphorus components independently. Refractory detrital material is remineralised to dissolved organic and inorganic substances. Particles contribute to the attenuation of light, sinks and enter the sediment layer where remineralisation processes continue.

Dissolved organic material is considered to be a pool of very refractory nature with very slow remineralisation time scales of about two years. Dissolved organic material is generated by remineralisation of pelagic and benthic labile detritus and refractory detritus and is modelled as independent carbon, nitrogen and phosphorus components. This material is remineralised by bacterial and chemical reaction to dissolved inorganic carbon, nitrogen and phosphorus. Enhanced concentrations of detritus in the sediment give rise to gradients in dissolved organic matter which diffuse into the pelagic layer.

Dissolved inorganic material is modelled as independent carbon, nitrogen and phosphorus pools. It is generated through inefficient feeding and excretion of zooplankton and by remineralisation of pelagic and benthic labile detritus, refractory detritus and dissolved organic material (Table 6). These transformations release nitrogen in the form of ammonium which depending on available oxygen, can undergo nitrification to nitrate and denitrification to nitrogen gas, which is then lost to the atmosphere. In the Derwent Estuary ammonium derived from point source input could also be nitrified and denitrified with associated drawdown of dissolved oxygen. Dissolved inorganic phosphorus can be adsorbed onto, or desorbed from, suspended sediment particles, which in turn may flocculate into larger particles with different sinking characteristics. Adsorption of phosphorus onto sediment

particles limits its availability for algal uptake and growth. Accumulation of labile and refractory detritus in the sediment leads to gradients in dissolved inorganic carbon and nutrient which diffuse back into the pelagic layer at rates enhanced by bio-irrigation. Dissolved inorganic nutrients are the final stage in the process of recycling organic material into bio-available nutrients for uptake by autotrophs.

To accommodate the large quantities of labile POC and DOC released into the estuary by the Norske Skog paper mill, these 2 additional tracers were added to the model and bacteria assimilation was explicitly included in the remineralisation process similar to the biogeochemical box model of the upper estuary by Parslow et al., (2001). Parameters added to represent the Norske Skog paper mill effluent and it's remineralisation are shown in Table 7.

Table 6 Modelled detritus parameter values and associated remineralisation rates.

Parameter	Value	Unit
Pelagic labile detritus breakdown rate	0.1	d^{-1}
Refractory detritus breakdown rate	0.0036	d^{-1}
Dissolved organic matter breakdown rate	0.00176	d^{-1}
Fraction of labile detritus converted to DOM	0.01	-
Fraction of labile detritus converted to refractory detritus	0.19	-
Fraction of refractory detritus converted to DOM	0.01	-
Maximum water column nitrification rate	0.1	d^{-1}
Maximum sediment nitrification rate	20	d^{-1}
Maximum nitrification efficiency	1.0	-
O2 half saturation rate for nitrification	500	mg O m^{-3}
Maximum denitrification rate	40	d^{-1}
O2 content at 50% denitrification rate	10000	mg O m^{-3}
O2 half saturation rate for aerobic respiration	500	mg O m^{-3}

Table 7 Modelled parameter values and rates for substances associated with Norske Skog paper mill effluent

Parameter	Value	Unit
Mill Attenuation Proxy	10.0	m^{-1}
Mill Effluent Decay Rate	20	d
Remineralisation rate of Labile Organic C	0.4	d^{-1}
Adsorption of LDOC onto LPOC	0.4	d^{-1}
Max growth rate of bacteria	0.4	d^{-1}
N half saturation for bacterial growth	3.0	mg N m^{-3}
P half saturation for bacterial growth	3.0	mg P m^{-3}

3.3.4 Biogeochemical Model Initialisation

The biogeochemical model was initialized in January 2003 with tracer concentrations derived from DEP observations made throughout the region (Appendix 10-4). Where suitable observations were unavailable historical data and literature values were used. Initialising a model in mid-summer is difficult as most biogeochemical tracers have strong vertical gradients associated with gradients in light, nutrients, phytoplankton biomass and mixing. Results from the first month of simulation should be treated with caution in case of artefacts from the initial condition.

In the absence of any data on phytoplankton species composition in the estuary in 2003, data collected off the CSIRO wharf in 1993 (Jameson, unpublished data) and qualitative data from Hallegraeff and McMinn collected in 2005 were used to partition observed chlorophyll data between model phytoplankton functional groups (see section 4.1.2). Phytoplankton samples were converted to biovolumes by assuming a mean size for each species of phytoplankton from previous observations (Pru Bonham unpublished data). Biovolumes were summed for each model compartment so large

phytoplankton contained mostly large diatoms small phytoplankton mostly flagellates and small diatoms and dinoflagellates containing large dinoflagellates. Observed chlorophyll concentrations in 2003 were then partitioned between the relative fractions of each algal group and translated to N biomass assuming a fixed nitrogen:chlorophyll ratio of 7 mgN: mgChl. For the dinoflagellate compartment the carbon concentration was calculated by assuming a fixed ration of 106C:16N (Redfield ratio).

In early simulations the marsh and wetland area above the Bridgewater Bridge was initialised with macrophyte biomass, and the remaining area of the estuary without macrophyte biomass. Macrophyte distribution was limited to the areas initialised with biomass and the model could not reproduce the small fringing beds found elsewhere in the estuary. In later simulations the whole model grid was initialised with a small uniform biomass of macrophytes and the model evolved spatial and temporal distributions of seagrass and macroalgae based on plant growth rates and bed access to light and nutrients. After ~6 months the placement of macrophyte beds correlated closely with observations although biomass in some areas took >2 years to approach steady state. [In these simulations the model generally overestimated seagrass growth compared with observations in Ralphs Bay].

Most model simulations ran from January 2003 until March 2004 to capture a full summer season. One simulation completed a full 2 years (with repeated 2003 annual forcing) to check for consistency in the seasonal cycle of biogeochemistry and to evaluate the temporal evolution of macrophytes.

3.4 Nutrient Sources into the Estuary

Loads of carbon, nitrogen and phosphorus enter the Derwent Estuary across the marine boundary, from the Derwent River and from a number of point source discharge locations throughout the region. Fluxes from marine and river sources are modelled as boundary conditions to the model; loads from industry, STPs and stormwater are included as point source loads delivered at a specified locations and depths into the model domain.

3.4.1 Marine Boundary

At the marine boundary of the model all tracer concentrations were specified with an upstream condition such that out-flowing concentrations were determined by the model whilst in-flowing concentrations were specified. Tracer concentrations were derived from the DEP 2003-4 time-series of surface and bottom observations at stations B1, B2 & B3 (Figure 3-4).

Seasonal cycles in the concentration of nitrate, ammonium, dissolved inorganic phosphate, labile and refractory detritus, suspended particulate matter, dissolved organic nitrogen, oxygen and plankton biomass were determined from the DEP observations (Appendix 10-5). Phytoplankton biomass was proportioned between small, large and dinoflagellate groups based on the time series of species composition collected off the CSIRO wharf in 1993 (Jameson, unpublished data) and 2005 data from Hallegraeff and McMinn (pers.comm.). The possible influence of elevated nutrient loads from fish farming activities in the adjacent D'Entrecasteaux Channel would have been included in the model as captured by the DEP data set [although sparse monthly sampling aliased by tidal state, could miss significant nutrient flux events].

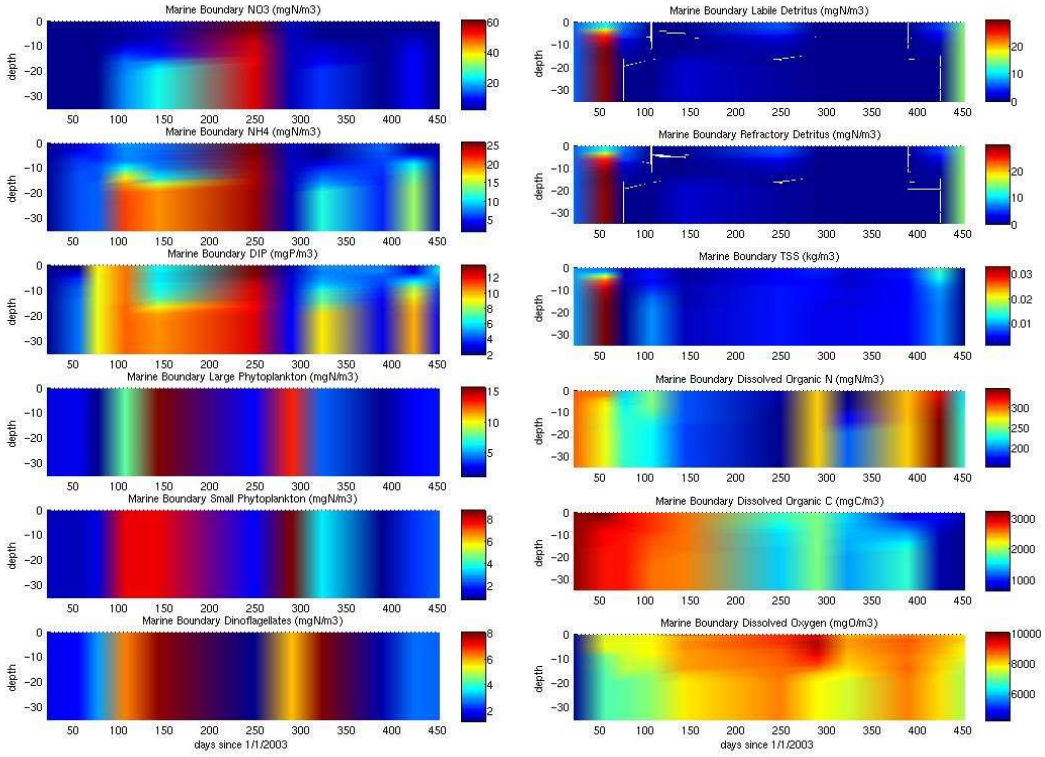

Figure 3-4 Time series of biogeochemical model substances supplied at marine model boundary (data are presented from the centre of the boundary; spatial variation along the boundary was included in the forcing file).

3.4.2 Derwent River

The model was forced at the northern end of the estuary with Derwent River flow derived from observations at Meadowbank (Figure 3-5) and the Tyenna River. No adjustments were made for additional flow from the Styx River or the Plenty River or for the time lag for flow to reach New Norfolk. During the modelled period Derwent flow varied from <50 m^3s^{-1} to >800 m^3s^{-1} with greatest flow occurring in August and September.

Tracer concentrations at the river boundary were derived from the DEP 2003-4 time-series of surface and bottom observations at New Norfolk (Figure 3-6). Observations included concentrations of nitrate, ammonium, dissolved inorganic phosphate, labile and refractory detritus, suspended particulate matter, dissolved organic nitrogen, oxygen and plankton biomass (Appendix 10-5). Phytoplankton biomass was proportioned between small, large and dinoflagellate groups based on the time series of species composition collected off the CSIRO wharf in 1993 (Jameson, unpublished data) and 2005 data from Hallegraeff and McMinn (pers.comm.). The modelled river boundary was implemented as an upstream boundary condition such that inflowing water contained the tracer concentrations derived from observations.

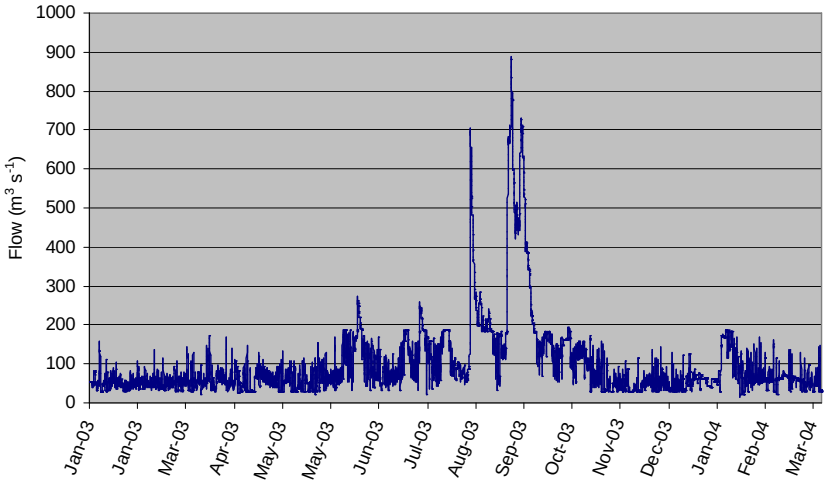

Figure 3-5 Derwent River flow at New Norfolk for 2003 model run.

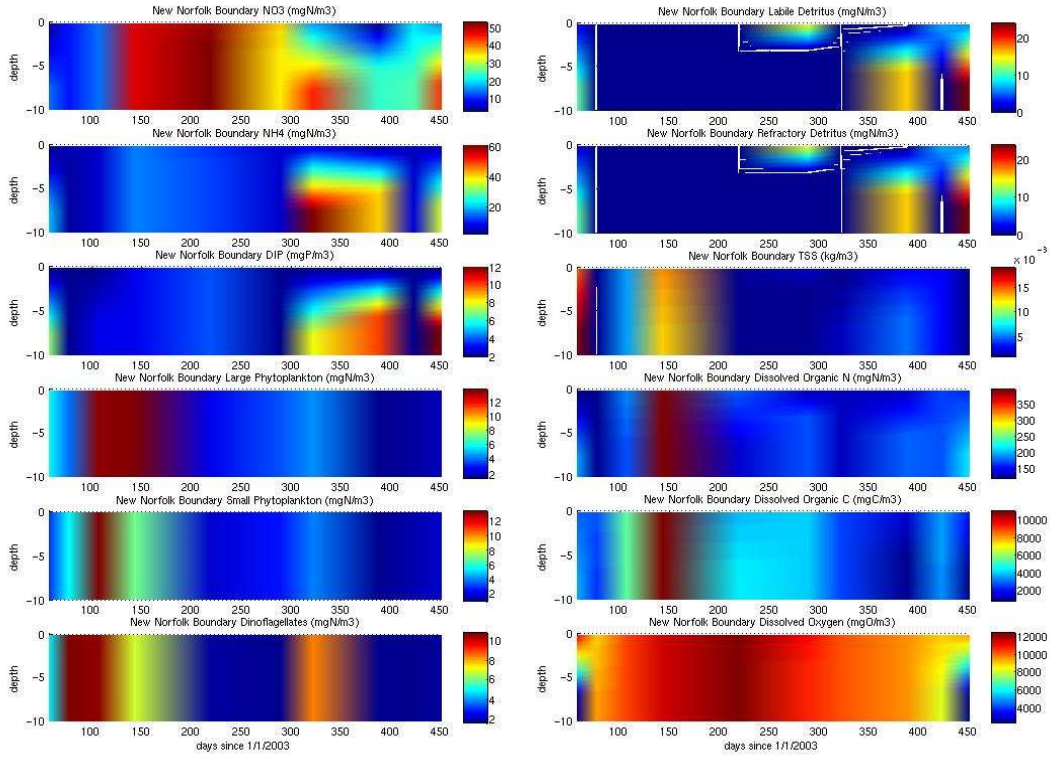

Figure 3-6 Time series of biogeochemical model substances supplied at New Norfolk model boundary.

3.4.3 Industry and Sewage Loads

Point source loads were included in the model for sewage treatment plants (STP) and industry (Figure 3-8). Nutrient and detrital data were collated for the model from DPIWE, industry and councils responsible for the sewage treatment plants. In 2003 STPs contributed the greatest point source load of nitrogen and phosphorus to the estuary, whilst industrial effluent contributed most carbon [primarily as DOC and POC from the Norske Skog paper mill] (Figure 3-7).

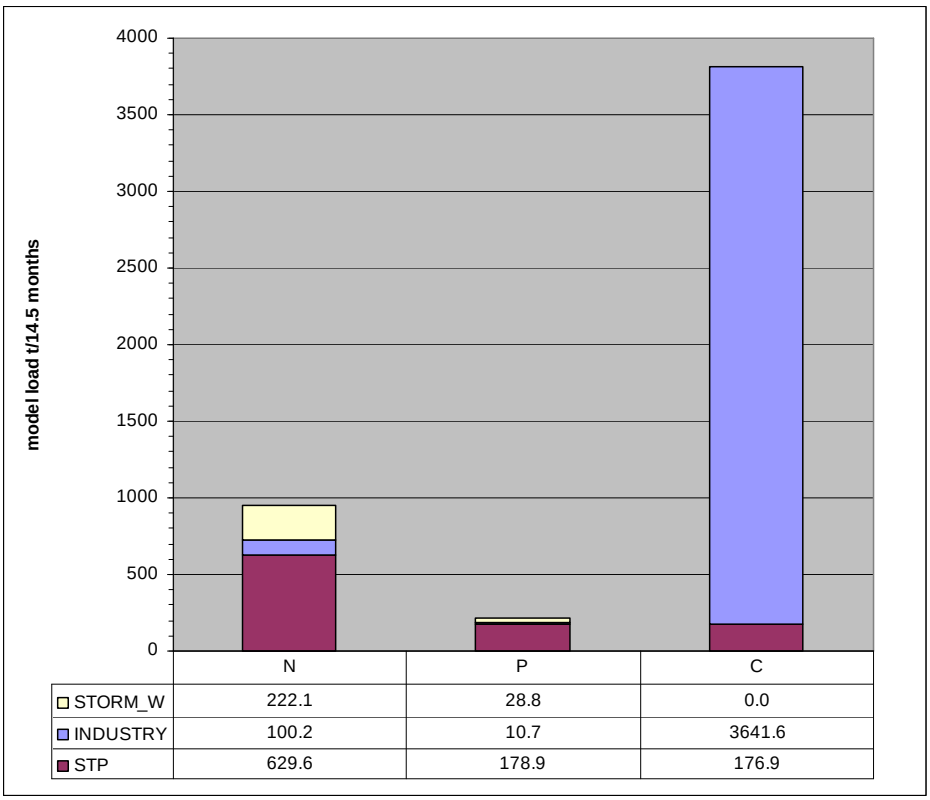

	N	P	C
STORM_W	222.1	28.8	0.0
INDUSTRY	100.2	10.7	3641.6
STP	629.6	178.9	176.9

Figure 3-7 Total loads of nitrogen, phosphorus and carbon supplied to the model from storm water, industry and sewerage treatment plants for the 14.5 month simulation period

In 2003, ten sewage treatment plants discharge treated wastewater to the Derwent estuary including 3 plants which process wastewater associated with larger industries (Prince of Wales Bay Cameron Bay and Macquarie Point). During 2003 sewage from the Bridgewater STP was totally re-used and there was no discharge from this STP into the estuary. For all other plants total suspended solids were converted to labile detrital particulate N and P at a fixed Redfield ratio (C:O:N:P=106:110:16:1). Refractory particulate detrital N and P were calculated by subtracting the labile components from the TN and TP respectively. Labile POC and DOC from Norske Skog and STPs were included to improve model resolution of detrital and dissolved oxygen dynamics. In addition to nutrient and carbon loads, an attenuation coefficient was specified for Norske Skog mill effluent to account for the strong colouration of resin acids in the effluent. Based on the optical model in Parslow et al., (2001) the attenuation coefficient was allowed to decay over a period of 20 days to simulate breakdown of the optically active components in the effluent. Effluent from Nyrstar zinc works and the adjacent company, Impact fertiliser, is discharged through the same outfall. Figure 3-8; Table 8 shows STP and industry locations, outfall depths, total flow volumes and nutrient discharge that were used as point source sinks for the model.

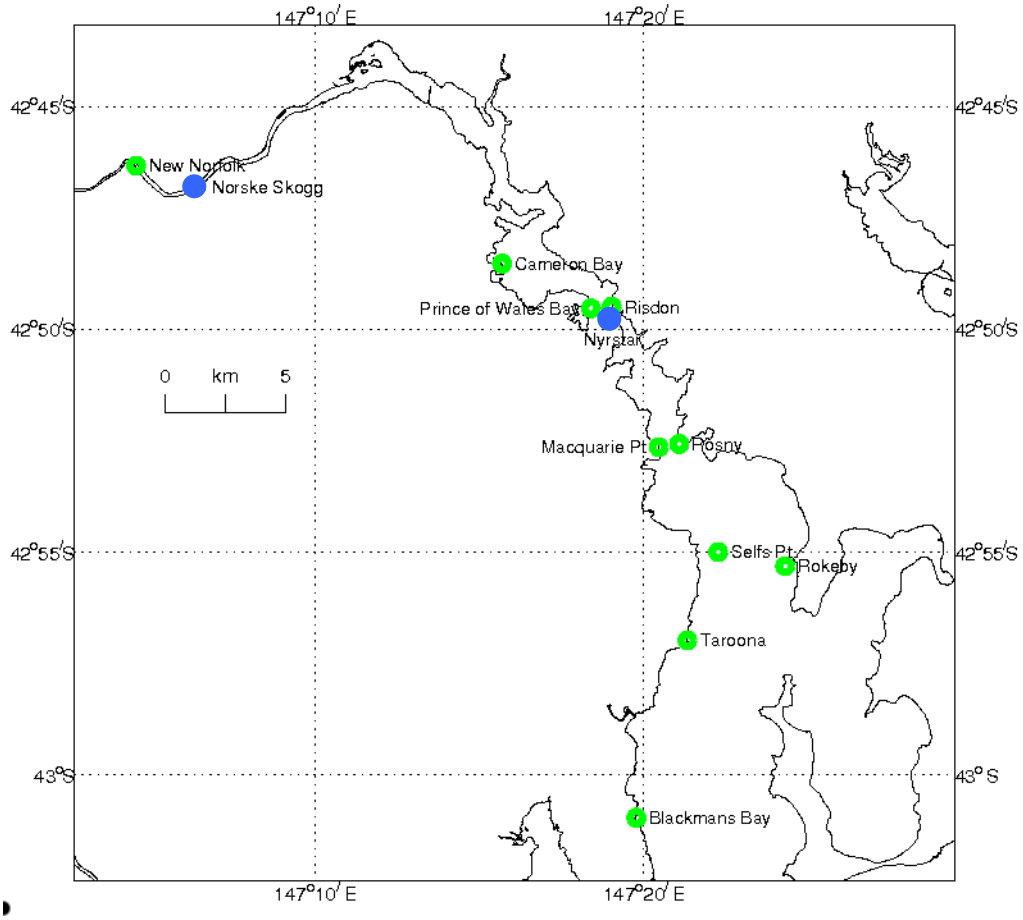

Figure 3-8 Map of Derwent Estuary indicating positions of sewerage treatment plants (green circles) and industry source loads (blue points).

Table 8 Locations of sewage treatment plants and industry outfalls in the Derwent Estuary – discharge depth, annual flow and loads used in model from DPIWE and industry source data.

Treatment Plant	Long. (deg.E)	Latitude (deg.S)	depth (m)	Discharge (ML/y)	Discharge (% total)	NH4 (tN/y)	NOx (tN/y)	TN (tN/y)	TP (tP/y)	DOC (tC/y)	POC (tC/y)
Taroona	147.355	42.95	0-1.6	0.27	1	7.7	0.3	9.7	2.4	7.4	0
Rokeby	147.405	42.922	22	0.81	3	1.1	1.9	3.5	1.7	6.1	0
Risdon	147.317	42.825	2	1.11	4	0.2	1	1.5	3.7	4.7	0
New Norfolk*	147.076	42.772	2	1.18	5	16.4	3.3	22.4	10.7	2.8	0
Blackmans Bay	147.33	43.016	2-3	1.64	7	60.2	0.5	64.6	15.3	7	0
Cameron Bay^	147.261	42.809	1.5	2.37	10	30.7	29	62.8	20.7	7.6	0
Rosny	147.351	42.876	17	3.09	12	77.4	0.9	93.4	21	34.9	0
Selfs Point	147.371	42.917	9	3.56	14	7.5	10.8	22.2	17	43.5	0
Prince of Wales Bay^	147.307	42.826	2	4.82	19	71.8	14.1	88	26.5	21.4	0
Macquarie Point	147.341	42.878	15	5.9	24	95.9	30.6	150.7	30.4	25.9	0
STP 2003 total				***24.8***	***100***	***369***	***92***	***149***	***149***	***161***	***0***
Impact Fertiliser #	147.11	42.777	Nov-16	0.003	0.01	0	0	0	1.7	0	0
Nyrstar (Zinc)	147.318	42.829	Nov-16	25.7	58	7.1	0	10.5	0	0	0
Norske Skog (Paper)	147.108	42.78	0-2	18.58	42	1.5	0.8	72.7	7.4	2192.6	802.2
Industry 2003 total				***44.3***	***100***	***9***	***1***	***83***	***9***	***2193***	***802***

^ Phosphate measured not TP
# Impact fertiliser uses Nyrstar's outfall
* 2002 data used for NHx, NOx, DIN and TP

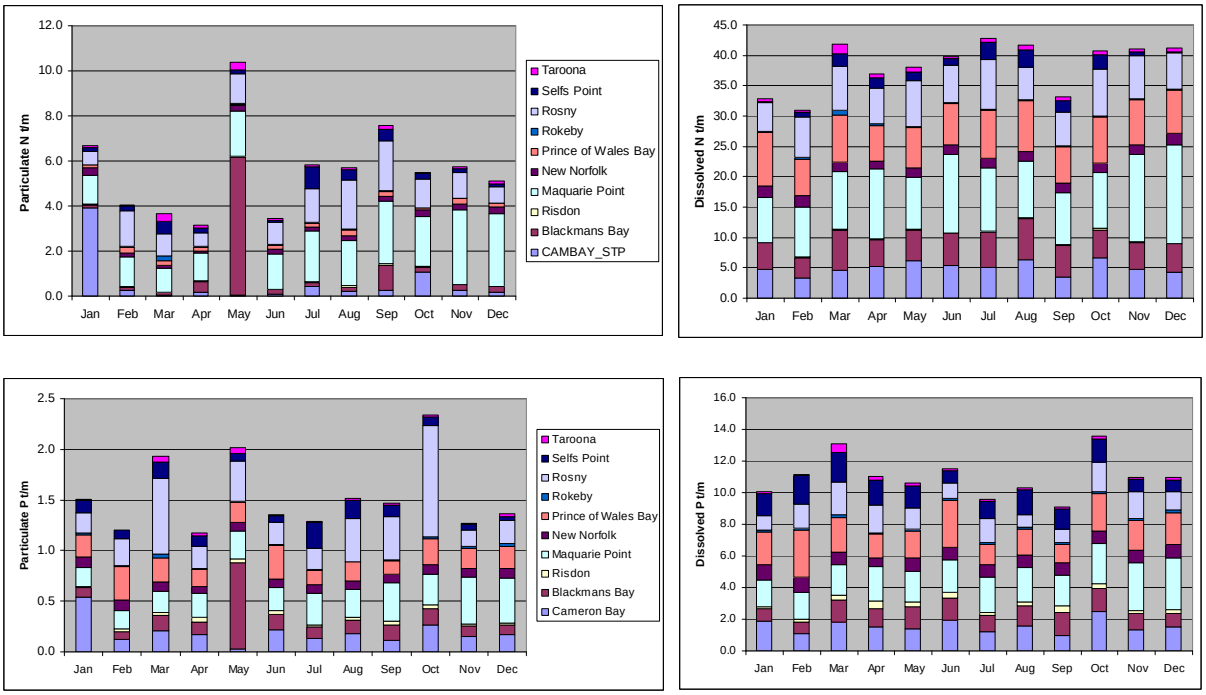

Figure 3-9 Monthly loads of particulate (left) and dissolved (right) nitrogen (upper panel) and phosphorus (lower panel) from STPs throughout the estuary in 2003.

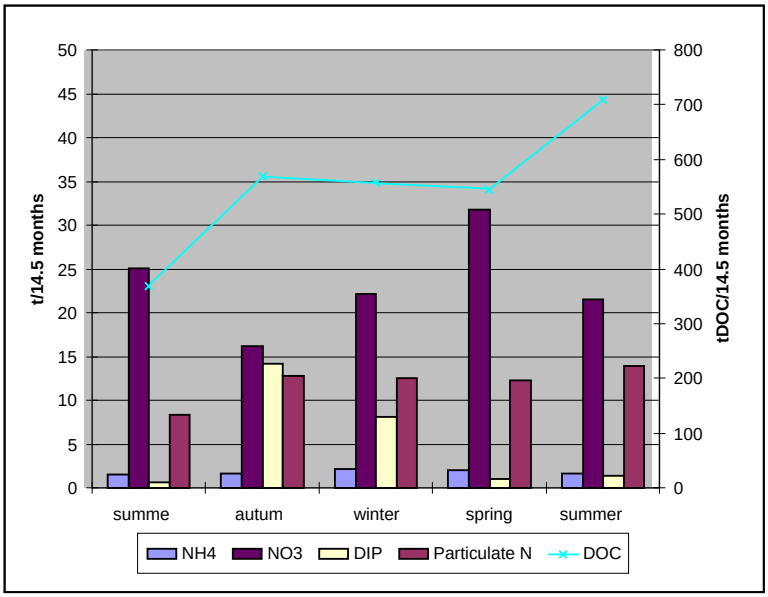

Figure 3-10 Seasonal loads of nutrients, particulate N and DOC from industry sources in 2003-4 (first summer is Jan – Feb '03; second summer is Dec'03 - Mar'04).

3.4.4 Stormwater Point Sources

Daily water volume and pollutant loading to the Derwent Estuary, from sub-catchments surrounding the greater Hobart region were modelled using MUSIC (Model for Urban Stormwater Improvement Conceptualisation) Version 3.0.1 software by Jason Whitehead et al., Derwent Estuary Program (Appendix 10-2).

Seventy four sub-catchments were identified and differentiated by their percentage of urban, rural and forested areas (Figure 3-11). These proportions were used to convert local rainfall data from the

region and Bureau of Meteorology into loads of TSS, TP and TN. A small set of nutrient observations in rivulets and stormwater entering the estuary were used to determine multipliers for the modelled loads and partition TN into ammonia and nitrate, and TSS into detrital labile nitrogen and detrital organic nitrogen (Table 9). Total suspended solids were converted to labile detrital particulate nitrogen at a fixed Redfield ratio of 16N:1P and refractory detrital organic nitrogen was gained by subtracting the labile components from TN. Point sources loads of nitrate, ammonia, detrital labile nitrogen and detrital organic nitrogen were included in the model for stormwater sources and rivulets (Table 9and

Appendix **10-3**).

Catchments were allocated to 96 point sources around the estuary with some catchments including multiple water courses (e.g. Opossum). Point source locations were placed with respect to stormwater outlets, geography and natural rivulets (Figure 3-12). Some smaller catchments were combined to form larger catchments as shown in Table 11 (Whitehead, pers. com.).

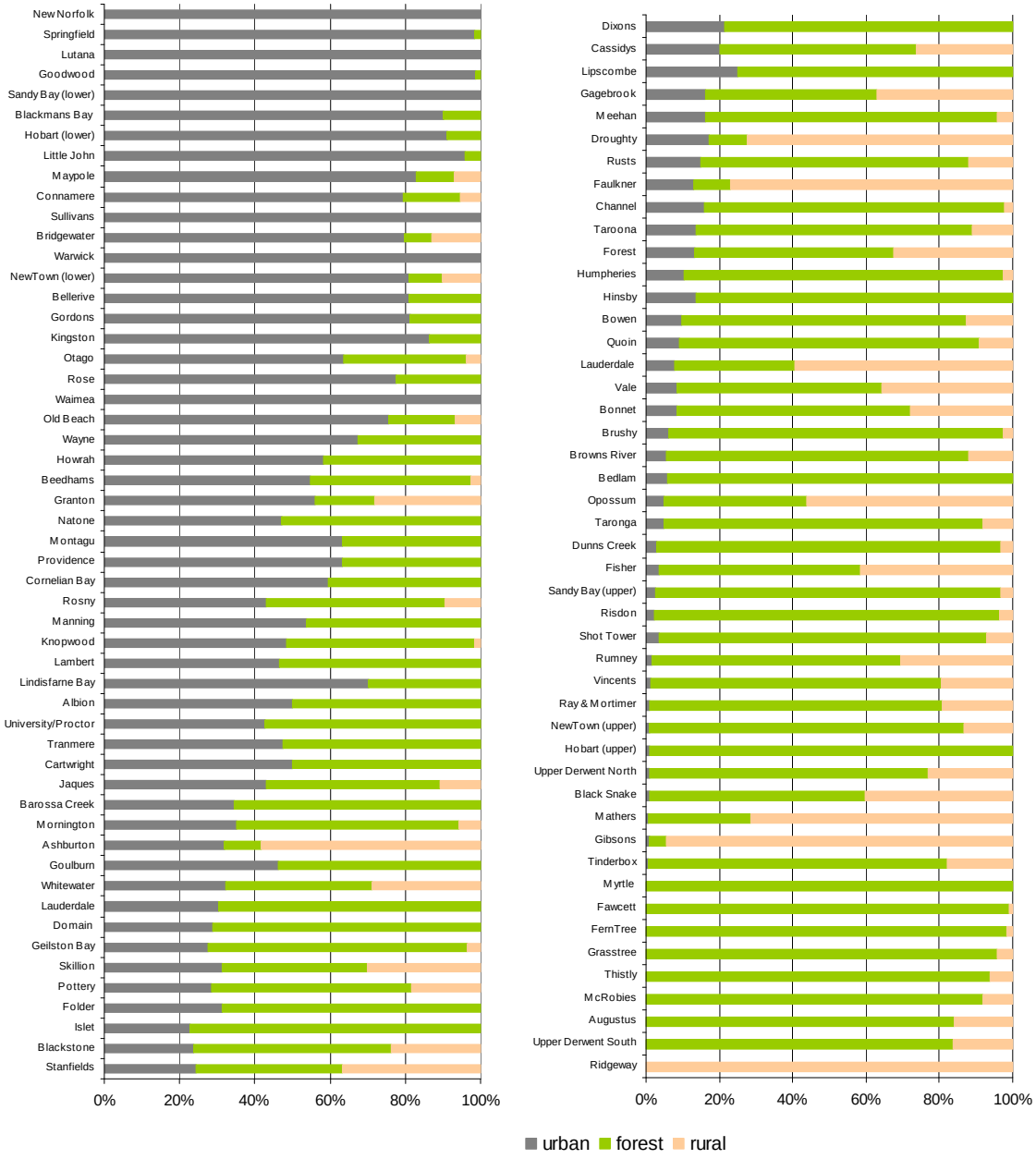

Figure 3-11 Stormwater catchment areas surrounding the Derwent Estuary showing designated proportions of rural, urban and forested catchment for the MUSIC model (source: Jason Whitehead et al., DEP).

Table 9 Catchment area multipliers and factors, used to partition N and P from MUSIC model between modelled substances.

	Humphreys	Rokeby	Browns	Urban western	Bridgewater	Lauderdale	Low urban	Rosny	Newtown	Sandy Bay	Hobart	North
No. of observations (TN)	15	3	5	5 (Sandy Bay)	3 (Rokeby)	3 (Rokeby)	3 (Rokeby)	10	22	5	15	15
DIN % NO3	100	100	100	100	100	100	95	92	86	65	65	65
DIN %NH3	0	0	0	0	0	0	5	8	14	35	35	35
DIN % of TN	23	23	45	36	23	23	23	34	39	36	36	36
DIP % of TP	18	30	18	18	18	20	18	18	29	18	18	18
TSS multiplier for DetPL_N	0.34	0.34	0.35	0.52	1	0.34	0.34	0.08	1	0.52	0.05	1
TN multiplier	0.8	1.1	0.32	1	1	1	1	0.53	0.1	0.61	0.14	1
TP multiplier	0.48	2.75	0.59	0.48	1	2.75	1	0.64	0.06	0.37	0.16	0.37
Multipliers above also used for these catchments	Faulkner Islet	Mather Droughty Gibson Rokeby Mortimer		Albion Bonnet Channel Cartwright Dixons Folder Hinsby Lipscombe Manning Shot Tower Taronga Taroona Waimea Wayne	Bridgewater Gagebrook Quoin Derwent north Derwent south New Norfolk	Lauderdale Stanfields	Bowen Old Beach Tinderbox Thistly Otago Opossum Bedlum Granton Cassidys Rusts Blacksnake Ashburton Blackstone	Risdon Mornington Vale Meehan Grasstree Geilston		Uni Sandy Bay Kingston Blackmans Bay Natone Lindisfarne Gordon Rose Montague Bellerive Howrah Knopwood Tranmere Skillion	Beedham Barossa	Little John Springfield Goodwood Sullivans Cornelian Connewarre Jacques

Table 10 Stormwater loads included in model (see

Appendix **10-3** for breakdown of individual loads for all stormwater catchments used).

Stormwater (tonnes/15 months)	**NO_3**	**NH_4**	**DIP**	**Labile Detrital Nitrogen**	**Dissolved Organic Nitrogen**
2003	55	4	7	161	2

Table 11 Some catchments were combined to form greater catchments for model runs (Jason Whitehead pers.com.)

Greater Hobart	**Greater Newtown**	**Greater Uni**	**Greater Risdon**	**Greater Rosny**	**Greater Rokeby**	**Greater Lauderdale**	**Greater Mortimer**
Hobart-low	Maypole	Lambert	Risdon	Rosny	Rokeby	Stanfields	Augustus
Hobart-up	Pottery	university/proctor	Vale	Mornington	Rumney	Lauderdale	Ray
Goulburn	Brushy	proctor	Meehan			lauderdale town	Mortimer
Warwick	NewTown Rivulet-up		Grasstree				Opossum
Providence	NewTown Rivulet-low						
Myrtle							
McRobies							

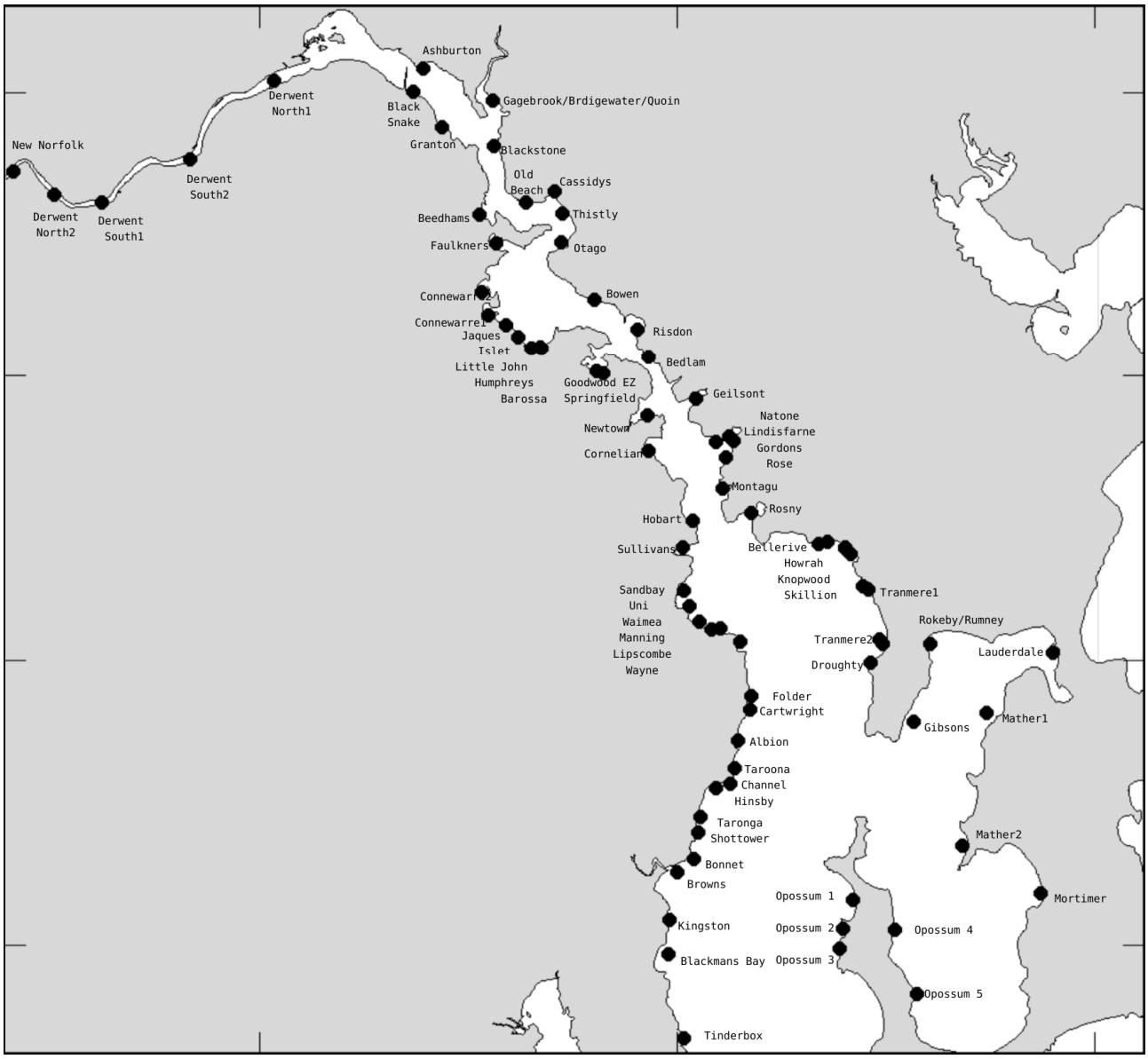

Figure 3-12 Stormwater and rivulet point sources used in the model. Entry points were placed at known stormwater drain and rivulet locations or with regard to the land contouring.

4. OBSERVATIONS

4.1 Pelagic

4.1.1 Water Quality

During 2003 the Derwent Estuary Program (DEP) collated monthly water quality surveys at 25 sites around the Derwent (Figure 4-1). Samples were taken from central river sites, 7 bays in inner Hobart and 3 sites from Ralphs Bay. Model and observed water column depths at the sites are shown in Table 12. There were some differences between the observed and modelled bathymetry of the estuary due primarily to averaging of water depth over each spatial grid cell. In some places, such as

U3, deep 'holes' in the estuary were not well represented by the model grid. In other places, small differences between observed and modelled depths are partially due to variation in tidal height during the surveys.

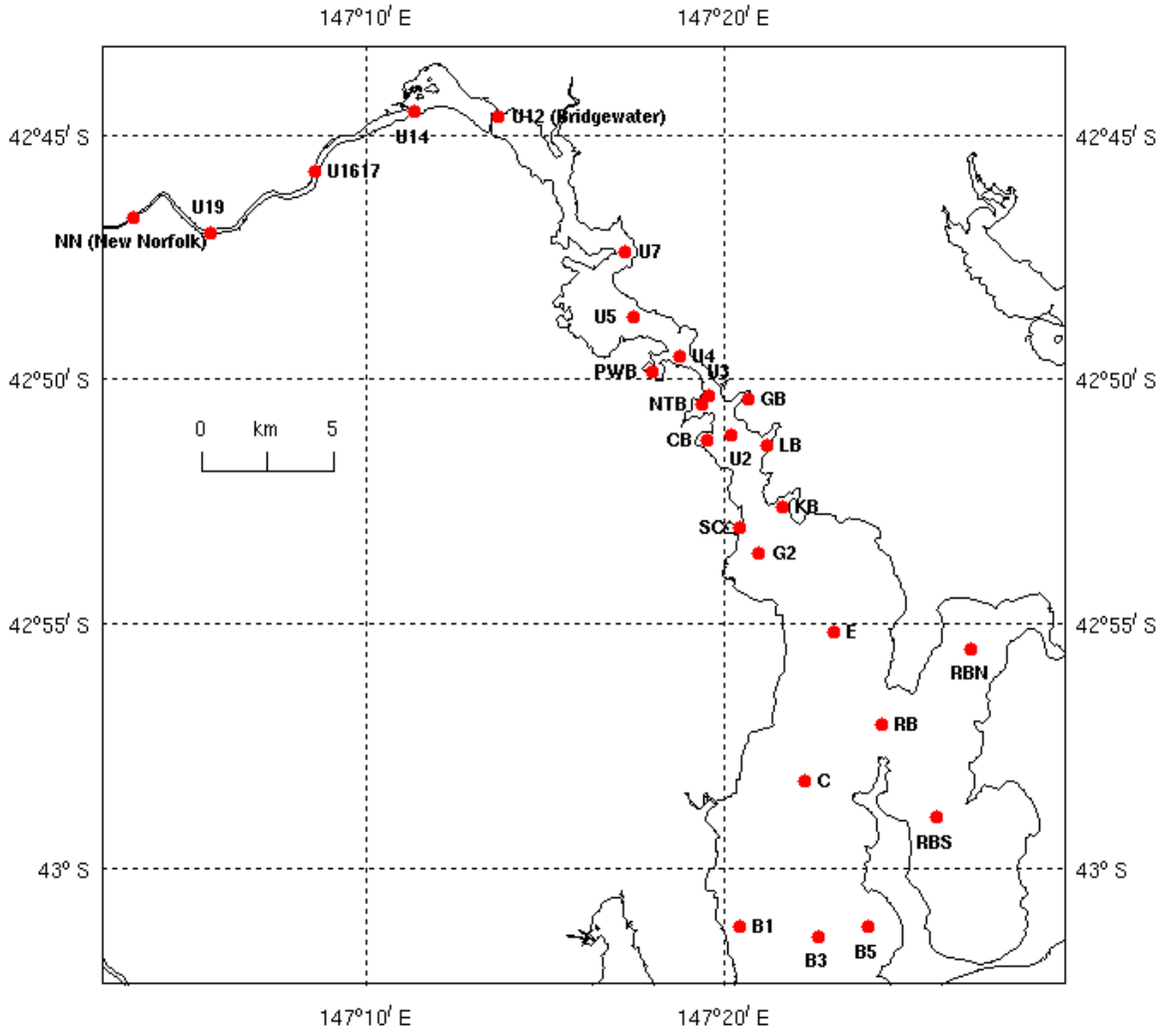

Figure 4-1 Map of Derwent Estuary from New Norfolk to Storm Bay showing sites where observations were taken.

At each site, surface and bottom water samples were analysed for temperature, salinity, dissolved oxygen (DO), dissolved organic carbon (DOC), turbidity, chlorophyll-*a*, total organic carbon (TOC) and total nitrogen, total phosphorus, total suspended solids (TSS), dissolved phosphate, ammonium, nitrate and nitrite. Other parameters were measured (e.g. zinc), but they are not included in this report as they were unresolved by the model

Norske Skog carried out extensive ambient monitoring in the upper estuary as part of their ecological risk assessment during 1999 and 2000 and in 2003 they monitored bi-monthly at 18 upper estuary sites (6 mid-river sites plus 2 cross-sections and fortnightly monitoring for DO, salinity, temperature and euphotic depth at 8 sites). The Norske Skog and DPIWE surveys have been coordinated around the same quarterly sampling dates since 1999. Both programs monitored the

Bridgewater causeway site (U12 Figure 4-1) to provide a comparative overlap and contribute results to the DEP database.

Table 12 Position of monitoring sites and water depth.

Site	Assigned region	Longitude	Latitude	Average water depth observed (m)	Water depth used in model grid (m)
NN	upper	147.0588	-42.7779	7	4.75
U19	upper	147.0950	-42.7832	8	5
U1617	upper	147.1431	-42.7623	6	4
U14	upper	147.1894	-42.7422	5	3.8
U12	upper	147.2283	-42.7438	6.5	5
U7	middle	147.2873	-42.7897	6	4.25
U5	middle	147.2905	-42.8122	2.5	3.75
U4	middle	147.3120	-42.8256	10	8.5
U3	middle	147.3255	-42.8391	25	5.75
U2	middle	147.3359	-42.8524	12	12
G2	middle	147.3492	-42.8927	20	19
E	outer	147.3838	-42.9194	24	23
C	outer	147.3700	-42.9701	26	26
B5	outer	147.4000	-43.0201	17	14
B3	outer	147.3767	-43.0235	18	23
B1	outer	147.3400	-43.0201	20	23
RB	outer	147.4058	-42.9514	20	19.5
RBS	outer bay	147.4317	-42.9828	2	2
RBN	outer bay	147.4473	-42.9252	6	4.75
SC	inner bay	147.3404	-42.8840	15	14
PWB	inner bay	147.2998	-42.8306	3	3
NTBO5	inner bay	147.3186	-42.8449	1.5	1.5
NTB13	inner bay	147.3230	-42.8426	5	4.25
NTB09	inner bay	147.3228	-42.8417	5	4
LB	inner bay	147.3525	-42.8560	8	6
KB	inner bay	147.3598	-42.8773	12	9
GB	inner bay	147.3439	-42.8400	3	5
CB	inner bay	147.3253	-42.8542	7	7

4.1.2 Phytoplankton

Despite housing Tasmania's capital city very little qualitative and quantitative data of phytoplankton species types or numbers are known in the Derwent. This is in contrast with the adjacent Huon Estuary which has more detailed information due to the presence of aquaculture and environmental requirements to register cell numbers and species types because of potential toxic algal blooms.

In the Derwent, broadly speaking the same pattern, of a spring diatom bloom and a late summer-autumn dinoflagellate bloom, occurs every year (Hallegraeff pers comm.). However, the timing of the diatom spring bloom can vary (Sept-Nov); *Gymnodinium catenatum* blooms occur according to the absence of wind conditions in autumn/late summer (i.e. not every year); the dominant species are *Ceratium, Dinophysis, Pseudo-nitzschia* and *Chaetoceros*, but the relative proportions of dinoflagellates compared with diatoms changes; and the influx of oceanic species into the Derwent varies. In recent years small episodic blooms of *Noctiluca* sp., often in side bays, have been a recurrent feature from late spring through to autumn.

4.1.3 Zooplankton

Few observations of zooplankton exist for the Derwent, although some data were collected by Nyan Taw in the early 1970's (Kerrie Swadling pers. comm.). We were unable to obtain any recent local data on zooplankton species or biomass to inform the model so these aspects of the model, whilst consistent with our understanding of the ecosystem, remain speculative. Zooplankton dynamics in the Derwent estuary are thought to be similar to the wider region of southeast Tasmania (Kerrie Swadling pers. comm.) with a cycle of abundance generally dominated by small inshore forms such as *Paracalanus indicus*, *Acartia tranteri* and *Gladioferens pectinatus*. There are occasional peaks of larger copepods such as *Sulcanus conflictus* and other plankton such as *Lucifer hanseni* and chaetognaths. Biomass is usually highest in December and January.

4.2 Macrophytes

The Derwent estuary contains about 159 km^2 of tidal flats (~ 1 km^2 vegetated in upper Derwent) and salt marshes, 2 km^2 of reef and 0.23 km^2 of seagrass. A comprehensive data set of maps from TAFI for 2001 (SEAMAP www.utas.edu.au/tafi/seamap) was used to ascertain the spatial extent of sea-grass, rocky reefs (i.e. substrate for macrophytes such as giant kelp) and macroalgae which also grow along the shoreline and in shallow inlets and bays through the region where favourable substrate exists.

Much of this data was difficult to reconcile with the model as it often described sub-gridscale features such as small areas of reef and seagrass beds. In addition the hydrodynamic model did not include wetting and drying of tidal flats so these regions could not be directly compared [recent advances in the model include the processes of wetting and drying of tidal flats, however realistic representation of these features requires a very high resolution model grid]. The maps provided by TAFI did not include quantitative information on macrophyte biomass and so it was impossible to correctly initialise and/or evaluate modelled macrophyte biomass or growth rate. Future mapping work in the Estuary might usefully quantify contrasting levels of seagrass, macroalgae and epiphytic algal biomass and some measurements of growth rates of the dominant species would be helpful.

5. BIOGEOCHEMICAL MODEL CALIBRATION

5.1 Model Validation Criteria

Model validation is achieved by evaluating the performance of a model against specific validation criteria (Rykiel, 1996). A model can only be declared 'fit for purpose' following successful validation; where validation is unsuccessful a model will require revision of parameters, and/or processes and/or concept design.

The purpose of the Derwent Estuary biogeochemical model is to reproduce the realistic seasonal dynamic cycling of carbon, nitrogen and phosphorus through dissolved and particulate organic and inorganic phases and the associated dynamics of dissolved oxygen. For this purpose 3 validation criteria are set:

The model must conserve mass of carbon, nitrogen, and phosphorus as it transforms and cycles material through various model substances; mass must also be conserved during advection and diffusion of tracers through the model domain and during sinking and resuspension of material between pelagic, benthic and epibenthic layers.

1. The model must reproduce the correct timing of the seasonal cycle in dissolved nutrients (nitrate, ammonium, dissolved inorganic phosphate), phytoplankton and dissolved oxygen compared with observations made at stations throughout the estuary over a year given the correct timing of the seasonal cycle of temperature, salinity and episodic flow events.
2. The model must simulate the correct magnitude of dissolved nutrients (nitrate, ammonium, dissolved inorganic phosphate), phytoplankton and dissolved oxygen compared with observations made at stations throughout the estuary over a year given the correct magnitude of the seasonal cycle of temperature, salinity and episodic flow events.

When comparing model results with observations it is important to remember that 1 model grid cell corresponds to many thousands of litres of water, whilst 1 sample taken for chemical analysis typically consists of <1 L of water. In regions of strong spatial gradients, such as river or rivulet plumes, small-scale patchiness may confound comparison of observations with model output. Conversely the high quantitative precision achieved by the model may exceed that achieved by sampling and analytical techniques.

5.2 Hydrodynamic and Sediment Model Calibration

The hydrodynamic and sediment models developed by Herzfeld et al., (2005a) and Margvelashvili (2005) respectively, were calibrated against time series of moored instrument observations collected in 2003. For the purposes of the biogeochemical model calibration the hydrodynamic and sediment models achieved all 3 validation criteria. Both models conserve mass during advection, diffusion, sinking and resuspension processes. The hydrodynamic model reproduces the timing and magnitude of the seasonal cycle in temperature and salinity and a number of high and low river flow events. The sediment model provides an accurate representation of sediment dynamics in the estuary, compared with observations, including the timing and magnitude of elevated suspended sediment events. Further details of the model calibration procedures can be found in Herzfeld et al. (2005a) and Margvelashvili (2005).

The hydrodynamic model and sediment model may be considered as ‘fit for purpose’ for coupling with the biogeochemical model to simulate the seasonal biogeochemical dynamics in the Derwent estuary.

5.3 Conservation of Mass in the Biogeochemical Model

The biogeochemical model code is processed in columns equating to the model grid. At the start of each time step total mass of carbon, nitrogen and phosphorus in the water column, epibenthos and sediment across all biogeochemical model tracers is summed. Computations then proceed for the uptake and transformation of substances within the biogeochemical model. At the end of the biogeochemical model time step the mass of all tracers is summed and checked against the initial value. Should a difference occur the model stops and the offending algorithm must be corrected in order to proceed.

In early simulations the biogeochemical model occasionally failed to conserve mass associated with the labile POC and DOC point source inputs from Norske Skog. Small numerical errors were identified in the code and rectified. Subsequent model runs achieved full conservation of mass for all carbon, nitrogen and phosphorus in the biogeochemical model and also during advection, diffusion, sinking and resuspension in the hydrodynamic and sediment model code.

5.4 Nutrient Calibration (Nitrogen and Phosphorus)

Summary plots of the model results for nutrients (N and P) compared with the observations can be seen in Figure 5-1 - Figure 5-3 and individual plots for all the stations and depths can be seen in **Appendix 10-6 - Appendix 10-12**. The summary plots show the stations grouped into upper reaches, middle reaches, outer reaches and bays and inner bays (Figure 5-1; see also Table 12). Median, minimum and maximum concentrations are shown for an ensemble of model grid cells and depth layers corresponding to the sampling site locations and depths.

The model median for DIN generally falls within the observational median. All sites show seasonal DIN with high levels in winter and low values over summer for both surface and bottom waters. Greatest DIN concentrations are found in bottom waters in the middle reaches of the estuary throughout the year and in surface waters of the inner bays from March through to November. There is very close agreement between model and observations. Occasional large spikes in modelled DIN are primarily due to stormwater inputs after heavy rainfall and thus show the impact of such events on the estuary's biogeochemistry. The higher levels of variance in the inner bays is primarily due to the shallow water and effect of the tidal flushing of the estuary but also due to the high levels of introduced nutrients in some of the bays (Prince of Wales and New Town bays in particular) which may not have been accurately resolved in the point source input file (see specific plots in **Appendix 10-6** to **Appendix 10-9**).

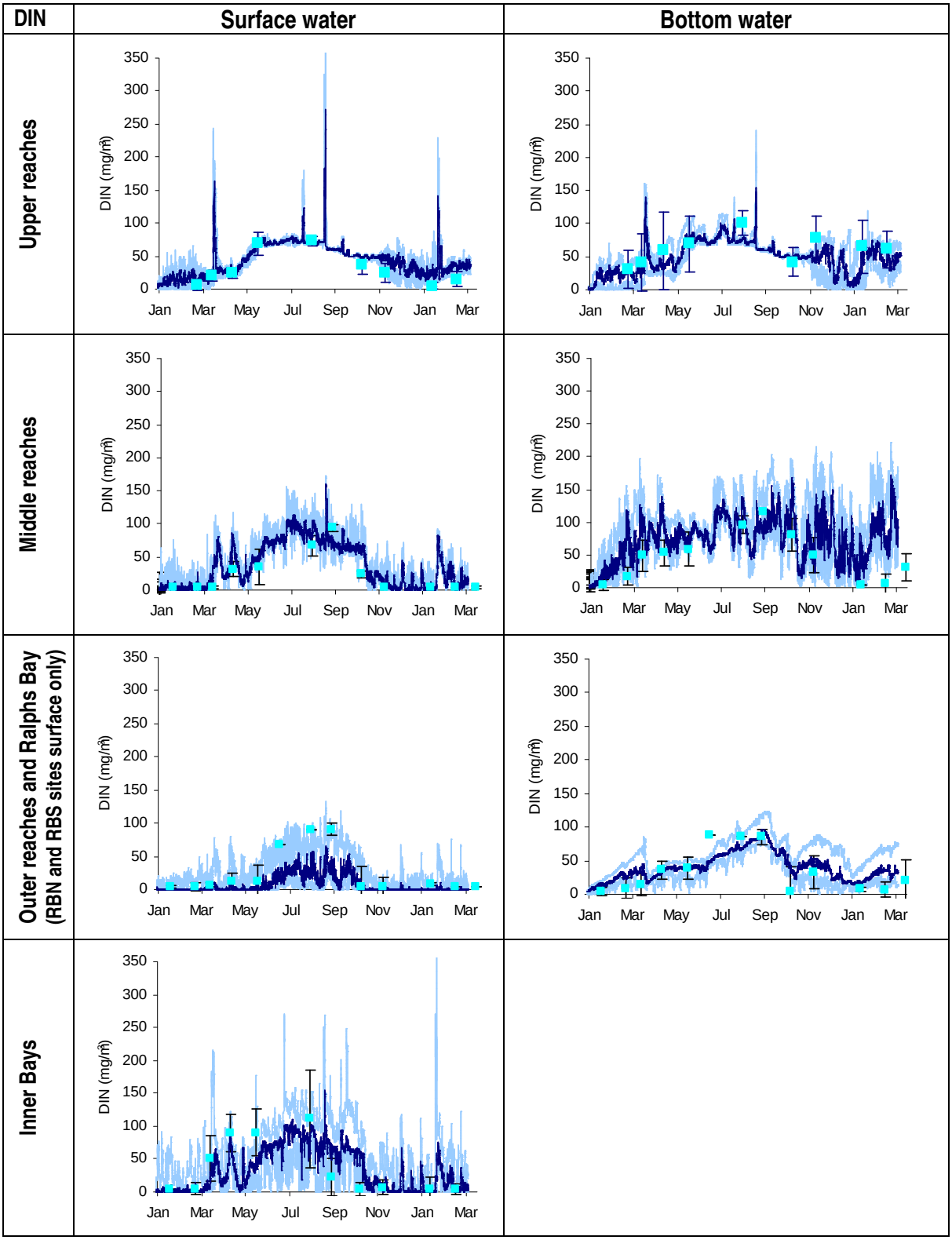

Figure 5-1 Dissolved Inorganic Nitrogen (DIN) concentrations in Derwent Estuary surface and bottom waters (n= no of sites used). Upper (n=5), middle (n=5), outer reaches and outer bays (n=9), inner bays (n=8). Blue squares are observations with error bars of 1 standard deviation [in the outer reaches DIN observations for June and July n=1]; dark blue line is model median and light blue lines show model range.

Nitrate contributes the largest portion of nitrogen to DIN in the estuary (Figure 5-2). Model results show a strong seasonal winter - summer cycle and correlate well with observed concentrations for all sub-regions of the estuary (Figure 5-2), although in surface water of the outer reaches and Ralphs Bay, sparse winter observations exceeded the modelled median concentration. The highest concentrations of nitrate are found in bottom waters of the middle reaches of the estuary. In surface waters nitrate concentrations are depleted first in the outer reaches (October) then the inner bays (late October) and middle reaches (late November). In the upper reaches low concentrations of nitrate remain in surface waters throughout the summer, likely due to point source and river nutrient supply exceeding assimilation by phytoplankton and macrophytes in this part of the estuary due to high attenuation and light limitation of autotroph growth. Summer depletion of nitrate in surface waters in the inner bays and middle reaches of the estuary (and less so in the outer reaches) is alleviated by episodic injection of nitrate, possibly associated with the springs – neaps tidal cycle, augmented by point source loads to the estuary. In late January 2004 a peak in nitrate concentration propagates through surface waters of the estuary due to a flood event.

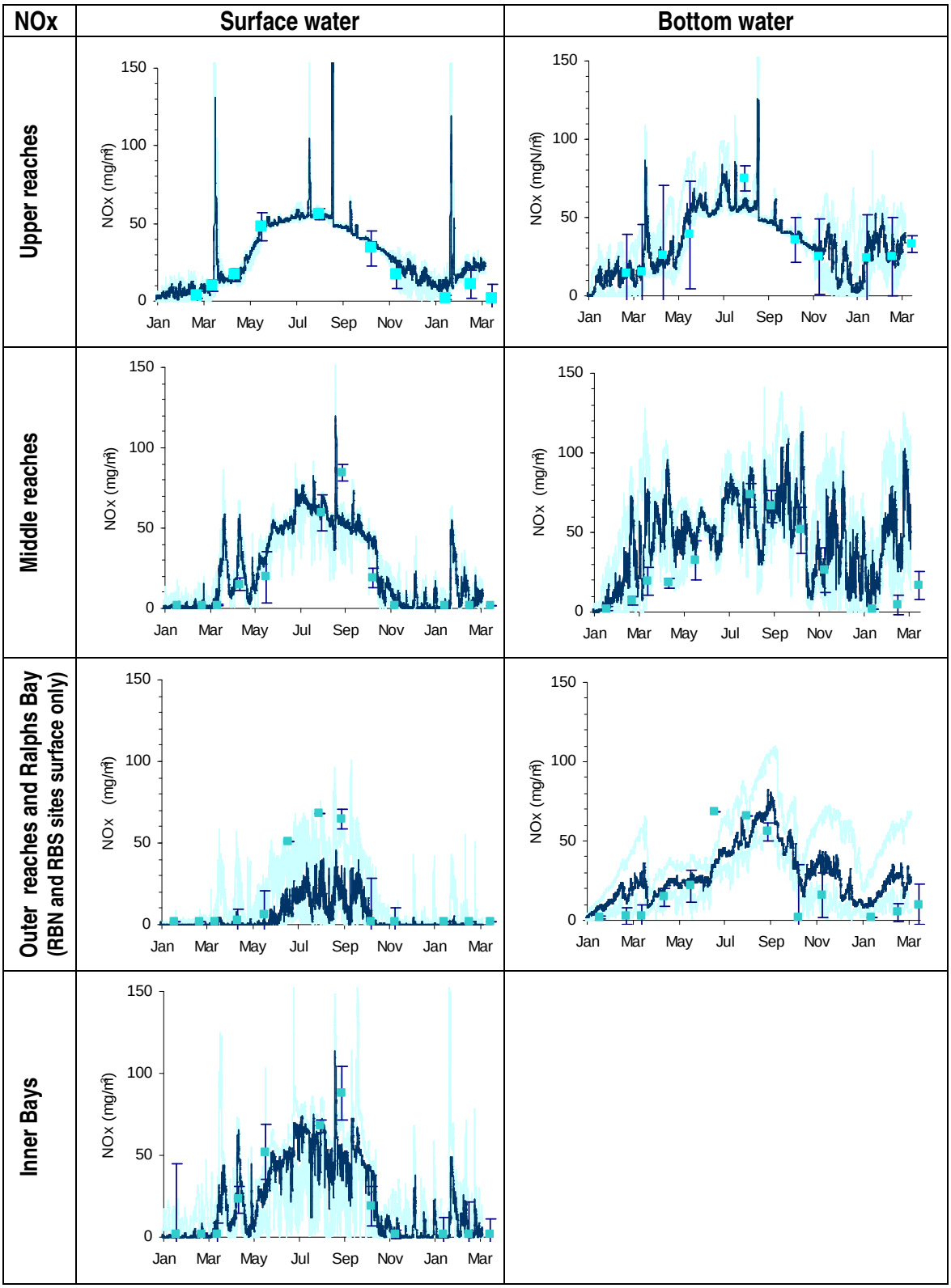

Figure 5-2 Nitrate concentrations in Derwent Estuary surface and bottom waters (n= no of sites used). Upper (n=5), middle (n=5), outer reaches and outer bays (n=9) inner bays (n=8).). Blue squares are observations with error bars of 1 standard deviation [in the outer reaches NOx observations for June and July n=1]; dark blue line is model median and light blue lines show model range.

Observations and model results for surface and bottom ammonia generally agreed for all sites (Figure 5-3). Observations in bottom water at stations U19 and U16/17 in the upper reaches, were consistently higher than the model possibly due to accumulation of ammonia in deep 'holes' which were unresolved in the modelled bathymetry. Bottom waters of the middle reaches contained the highest concentrations although surface concentrations in the inner bays were also high and extremely variable likely due to variability in point source loads. Although ammonia had very good correlation with observations for most of the inner bays an exception was Prince of Wales Bay (PWB) where observed levels were more than double model results possibly due to underestimation of point source load, an overestimation of local denitrification or sampling of sub grid-scale gradients in concentration (**Appendix 10-8**). In the middle reaches of the estuary, from sites U3 to U7 in surface waters (**Appendix 10-8**), modelled ammonia concentrations in winter were ~1 μM higher than observations, possibly due to excessive attenuation in the model limiting phytoplankton uptake or poor resolution of point source loads in this part of the estuary.

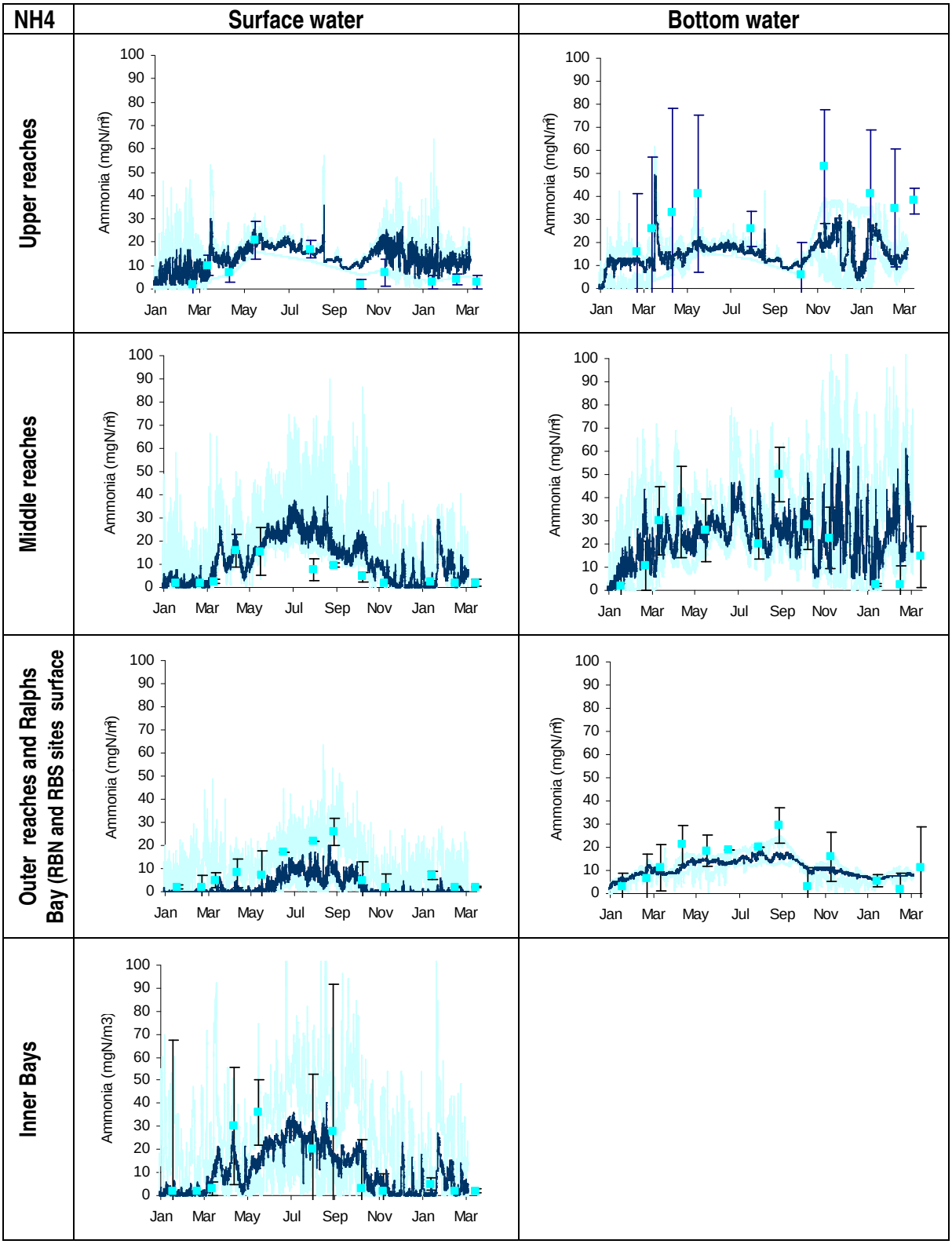

Figure 5-3 Ammonia concentrations in Derwent Estuary surface and bottom waters (n= no of sites used). Upper (n=5), middle (n=5), outer reaches and outer bays (n=9), inner bays (n=8). Blue squares are observations with error bars of 1 standard deviation [in the outer reaches NH_4 observations for June and July n=1]; dark blue line is model median and light blue lines show model range.

Observed phosphate concentrations were reasonably well simulated by the model (Figure 5-4) although in the upper estuary modelled surface concentrations were a little higher and bottom water concentrations, a little lower than observed in autumn. As the modelled upper estuary has fairly course grid resolution relative to its complex channel bathymetry there is more uncertainty in the modelled hydrodynamics in this part of the estuary. In the middle reaches observations showed a drawdown of surface phosphate in summer and also spring 2003 that was not captured by the model. In other parts of the estuary there was little seasonality in concentration and no evidence of summer drawdown in concentration which might limit phytoplankton or macrophyte growth. Concentrations were consistently highest in the bottom water of the middle reaches. In the outer reaches and Ralphs Bay modelled bottom water phosphate was lower than observed at stations E and RB possibly due to underestimation of marine flux into the model domain. In the upper reaches occasional spikes in concentration correspond to heavy rainfall events.

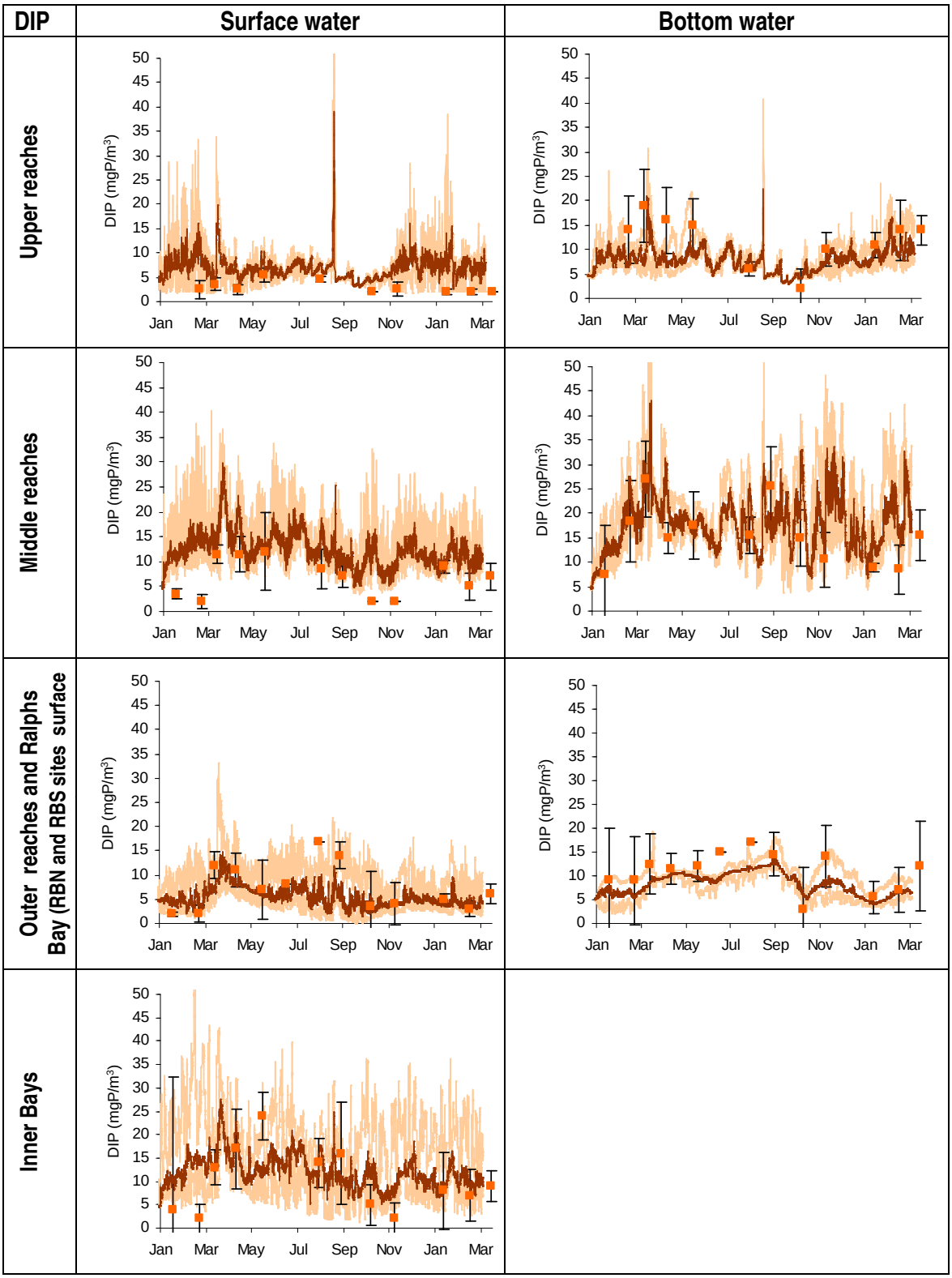

Figure 5-4 Dissolved Inorganic Phosphate concentrations in Derwent Estuary surface and bottom waters (n= no of sites used). Upper (n=5), middle (n=5), outer reaches and outer bays (n=9), inner bays (n=8). Orange squares are observations with error bars of 1 standard deviation [in the outer reaches DIP observations for June and July n=1]; dark brown line is model median and light brown lines show model range.

5.5 Chlorophyll, Dissolved Oxygen and DOC Calibration

The model reproduces the general features of the observed seasonal cycle in chlorophyll throughout the estuary (Figure 5-5; **Appendix 10-12**). The model describes distinct autumn and spring elevations in chlorophyll concentration within the estuary and inner bays, although the amplitude of this seasonal cycle is much smaller in the outer reaches and Ralphs Bay and confounded by variability. Highest concentrations of chlorophyll were simulated in the middle reaches and inner bays and the observed timing and amplitude of the spring bloom was well captured by the model.

In the upper reaches simulated chlorophyll concentrations exceeded observed values in autumn, possibly due to underestimation of attenuating substances in the water column and propagation of excess light facilitating phytoplankton growth. In the middle reaches and inner bays the modelled autumn bloom persisted longer than observed possibly due to under representation of zooplankton growth and grazing in the model [no zooplankton data exists for the time period of the simulation to confirm their dynamics].

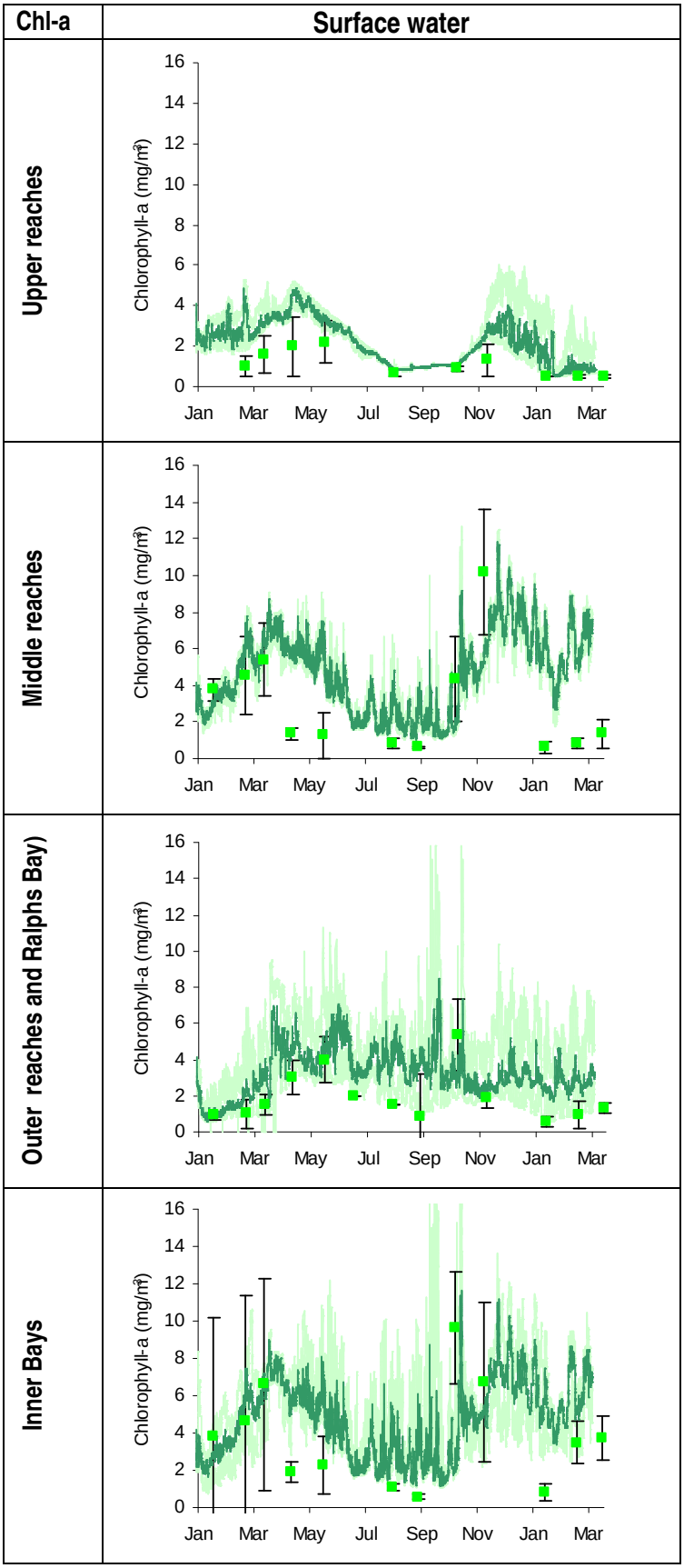

Figure 5-5 Chlorophyll concentrations in Derwent Estuary surface waters (n= no of sites used). Upper (n=5), middle (n=5), outer reaches and outer bays (n=9), inner bays (n=8). Green squares are observations with error bars of 1 standard deviation [in the outer reaches chlorophyll observations for June and July n=1]; dark green line is model median and light green lines show model range.

Modelled chlorophyll comprises pigment from large and small phytoplankton, dinoflagellate and microphytobenthos populations. Although the absence of species composition data for the Derwent estuary precludes comprehensive validation of this aspect of the model, the simulated succession of species is consistent with our broad understanding of estuarine phytoplankton dynamics. The model simulated relatively constant levels of small phytoplankton biomass throughout the year; large phytoplankton (representing a diatom-dominated population) were elevated in spring and dinoflagellate biomass increased in summer and autumn. A more detailed description of the species succession is included in Section 6.4

The model reproduced the observed drawdown in % saturation of dissolved oxygen in bottom waters well for the lower reaches of the estuary and Ralphs Bay (Figure 5-6). Modelled concentrations in the middle reaches and inner bays were consistently higher than observed by 20 - 30% (Appendix 10-13). On closer examination of the data, observed surface concentrations at these stations were unusually low with year round values of 70 – 80% (cf. typical 100% saturation). This suggested a possible offset in the dissolved oxygen sensor for both surface and bottom water dissolved oxygen readings for stations in the middle reaches and inner bays of the estuary [these stations correspond to those routinely sampled by the Nyrstar field work team]. In the absence of calibration samples (by Winkler titration or similar) it is impossible to confirm these unusual observations. In the upper reaches of the estuary, sparse data in 2003 precluded rigorous comparison of model and observations.

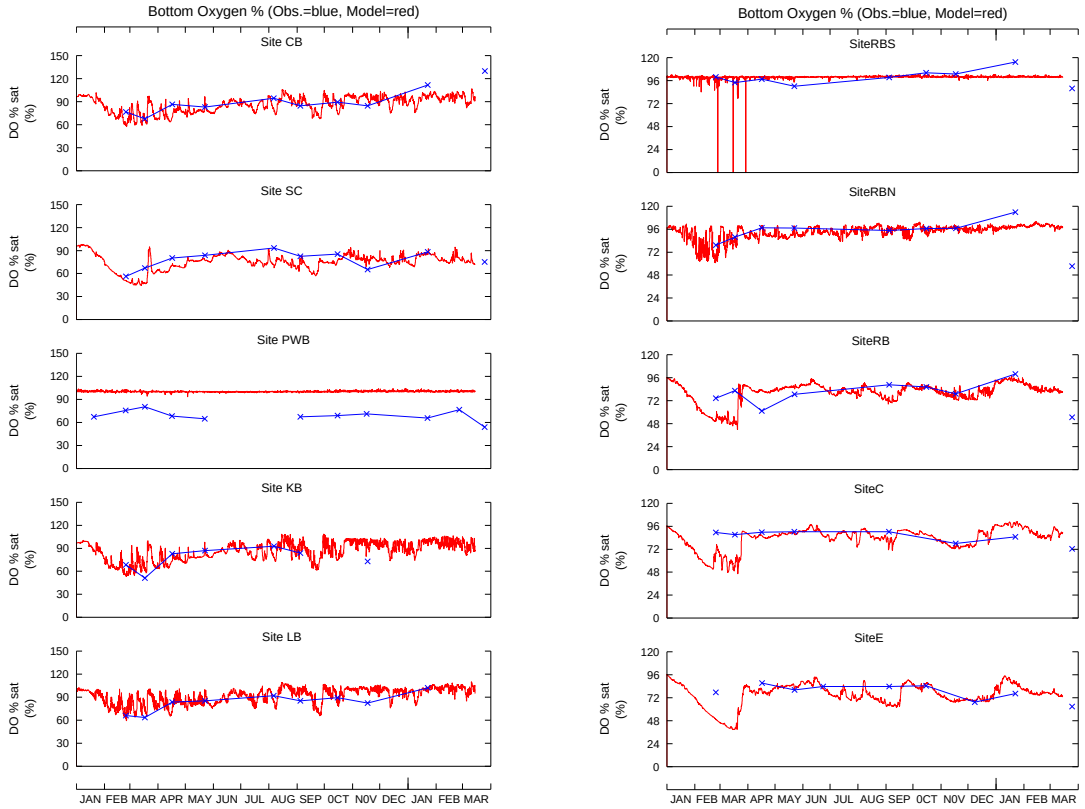

Figure 5-6 Modelled (red) and observed (blue) bottom water dissolved oxygen saturation at stations in the outer reaches, Ralphs Bay and some side bays [CB – Cornelian bay; SC – Sullivans Cove; PWB – Prince of Wales Bay; KB – Kangaroo Bay; LB – Lindisfarne bay; RB N/S – Ralphs Bay north/south; C/E DEP sites C/E].

Observed and simulated dissolved organic carbon agreed well for most sites in the estuary (Figure 5-7; **Appendix 10-14 - Appendix 10-15**). In general there was a steady decline in DOC concentration over the period of simulation. In the upper reaches, a peak in DOC concentration in May propagated

downstream more efficiently in the model than observed. This resulted in over-estimation of DOC concentration at a number of modelled sites throughout the estuary likely due to under representation of winter time bacterial uptake and remineralisation rates.

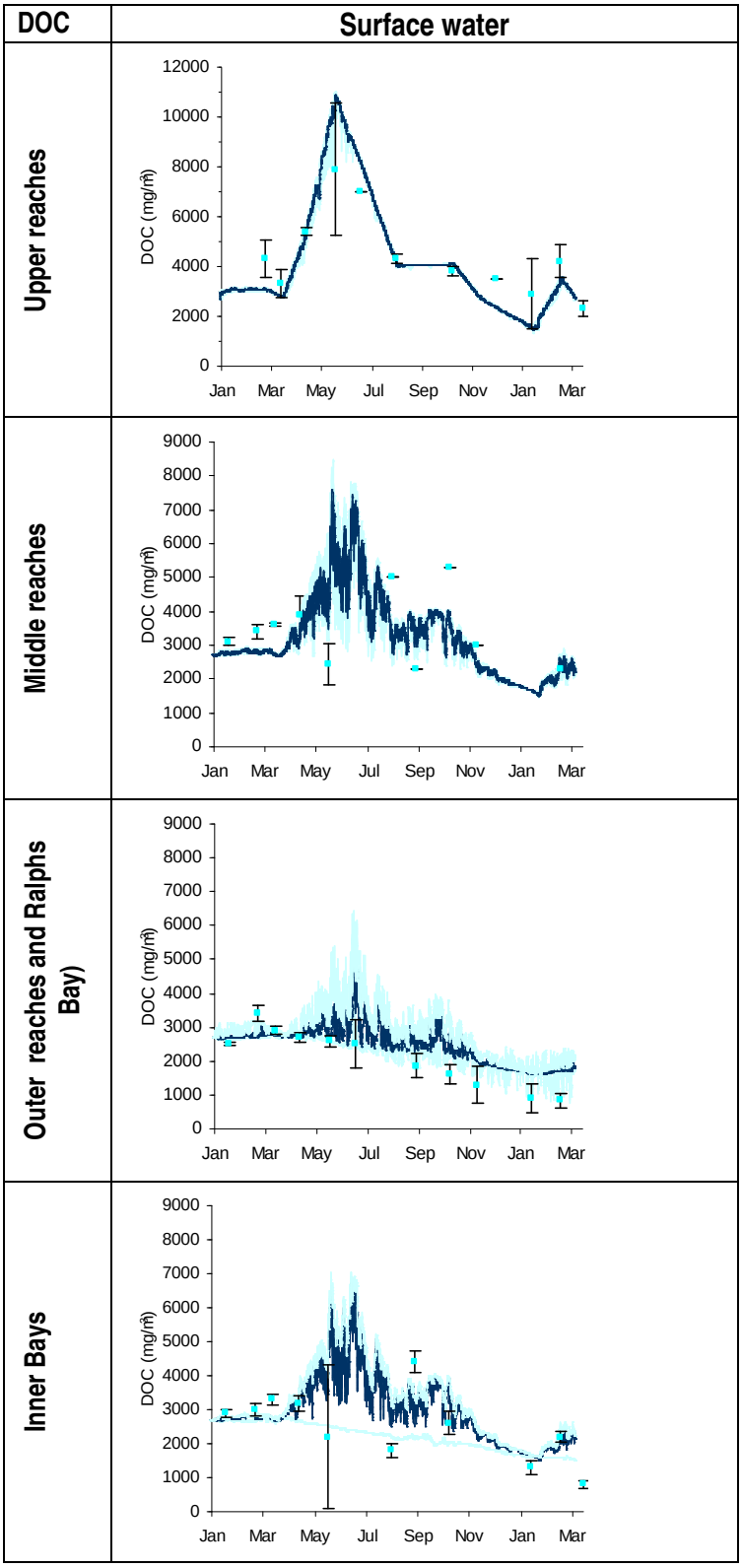

Figure 5-7 DOC concentrations in Derwent Estuary surface waters (n= no of sites used). Upper (n=5) middle (n=5) outer reaches and outer bays (n=9) inner bays (n=8). Blue squares are median observations with error bars of 1 standard deviation [in the Middle and Upper reaches DOC observations for Aug 03 – Mar 04 and Jul – Dec, respectively, n=1] ; dark blue line is model median and light blue lines show model range.

5.6 Calibration Summary

The Derwent estuary biogeochemical model fulfilled all 3 validation criteria:

1. The model conserved mass including carbon, nitrogen and phosphorus through all biogeochemical transformations and during physical advection and diffusion, and sinking and resuspension between pelagic, epi-benthic and sediment layers.

2. The model reproduced the correct timing of seasonal fluctuations and episodic events in observed dissolved nitrate, ammonium, dissolved inorganic phosphate, phytoplankton, dissolved organic carbon and dissolved oxygen made at stations throughout the estuary in 2003-4.

3. The model simulated the correct magnitude of dissolved nutrients (nitrate, ammonium, dissolved inorganic phosphate), phytoplankton and dissolved oxygen compared with observations made at stations throughout the estuary in 2003-4.

In summary, the general biogeochemical dynamics of the estuary including nutrient [nitrate, ammonium, phosphate], chlorophyll, dissolved oxygen and dissolved organic carbon concentrations, are well captured by the model and its parameter values. Embayments and the middle reaches of the estuary, which have a high surrounding urban density, had elevated levels of nutrients and chlorophyll compared to the upper reaches and the outer marine sites and bays (including Ralphs Bay) and this was reflected in the model. Prince of Wales and Newtown bays had sporadic but high levels of nutrient and algal blooms which were not always completely captured by the model, likely due to sub-grid scale gradients within these bays and/or sub-optimal resolution of local point source loads from industry, STPs and stormwater. In the upper estuary the model grid was coarse relative to the complex channel bathymetry precluding full resolution of the estuarine dynamics, however model results were generally consistent with the observations, except in the proximity of unresolved deep ‘holes’ in the bathymetry.

In some parts of the estuary model results show high frequency fluctuations which mostly result from tidal advection of gradients past the observation site. In the absence of high frequency observations these features should be treated with caution, however they may be considered indicative of natural variability at each site which is not resolved by a monthly sampling program.

There were insufficient observations to fully validate model simulations of phytoplankton group composition, zooplankton biomass and group composition, macrophyte biomass and sediment biogeochemistry. Whilst results from these elements of the model appear realistic and are consistent with our understanding of the system they should be treated with caution [results for these components are presented with more detail in the following section].

6. MODELLED BIOGEOCHEMISTRY OF THE DERWENT ESTUARY

Monthly mean concentrations of salinity, nutrients, chlorophyll and dissolved oxygen are given in the following sections. For nutrients and chlorophyll, spatial distributions are shown for near-surface concentrations to represent concentrations in the more biologically active euphotic zone. The near-surface layer is computed as the mean concentration in the top 11 m of the water column or less where the bathymetry is shallower (Figure 6-1). This may result in aliasing in depth mean concentrations in shallow water proportional to the water depth. Plots should therefore be interpreted with consideration of the regional bathymetry.

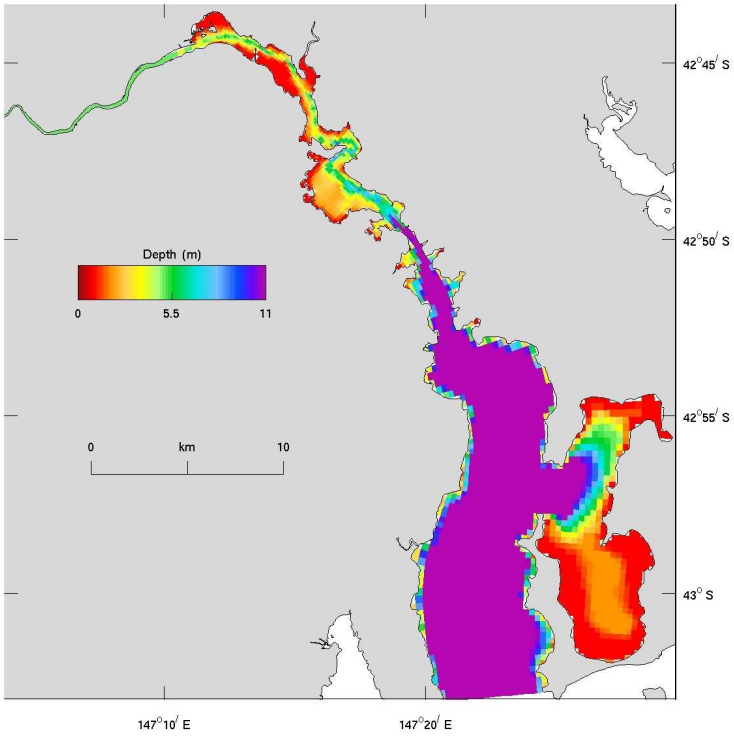

Figure 6-1 Derwent estuary bathymetry detailing area <11 m deep.

Monthly mean cross-section plots are shown for transect along the axis of the estuary from New Norfolk (left) to Iron Pot (right). The approximate location of sampling stations along the transect is shown in Figure 6-2.

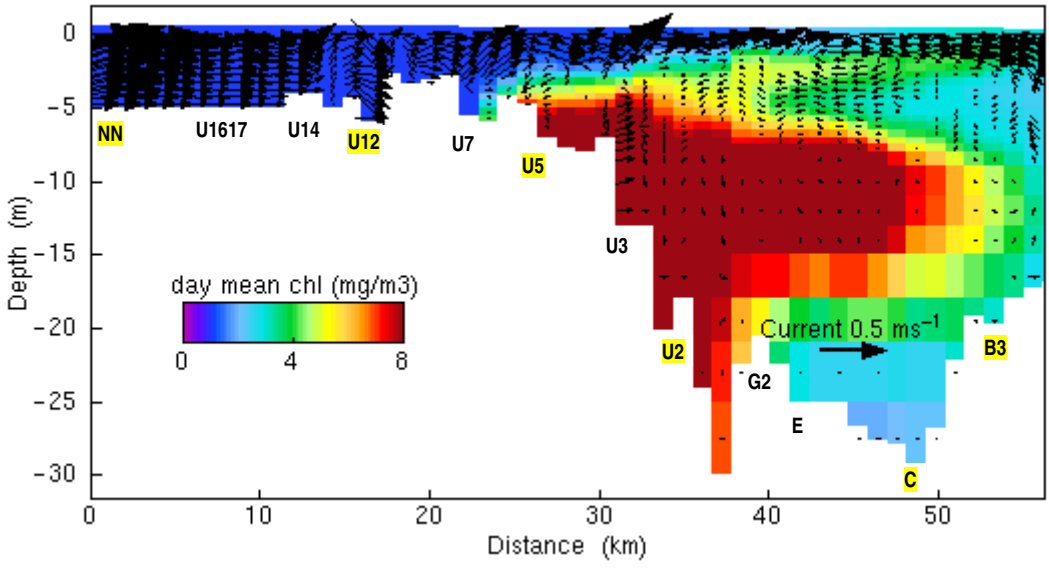

Figure 6-2 Approximate location of sampling sites along a cross section along the axis of the estuary from New Norfolk (NN) to Iron Pot [U12 is Bridgewater Bridge, U5 is southern end of Elwick Bay above Bowen Bridge, U2 is north of Tasman Bridge, C is across from Hinsby Beach, B3 is across from Half Moon Bay]. Contours show a snapshot of daily mean chlorophyll concentration and circulation.

6.1 Salinity

The Derwent estuary has a persistent salt wedge structure with fresher water originating from the catchment overlying more salty marine water. During the model simulation the intrusion of salt water was greatest in January 2003 with the influence of fresh water increasing through the year until October. In September and October monthly mean salinities of <20 PSU were found in surface waters of Ralphs Bay and along the eastern side of the lower estuary (Figure 6-3).

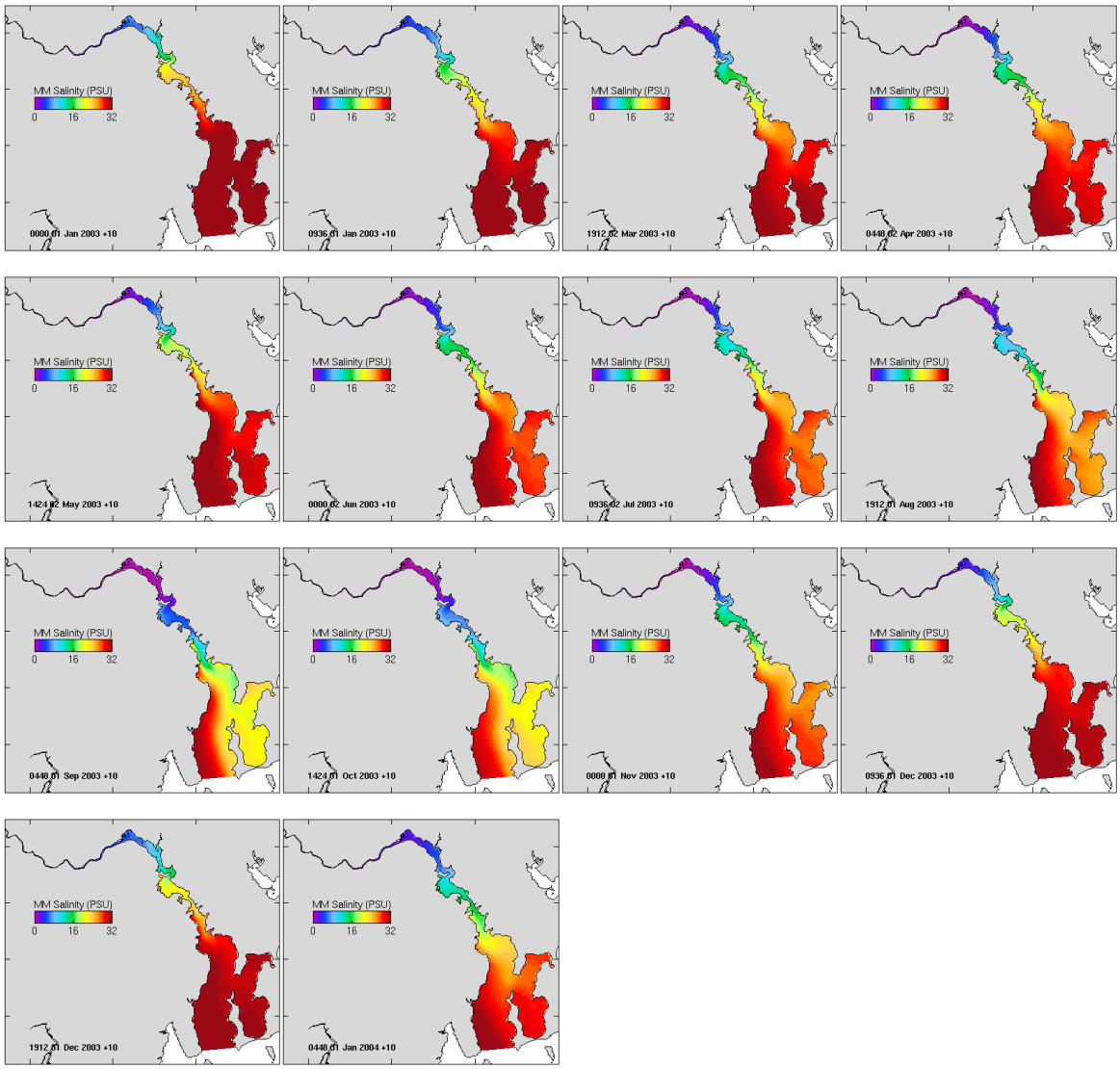

Figure 6-3 Monthly mean surface salinity from 1 Jan 2003 – 31 Jan 2004.

Cross sections along the axis of the estuary illustrate the consistency of the salt wedge structure with surface waters of the upper estuary remaining fresh and bottom waters of the lower reaches remaining fully marine for the whole year (Figure 6-4). Whilst the surface signature of salinity varies in spatial extent throughout the estuary, the intersection of the front with the bed remains fairly consistently located at site U7 (Figure 6-2). In summer months, when river flow is seasonally lowest, salty bottom water propagates up the estuary to New Norfolk.

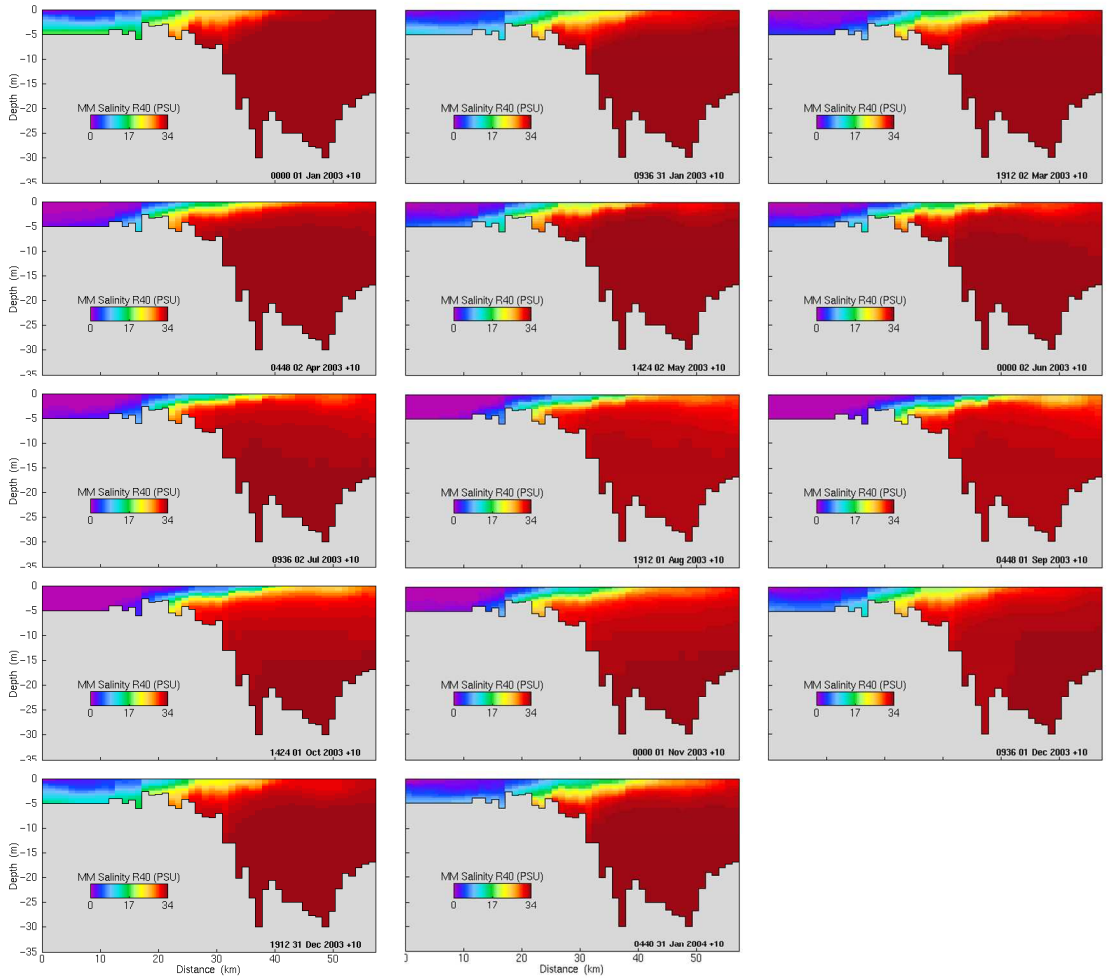

Figure 6-4 Monthly mean salinity cross-section along the axis of the estuary from New Norfolk to Iron Pot from 1 Jan 2003 – 31 Jan 2004.

6.2 Water Quality

6.2.1 Nitrogen

Near-surface monthly mean concentrations of DIN (Figure 6-5) show low concentrations of DIN in the summer and autumn months particularly in the upper reaches, the outer reaches and outer bays. The middle reaches are generally high in DIN throughout the year particularly between sites U2 and U5. There is a higher concentration of nutrients (half moon shape) at the entrance of Ralphs Bay for much of the year showing the effect of bathymetry and the associated currents in this area during 2003.

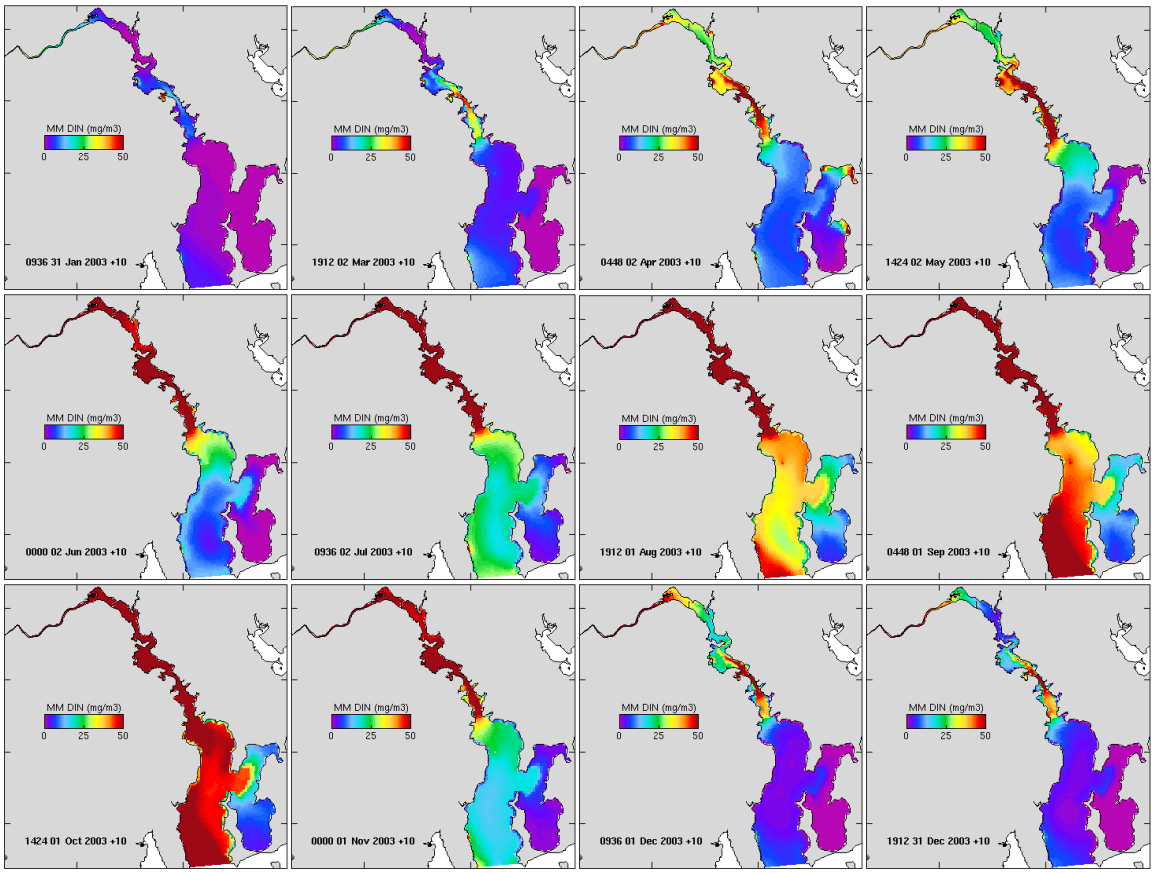

Figure 6-5 Monthly mean near-surface (0-11m) concentration of DIN from 31 Jan 2003 – 31 Jan 2004.

Monthly mean cross-sections of nitrate and ammonia along the axis of the estuary (Figure 6-6 and Figure 6-7) show a seasonal cycle in surface concentration. Over winter nitrogen concentrations increase in the upper estuary due to higher river, anthropogenic point source and storm water loads, and in the outer reaches by marine influx. In other seasons surface marine influx is small whilst river and point source loads in the mid estuary maintain elevated surface DIN. In spring through autumn surface nutrient concentrations are depleted throughout much of the estuary by autotroph assimilation except in the upper and mid estuary. In the upper estuary surface nutrients persist because high attenuation limits local phytoplankton growth; in the mid estuary surface nutrient supply typically exceeds autotroph uptake.

In deeper water there is persistent elevation of nitrogen concentrations in the mid-estuary. Nitrogen appears to accumulate and be retained in this part of the estuary most likely due to the combination of estuarine re-circulation of point source loads and detrital remineralisation. In the mid-estuary outcropping of deep nutrients into surface waters appears to coincide with the location of the salt wedge front and could result from an increase in vertical velocity associated with the interaction of currents with the bathymetry and the halocline.

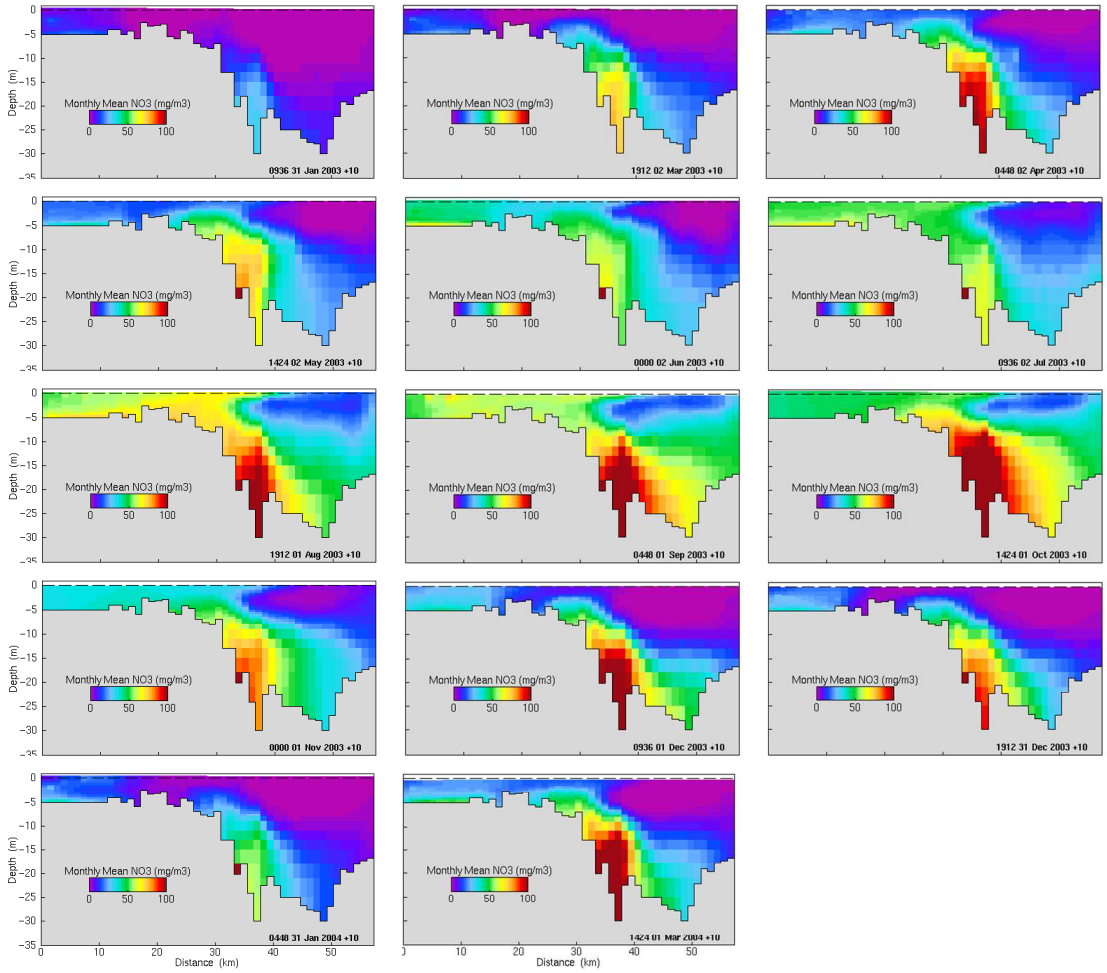

Figure 6-6 Cross section of monthly mean concentrations of nitrate along the axis of the estuary (from New Norfolk to Iron Pot).

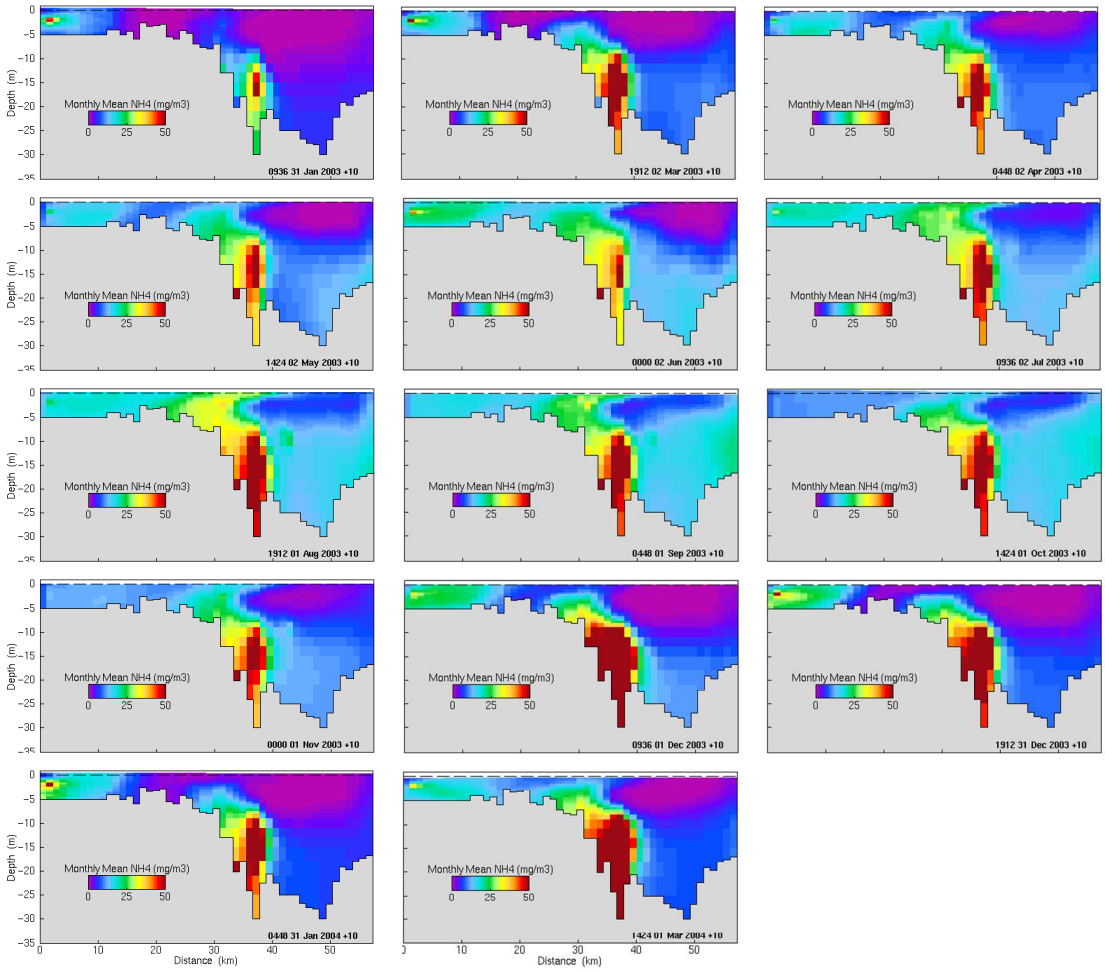

Figure 6-7 Cross section of monthly mean concentrations of ammonia along the axis of the estuary (from New Norfolk to Iron Pot).

6.2.2 Phosphorus

Near-surface monthly mean concentrations of DIP (Figure 6-8) show high levels of DIP in the middle reaches of the estuary throughout the year and the relatively low concentrations of DIP in other regions of the estuary. Gradients in DIP concentration adjacent to the shore are due primarily to STP and stormwater inputs throughout the year. There is a general increase in DIP concentration throughout the estuary in autumn and winter and a decline in concentration in spring and summer associated with phytoplankton assimilation. In comparison with nitrogen, phosphorus concentrations remain in excess of Redfield ratio (16N:1P) and are therefore not thought to limit primary production in the estuary.

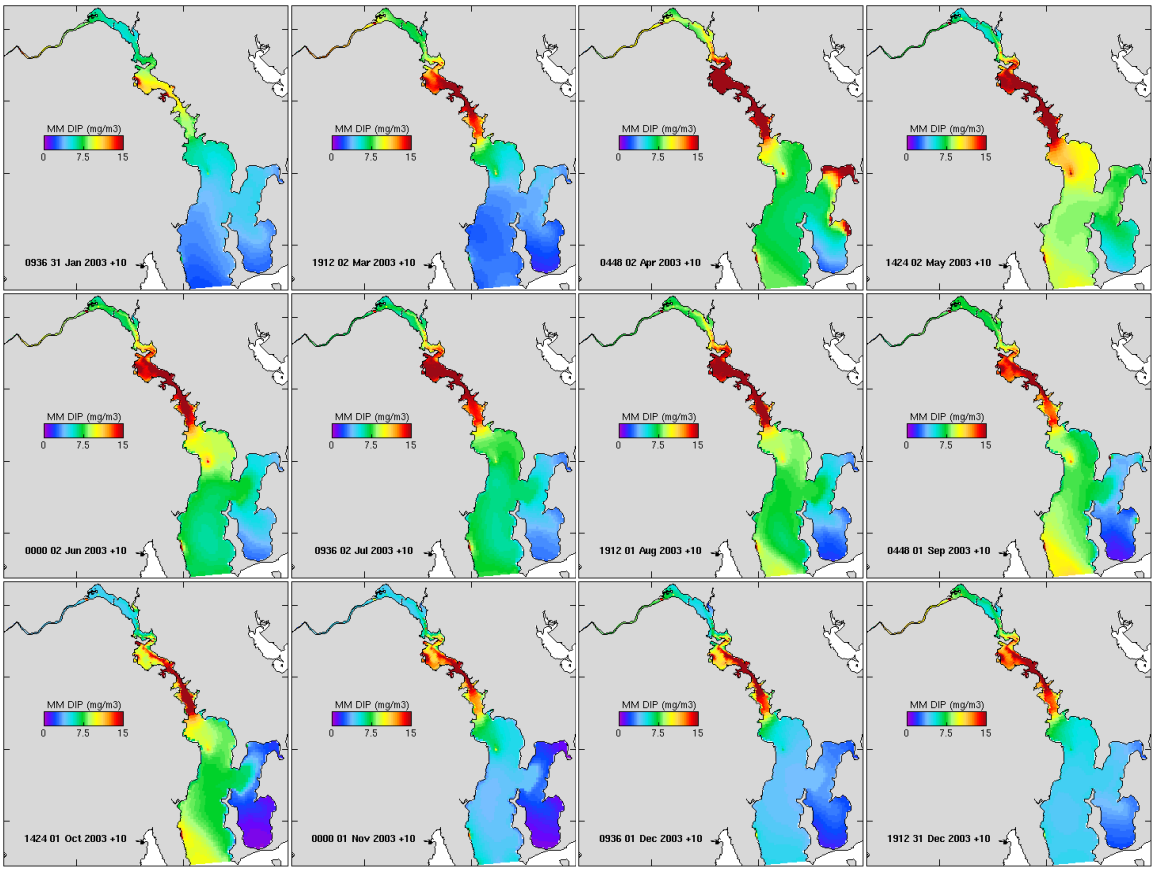

Figure 6-8 Monthly mean near-surface (0-11m) concentrations of DIP from 31 Jan 2003 – 31 Jan 2004.

Cross-sections of DIP concentration along the axis of the estuary (Figure 6-9) show a similar distribution of elevated concentration to that of nitrate and ammonium and the influx of STP loads in the upper estuary is clearly visible through much of the year. There is persistent accumulation of DIP in bottom waters of the middle estuary and this appears to outcrop into surface waters in the vicinity of the salt wedge front.

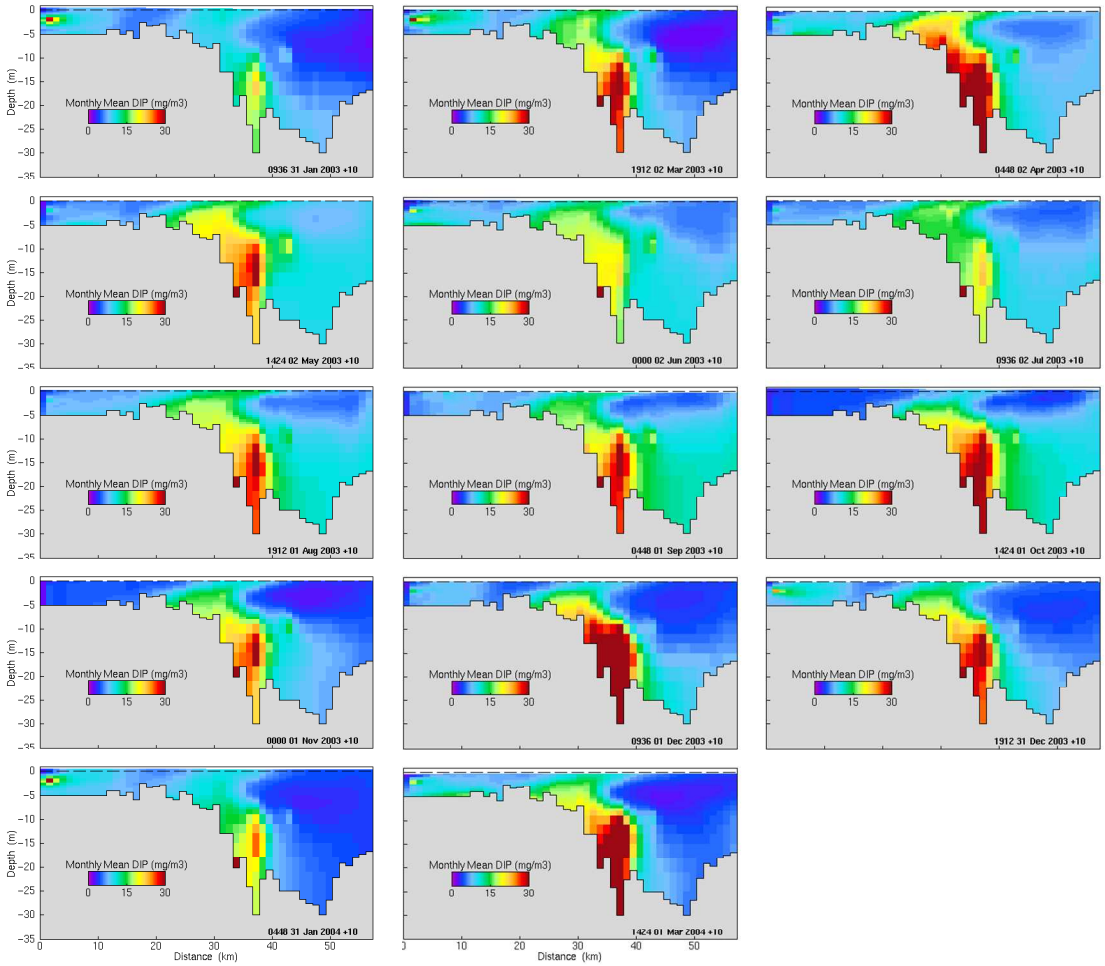

Figure 6-9 Cross section of monthly mean concentrations of dissolved inorganic phosphate along the axis of the estuary (from New Norfolk to Iron Pot).

6.2.3 Chlorophyll

In the upper estuary near-surface chlorophyll concentrations (Figure 6-10) were elevated in autumn Mar'03 – May'03 and summer (Dec'03 – Feb'04). In the mid-estuary the autumn increase in concentration occurred over a longer period (Mar'03-Jul'03) dipped slightly in Aug'03 then increased steadily through spring and summer (Sep'03-Feb'04). In the lower estuary and Ralphs Bay chlorophyll concentrations were elevated through winter and spring (May'03-Nov'03) with moderate levels of chlorophyll remaining in Ralphs Bay through summer to Feb'04. A semi-circular area of elevated near-surface chlorophyll and nutrient (Figure 6-5 and Figure 6-8) concentrations frequently shown in the centre of Ralphs Bay results from shoaling contours in bathymetry.

In general near-surface monthly mean concentrations of chlorophyll were lower in the upper estuary and outer reaches whilst the mid-estuary had consistently higher chlorophyll concentrations throughout the year (>4 mg m^{-3}). The middle and lower reaches had highest chlorophyll adjacent to the shore, in the proximity of STP and stormwater inputs. The spatial and temporal distribution of phytoplankton biomass in different regions of the estuary is due primarily to contrasting availability of light and nutrients essential for growth. In addition, sinking, resuspension and circulation of cells through the model will contribute to the resulting distribution of phytoplankton biomass.

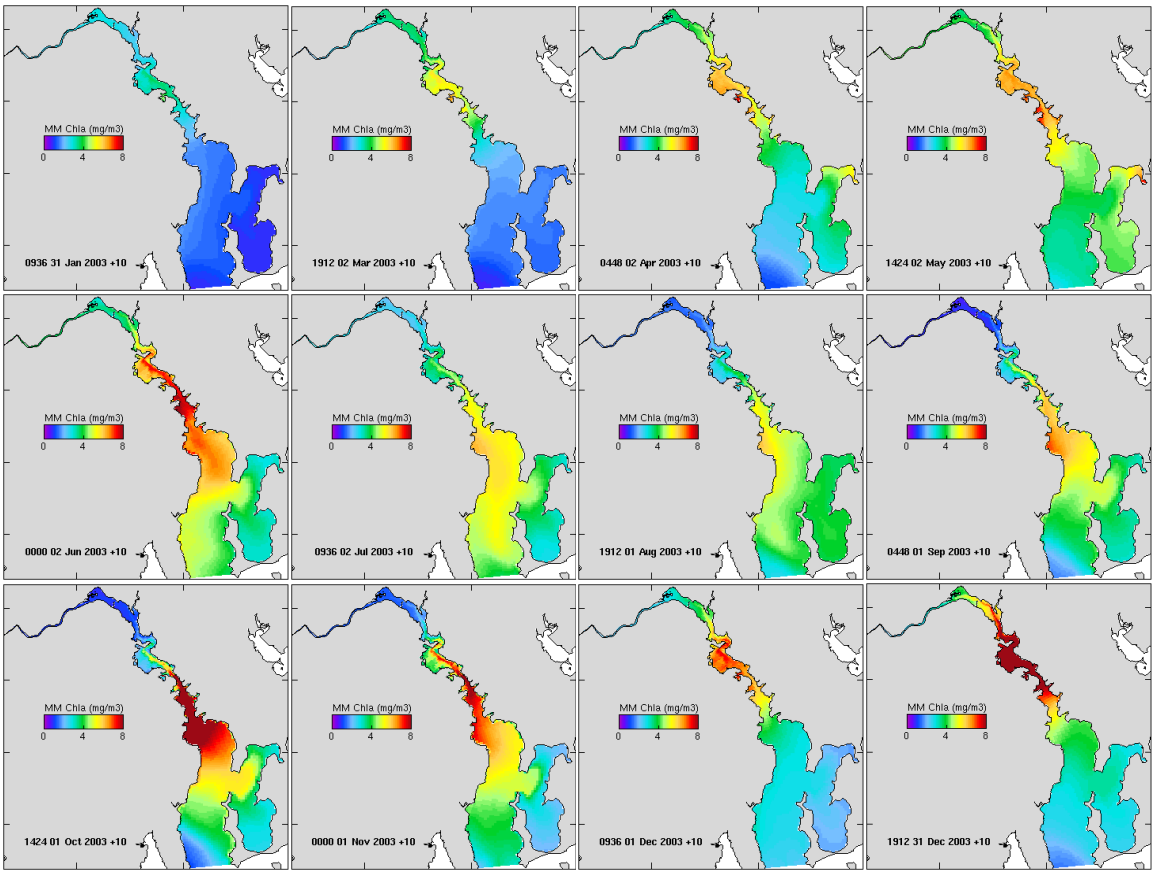

Figure 6-10 Monthly mean near-surface (0-11m) concentrations of chlorophyll from 31 Jan 2003 – 31 Jan 2004.

Cross-sections of chlorophyll concentration along the axis of the estuary (Figure 6-11) show a persistent plume of elevated concentration in the mid-estuary outcropping into surface waters in the vicinity of the salt wedge front similar to the distribution of nutrients (Figure 6-6 and Figure 6-7). The chlorophyll concentration and location suggests that phytoplankton from the inner reaches of the estuary may seed the blooms in the outer reaches of the estuary. High chlorophyll levels in the outer reaches can occur at greater depths (~10 m) due to lower levels of attenuation and increased propagation of light in this region. These results are supported by observations taken in the outer reaches of the estuary which show higher chlorophyll concentrations in deeper waters (DEP pers. comm.).

The amplitude of chlorophyll concentration varies with highest concentrations shown in winter (Jun'03) and spring-summer (Oct'03-Jan'04). During winter and spring elevated phytoplankton biomass occurs at depths in excess of 20 m due to sinking and advection of near-surface populations. Phytoplankton in deep water have low ambient growth rate due to light limitation, however growth may increase if they are advected to a more favourable light environment by the estuarine circulation.

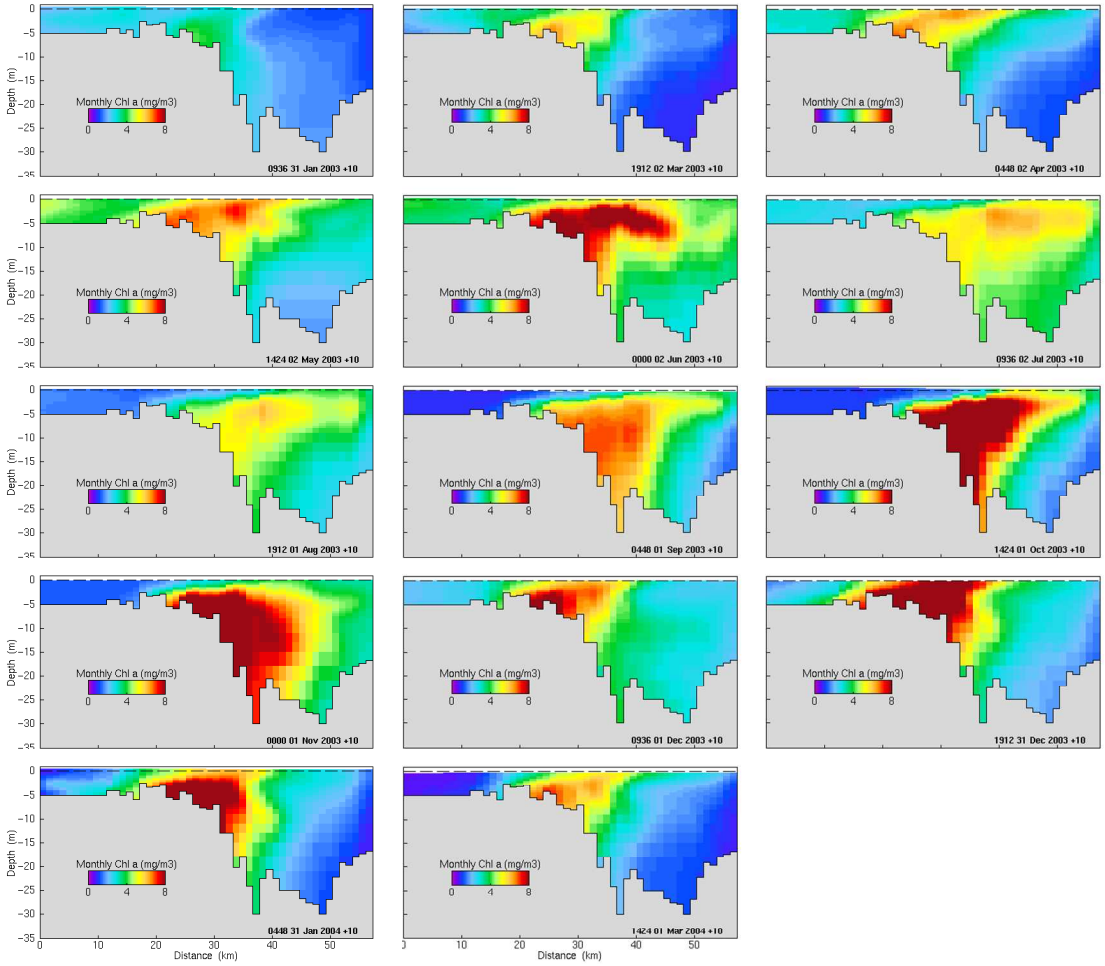

Figure 6-11 Cross section of monthly mean concentrations of chlorophyll along the axis of the estuary (from New Norfolk to Iron Pot).

6.2.4 Attenuation of Light

Attenuation of light by coloured dissolved organic material, industrial effluent, and suspended particulate material determines the propagation of light through the water column and the amount of photosynthetically active radiation (PAR) available at different depths for phytoplankton and macrophyte photosynthesis. Where attenuation is high propagation of light is low and autotroph photosynthesis is constrained. In the Derwent Estuary few profiles of attenuation have been measured and this aspect of the model, whilst consistent with our understanding of the dynamics of optically active substances, has not been validated against observations.

Plots of modelled near-surface monthly mean attenuation coefficient (Figure 6-12) show high levels of attenuation in the upper estuary throughout the year. Attenuation is greatest in winter months when the seasonal influx of river water containing elevated concentrations of CDOM is greatest. In Dec-Jan ’04 attenuation was also high in the upper estuary corresponding to elevated river flow (Figure 3-5). In southern Ralphs Bay modelled attenuation is elevated compared with the outer estuary due to resuspension of bottom material in the shallow bay. Water quality surveys in the area are not thought to support this (Coughanowr pers.com.) which suggests the modelled sediment may be too easily resuspended in this part of the model domain.

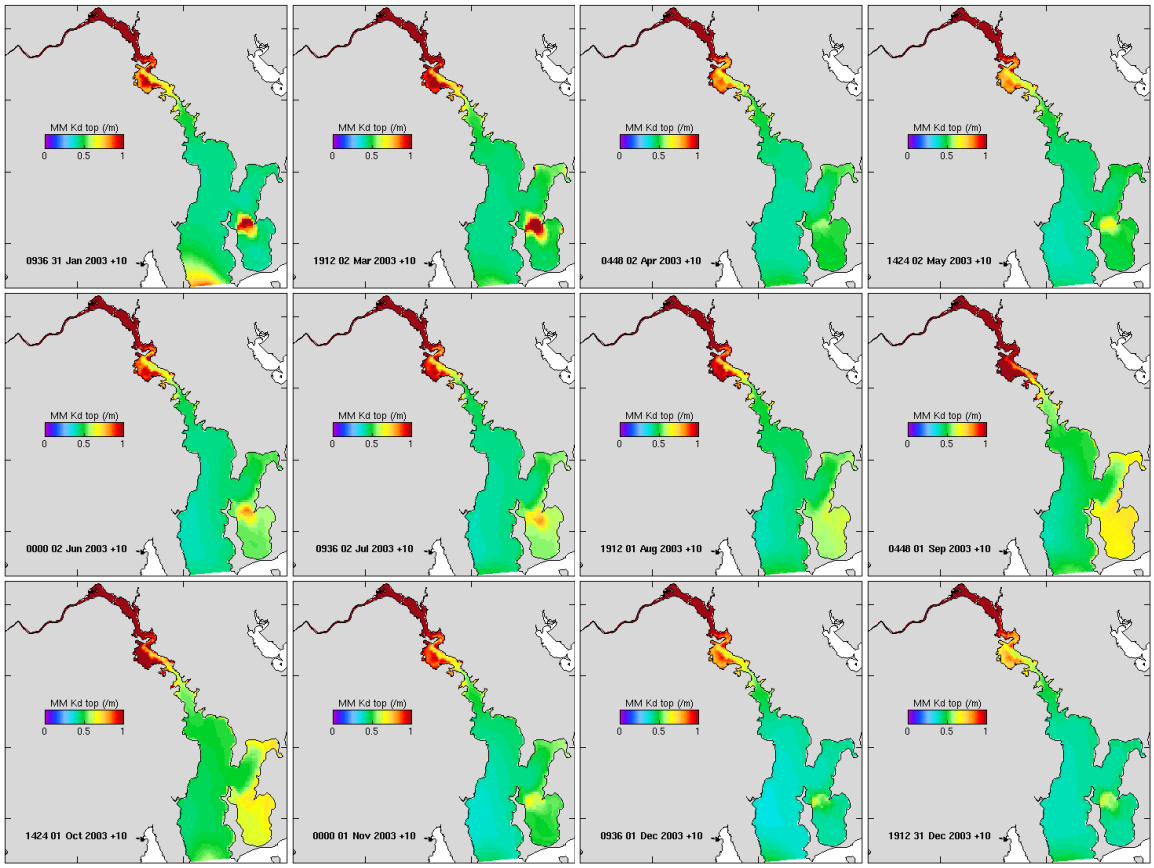

Figure 6-12 Monthly mean near-surface (0-11m) attenuation coefficient from 31 Jan 2003 – 31 Jan 2004.

Cross sections of attenuation coefficient along the axis of the estuary (Figure 6-13) clearly show the contribution of CDOM-rich river waters to the optical climate. Peaks in attenuation coefficient near New Norfolk are visible in summer months associated with the strongly coloured effluent discharged from Norske Skog. Dispersion and degradation of the effluent limits the optical impact of the effluent to the upper estuary. In general, waters upstream of the salt wedge front are strongly attenuating limiting available light for autotroph growth, whilst waters downstream of the front are considerably clearer.

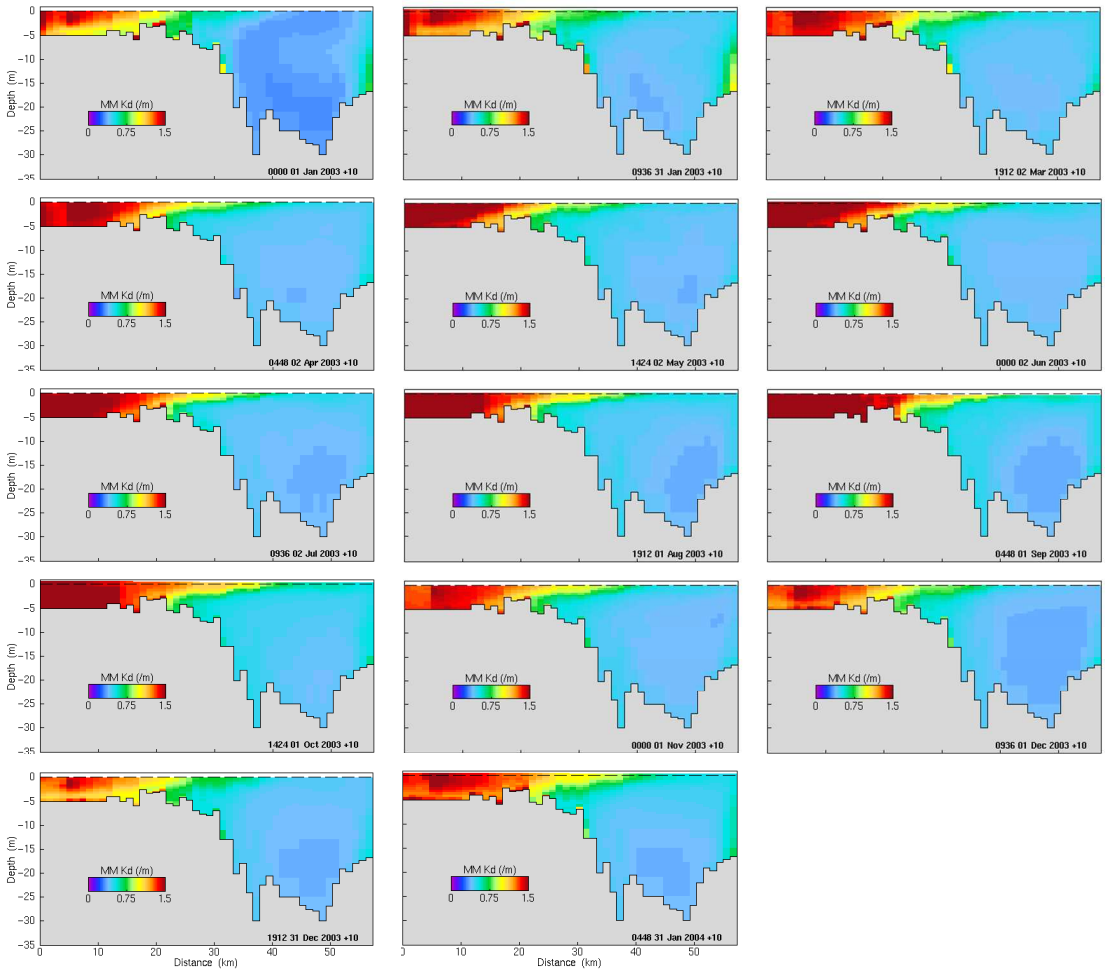

Figure 6-13 Cross section of monthly mean attenuation coefficients along the axis of the estuary (from New Norfolk to Iron Pot).

6.2.5 Dissolved Oxygen

Plots of modelled monthly mean bottom water dissolved oxygen content (% saturation) (Figure 6-14) shows low levels of dissolved oxygen (<75% saturation) in the middle reaches of the estuary out to the deeper outer reaches (near the entrance of Ralphs Bay) throughout much of the year, but particularly in autumn (<50% saturation). In comparison the inner and outer bays are well oxygenated due primarily to their shallow depths. The upper reaches of the estuary also has shallow depth but intrusion of salty water in summer and autumn brings waters with lower oxygen content upstream.

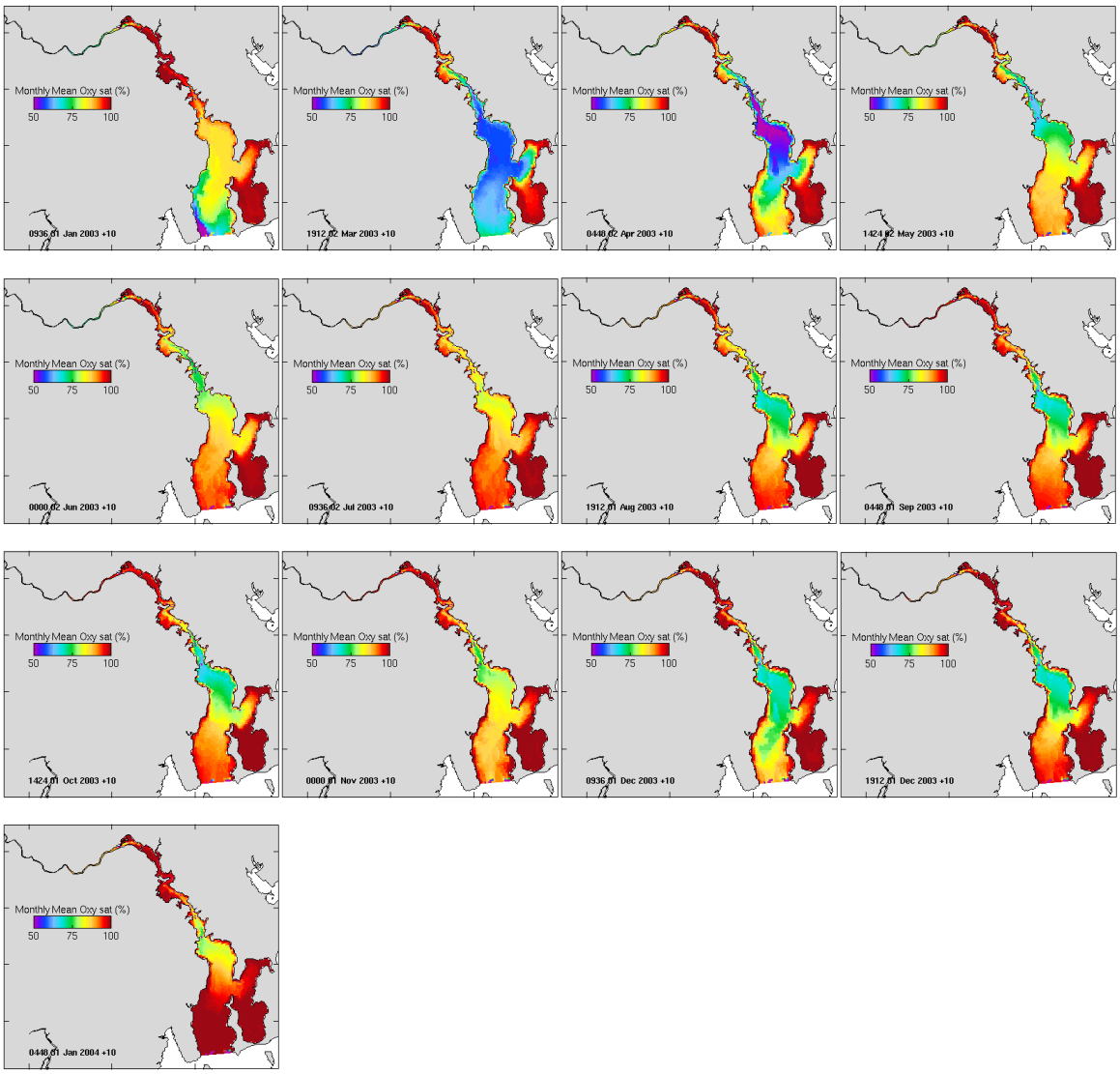

Figure 6-14 Monthly mean bottom water dissolved oxygen % saturation from 31 Jan 2003 – 31 Jan 2004.

The cross sections of monthly mean dissolved oxygen content (% saturation) show low oxygen levels in the deeper water of the mid-estuary for most of the year (< 75% saturation; Figure 6-15). The section also has a number of deeper “holes” which accumulate organic particles and are less well ventilated than smoother sections of bathymetry. In these locations dissolved oxygen saturation is consistently very low throughout the year (<50% saturation).

Seasonally autumn is the period which has the lowest dissolved oxygen levels in the middle reaches with values falling to below 50% saturation in the bottom 10 m of the water column. Low oxygen saturation was also simulated in the upper reaches of the estuary for the summer and autumn months in the salt wedge.

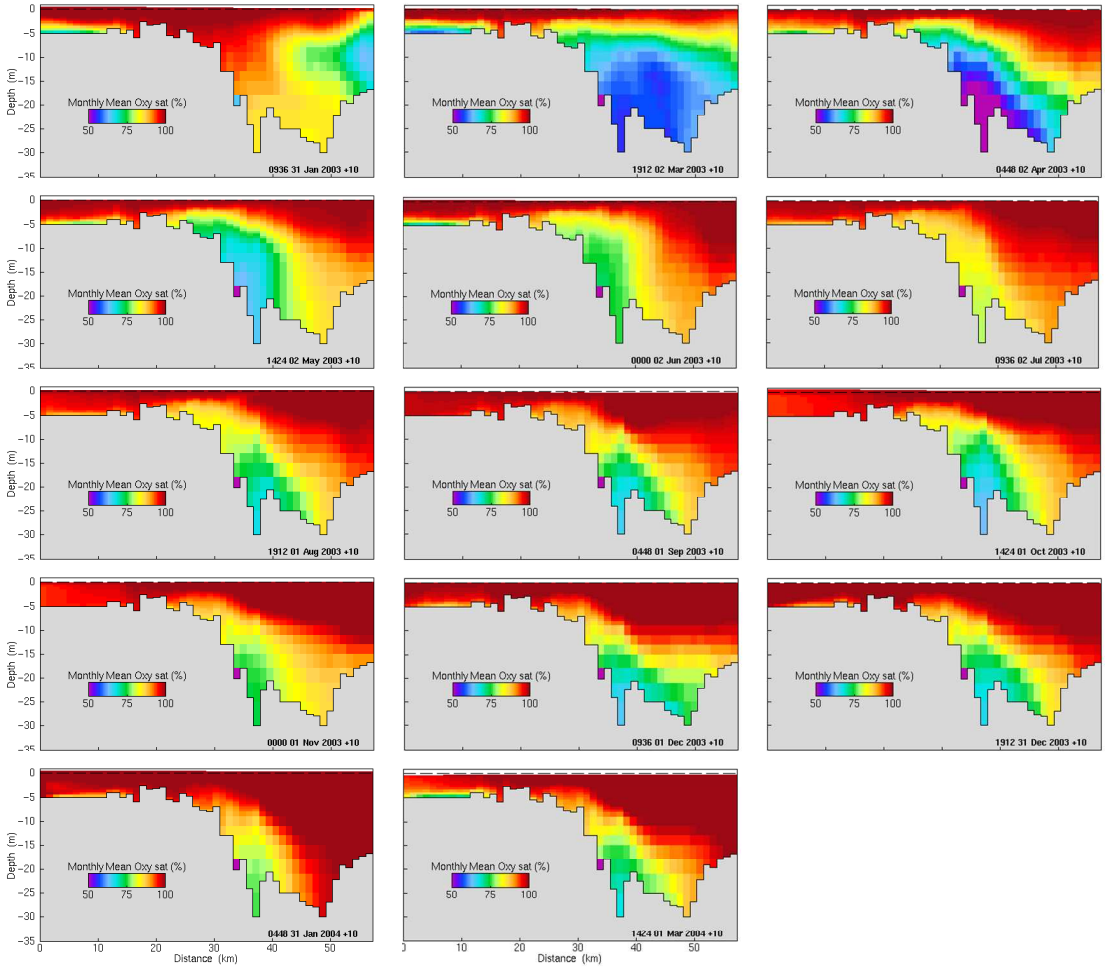

Figure 6-15 Cross section of monthly mean concentration of Dissolved Oxygen percent saturation along the axis of the estuary (from New Norfolk to Iron Pot).

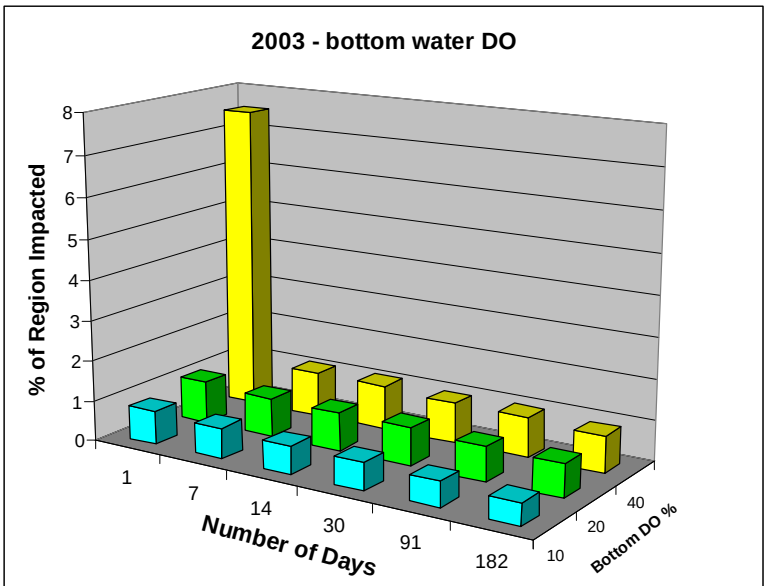

	1	7	14	30	91	182
10	0.8	0.8	0.7	0.7	0.6	0.5
20	1.0	1.0	0.9	0.9	0.8	0.8
40	7.5	1.1	1.1	1.0	1.0	0.9

Figure 6-16 Area of estuary (%) and duration (days) when bottom water dissolved oxygen saturation falls below thresholds of 40, 20 and 10 % saturation.

By summing the model results over space and time the extent of low bottom water dissolved oxygen levels can be understood more easily (Figure 6-16). In 2003-4 7.5% of the estuary, by area, experienced bottom water dissolved oxygen saturation less than 40% for 1 day; whilst 1% of the estuary area experienced less than 20% saturation for 7 days. [This analysis sums all days which are not necessarily sequential]. In the context of the whole estuary, the model suggests that only a very small area experienced low bottom water dissolved oxygen concentrations of concern in 2003-4. In the upper estuary where complex bathymetry is unresolved by the model and the biogeochemistry is simulated with less reliability low bottom water dissolved oxygen events may not be fully captured by the model. In this respect the model may underestimate the true, extent of low bottom water oxygen and results should be treated with caution.

6.3 Benthos

Few data exist in the Derwent Estuary to validate the modelled epi-benthic macrophytes and sediment biogeochemistry. Where data do exist they show large variation in properties over small space scales which are difficult to reconcile with the comparatively large model grid. Sediment observations are difficult to make and time consuming to analyse resulting in spatially and temporally sparse data confounded by the high natural spatial variability. Accordingly it has not been possible to validate any of the benthic model results with concurrent observations made in 2003-4. Model results and their interpretation in this section should therefore be treated as unvalidated, although the results are consistent with our modelled understanding of benthic-pelagic interactions.

6.3.1 Light

The amount of light reaching the epi-benthos determines the level of autotroph photosynthesis and production. Propagation of light depends on the intensity of incident light, the concentration of attenuating substances in the water and the depth of overlying water. Plots of modelled monthly time-integrated photosynthetically active radiation (PAR) reaching the epi-benthos (Figure 6-17, Figure 6-18) show the seasonal cycle in day length and light intensity with highest values in summer and lowest light levels simulated in winter. Regions of shallow water in the lower estuary and Ralphs Bay have extensive areas where significant irradiation reaches the epi-benthos. In the upper estuary, where attenuation in the water column is typically higher, the area receiving elevated levels of irradiation is confined to the shallowest water adjacent to the shore.

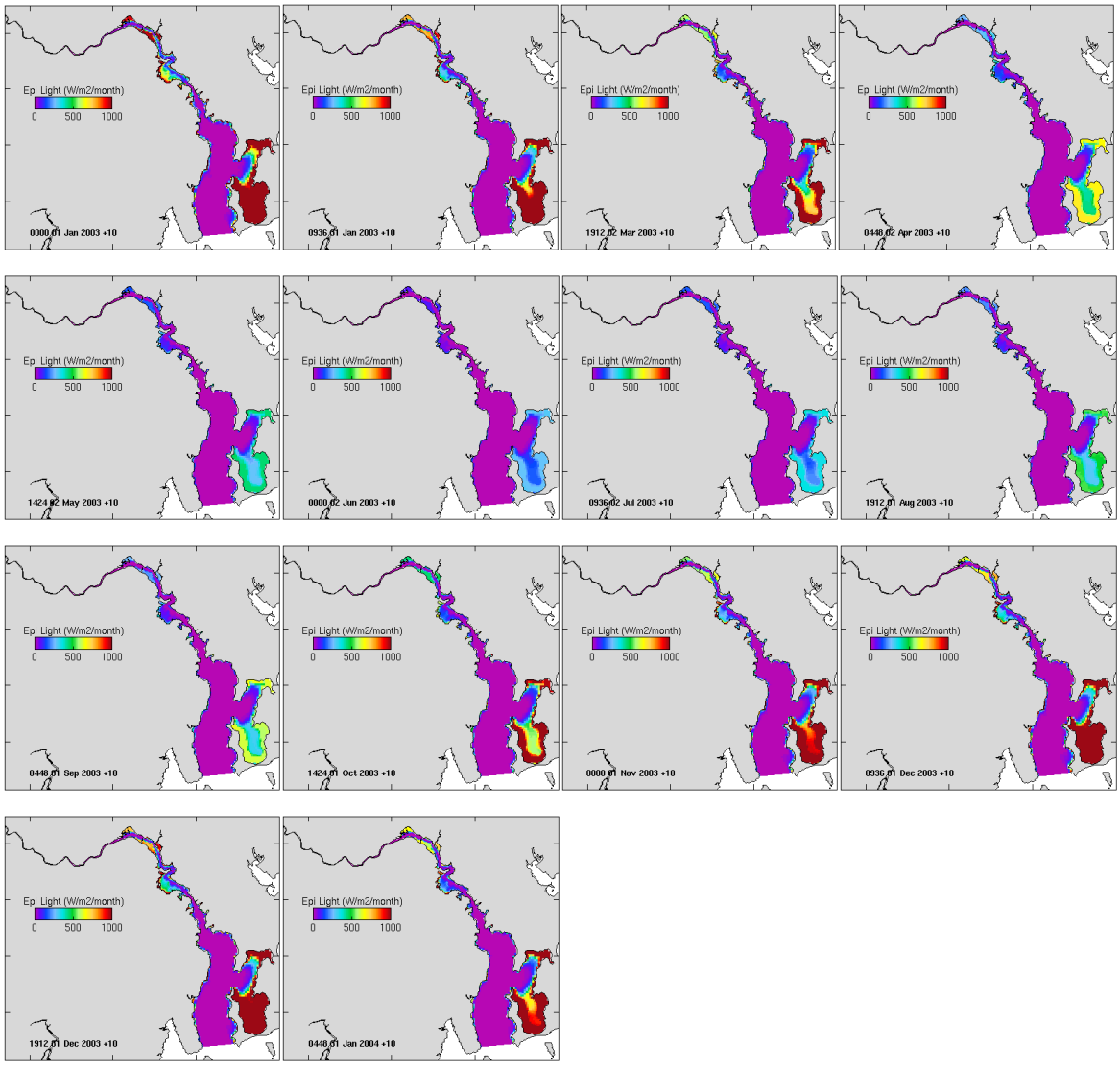

Figure 6-17 Monthly integrated PAR reaching the epi-benthos from 1 Jan 2003 – 31 Jan 2004.

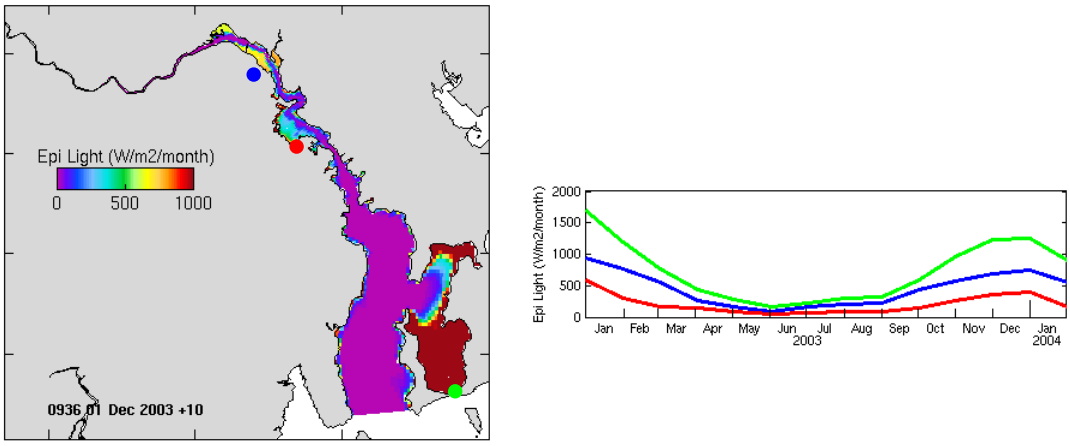

Figure 6-18 Monthly integrated PAR reaching the epi-benthos at stations throughout the estuary (red = 2.5 m, blue = 1 m, green = 2 m deep).

On an annual basis the amount of PAR reaching the epi-benthos in 2003 is shown in

Figure 6-19. The edges of Ralphs Bay received the most irradiation followed by the areas of shallow water in the vicinity of Bridgewater Bridge. Waters deeper than 10 m received little light and would be unlikely to support significant epi-benthic photosynthesis by seagrass, macroalgae or microphytobenthos.

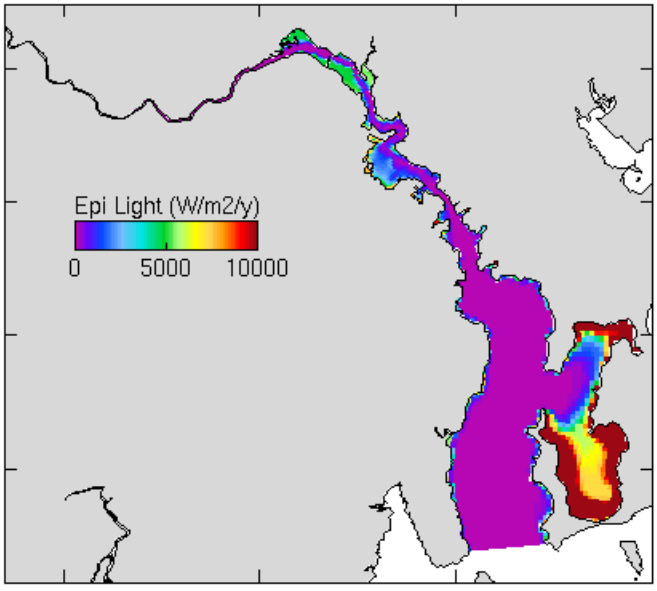

Figure 6-19 Annual integrated light reaching epi-benthos.

6.3.2 Macrophytes

In the simulation results shown seagrass and epiphytic macroalgae were allowed to propagate in the model following initialisation with a uniform low biomass throughout the model domain (rational discussed in Section 3.3.4). The model does not resolve variations in substrate which may influence the establishment of macrophytes and may generally under-predict epibenthic light and photosynthesis where the model grid only coarsely resolves gradients in depth. The results shown should therefore be interpreted as the minimum set of locations where modelled light and nutrients favour seagrass and macrophyte growth.

The modelled monthly mean biomass of seagrass and macroalgae in Dec'03 is shown in., Figure 6-20. In summer 2003-4 seagrass and macroalgae are shown in Elwick Bay and along the edges of the channel above the Bridgewater Bridge in the upper reaches of the estuary. Despite an extensive area of elevated epi-benthic PAR in Ralphs Bay the biomass of macrophytes in the bay is smaller than in the middle and upper reaches of the estuary, due to the smaller contribution of macroalgae to the net biomass. In the upper estuary, epiphytic macroalgae, are more successful due to elevated ambient nutrient concentrations. They grow fast and shade seagrass reducing the growth rate of seagrasses further. Ralphs Bay generally experiences lower ambient nutrient concentrations which limits the growth of epiphytic macroalgae and favours growth of seagrass in the model (Figure 6-21).

Observed maps of macrophyte presence in general correlate well with the locations where the model simulated seagrass and macroalgae although in Ralphs Bay little seagrass has been observed, whilst the model suggests conditions should favour growth. Also in the upper estuary extensive beds of seagrasses are found whilst the model suggests macroalgae should dominate. These comparisons show considerable uncertainty in the modelled macrophyte distributions and emphasise the need to better constrain the macrophyte model preferably with observed species information, biomass, growth rates and nutrient stochiometry. In addition it would be valuable to include spatial distribution of substrate and substrate disturbance information in the model.

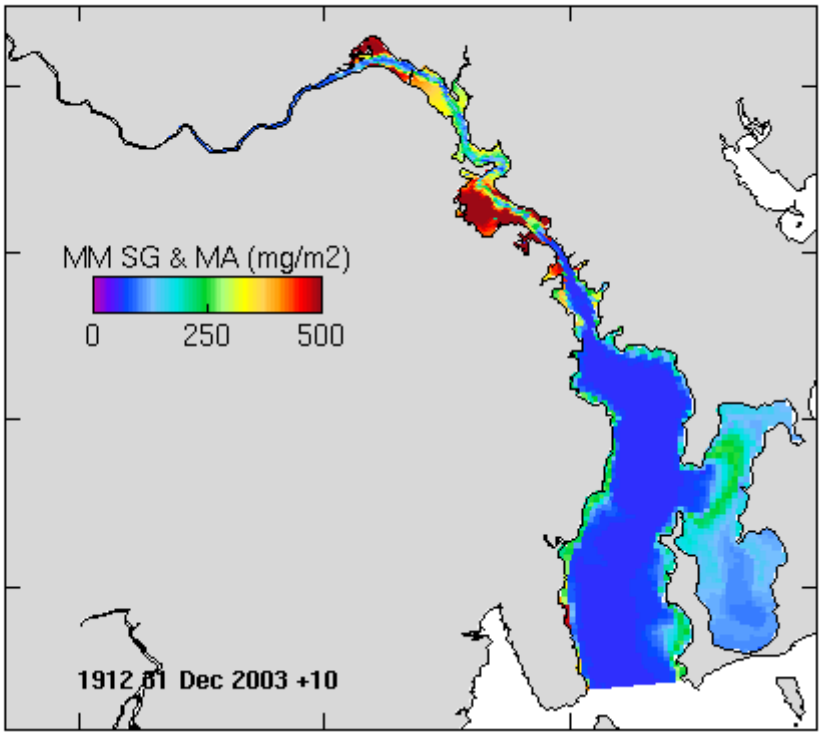

Figure 6-20 Monthly mean biomass of macrophytes (seagrass and macroalgae) simulated in Feb 2004.

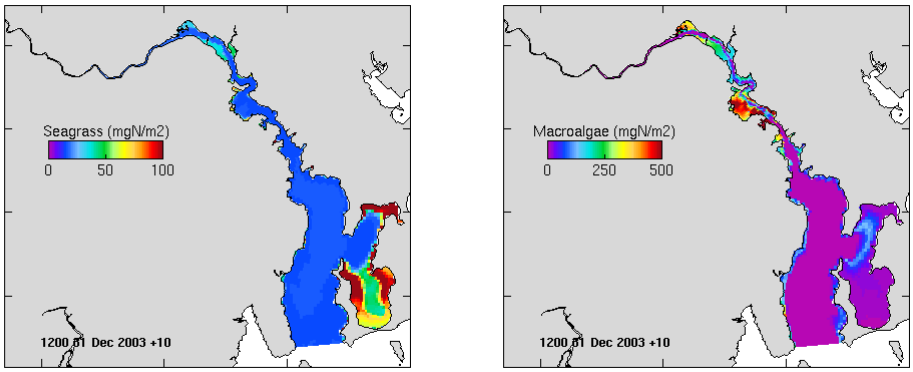

Figure 6-21 Nitrogen biomass of modelled seagrass (left) and macroalgae (right) on 31 Dec'03.

6.3.3 Sediment Oxygen

The modelled spatial distribution of dissolved oxygen content (% saturation) of the surface sediment (Figure 6-22) is similar to the distribution of bottom water dissolved oxygen saturation (Figure 6-14). Values are typically lower in the sediment due to aerobic respiration, associated with detrital remineralisation, which exceeds benthic-pelagic oxygen exchange and results in the sedimentary drawdown. Dissolved oxygen saturation is lowest in the mid-estuary to outer reaches where levels fall below 40% saturation during autumn and early spring. High concentrations of

sediment oxygen correspond to regions of shallow water where macrophytes and microphytobenthos augment surface exchange by releasing dissolved oxygen during photosynthesis.

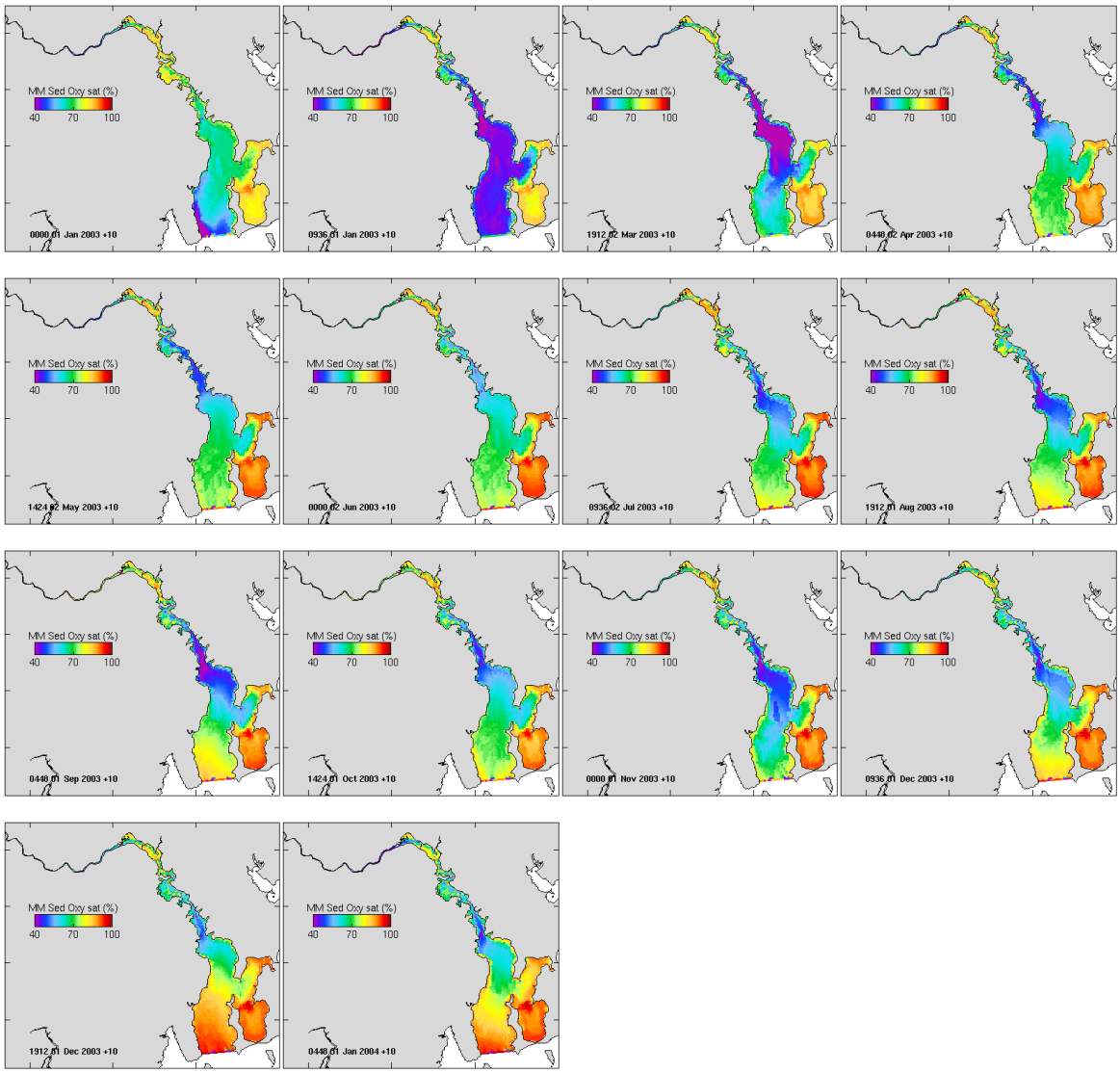

Figure 6-22 Monthly mean surface sediment dissolved oxygen percent saturation from 1 Jan 2003 – 31 Jan 2004.

Figure 6-23 shows the monthly 10 percentile dissolved oxygen content (% saturation) of the surface sediment. For 10% of the time in Mar'03, sediment oxygen values fell to 20% saturation in a small area by the Tasman Bridge. Elsewhere in the mid and lower estuary values of <50% saturation occurred for 10% of the time during Feb'03 – Apr'03 and Aug'03 - Nov'03 over larger areas of the estuary.

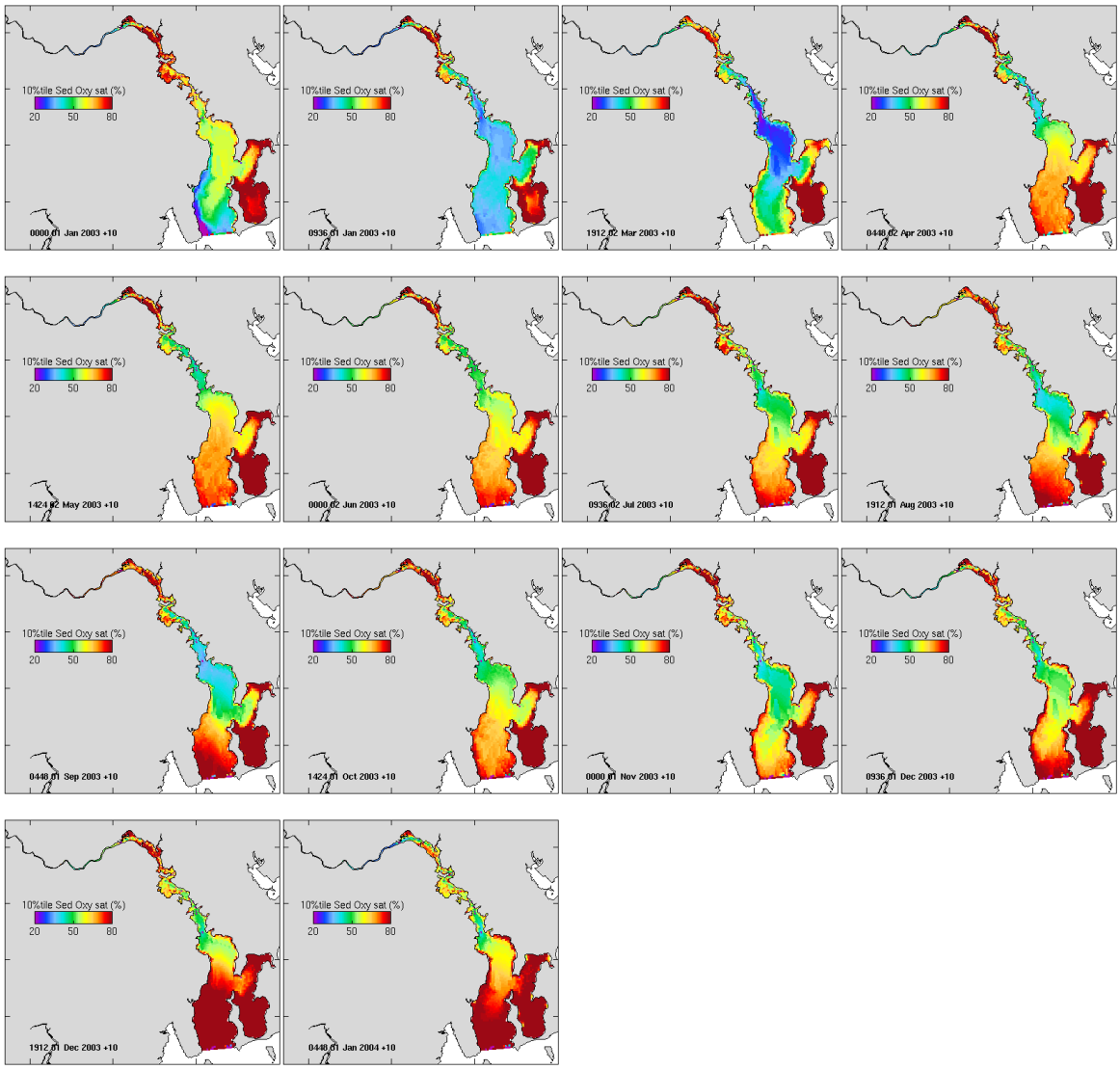

Figure 6-23 Monthly 10 percentile surface sediment dissolved oxygen % saturation from 1 Jan 2003 – 31 Jan 2004.

6.3.4 Denitrification

There were no observations of denitrification in Derwent Estuary sediments in 2003-4 so these results from the model have not been rigorously validated against observations. Recent observations of denitrification in 2008 (Jeff Ross pers. com.), show small scale spatial and temporal variability in benthic-pelagic fluxes, likely due to sediment heterogeneity in grain size, porosity, nutrient load, bioturbation and irrigation by benthic fauna. The model cannot reproduce this sub-grid scale patchiness, which confounds comparison of model results with the observations made to date [although model results are of similar magnitude to the observations]. For the purposes of model validation, it would be useful to observe denitrification rates over wider spatial and temporal scales throughout the estuary. It would also be of value to extend the biogeochemical model to include diurnal cycles in autotroph growth and respiration, and gradients in sediment bioturbation and irrigation by benthic fauna.

Modelled monthly mean denitrification flux out of the Derwent estuary sediments shows a seasonal cycle with elevated flux in spring (Figure 6-24). Highest denitrification rates were consistently found

in the mid-estuary and the narrow channel of the upper estuary where elevated sediment ammonia (Figure 6-25) concentrations and low dissolved oxygen saturation favoured the coupled nitrification – denitrification reaction implemented in the model. In the middle reaches of the estuary and in Elwick Bay there are 'hot spots' of increased denitrification flux. These correspond to depressions in the bathymetry where sediment ammonia concentrations are high, and dissolved oxygen concentrations low, from remineralisation of organic material accumulating on the sea bed.

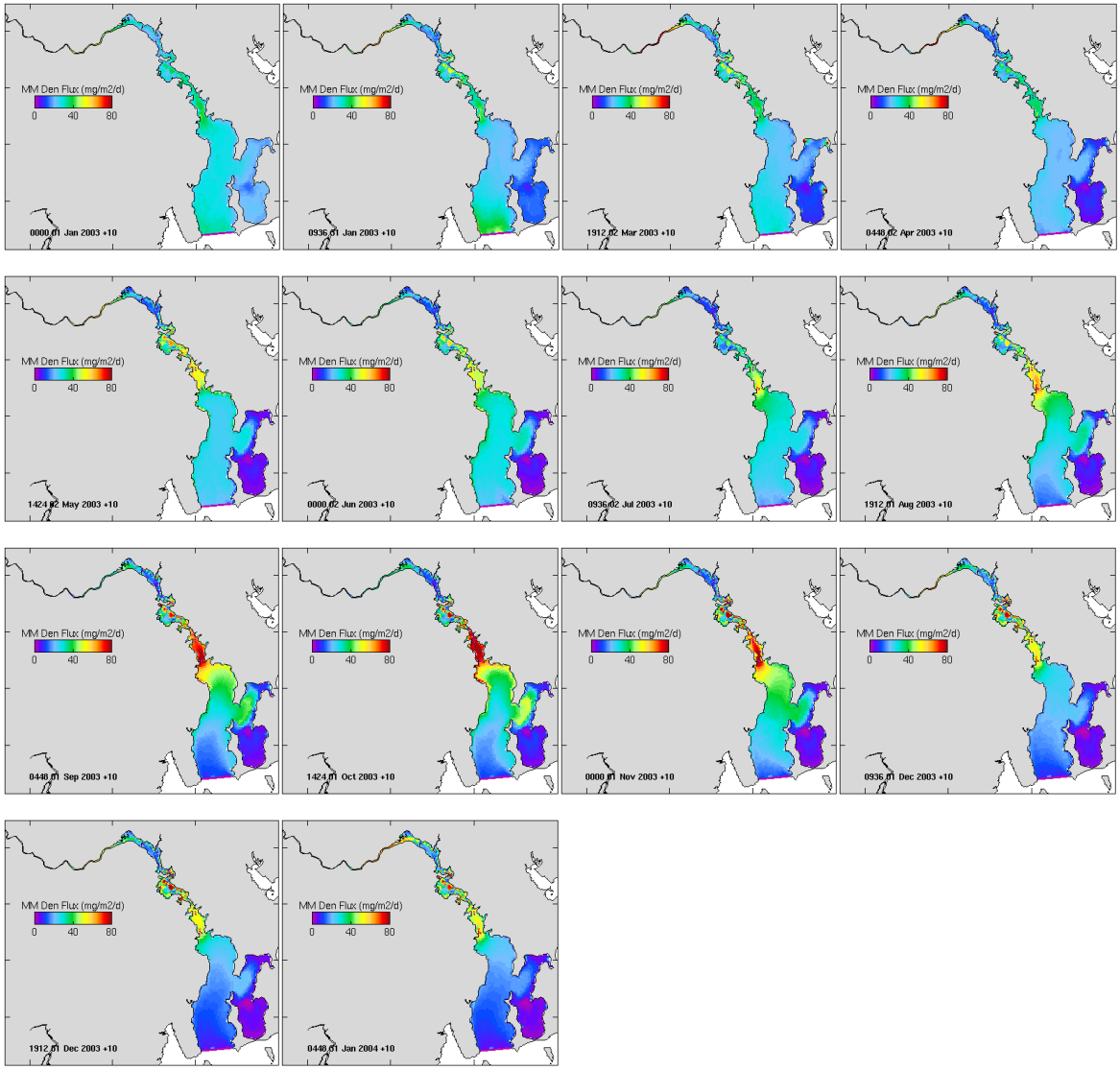

Figure 6-24 Monthly mean denitrification flux out of the sediment from 1 Jan 2003 – 31 Jan 2004.

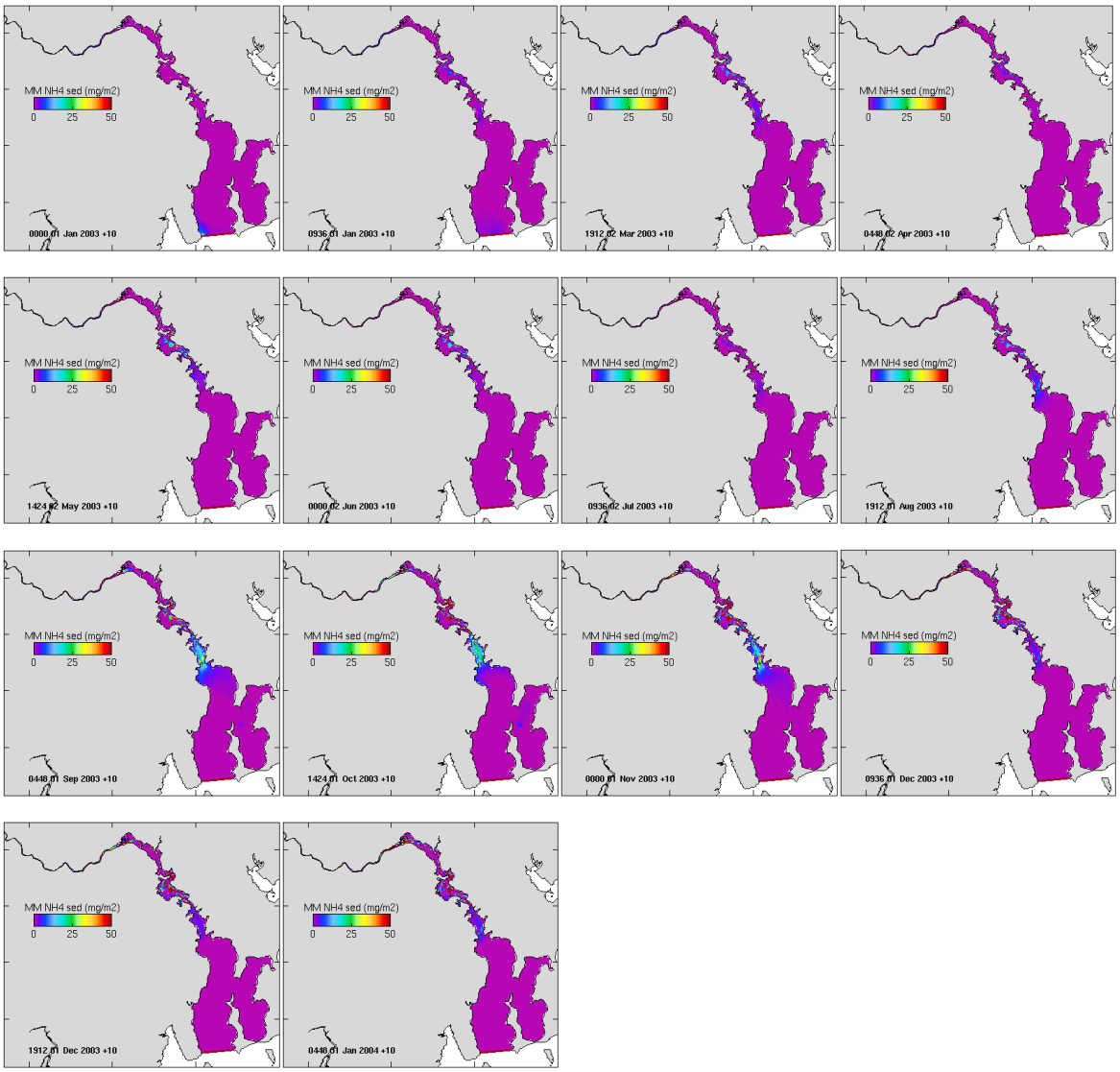

Figure 6-25 Monthly mean sediment ammonia content (depth-integrated over top 21 cm).

The modelled total annual denitrification flux shows a high denitrification flux in the upper and mid-estuary (Figure 6-26). In Ralphs Bay north and south and the shallow region above and below Bridgewater, denitrification flux was lower likely due to higher modelled sediment oxygen concentrations in these parts of the estuary inhibiting the denitrification process. [It should be noted that the model does not rigorously include bioturbation and irrigation of sediments by burrowing and filter feeding organisms which have the capacity to significantly modify local sediment biogeochemical processes.]

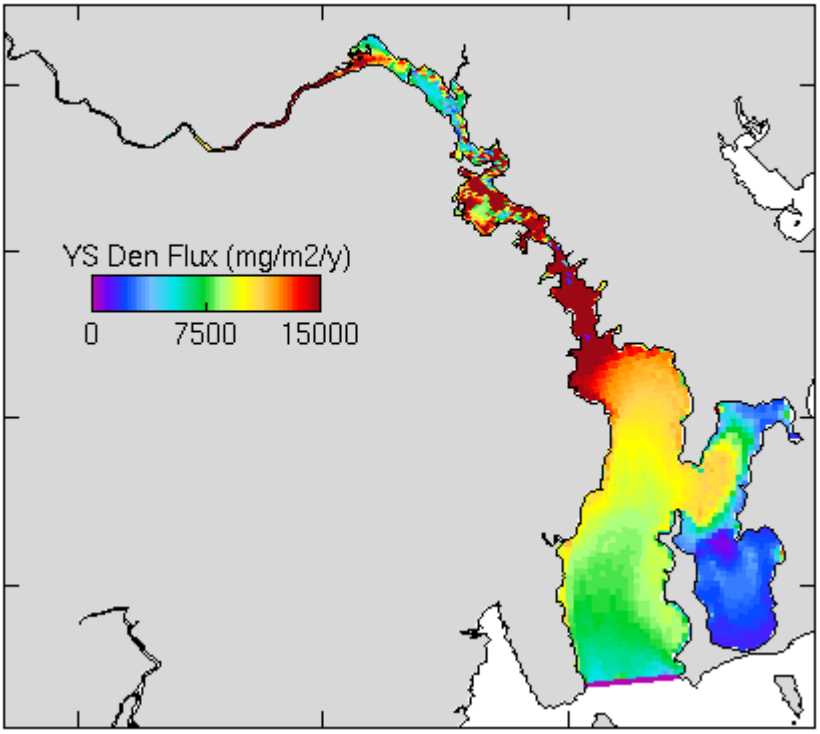

Figure 6-26 Annual integrated denitrification flux.

6.4 Plankton Communities and Succession

6.4.1 Phytoplankton

In 2003-4 there were no observations of phytoplankton species to compare with model results, however, the model did reproduced observed concentrations of chlorophyll throughout the estuary. Modelled chlorophyll is the sum of contributions from small phytoplankton, large phytoplankton, dinoflagellate and microphytobenthos groups. The model predicts a succession of phytoplankton groups and contrasting depth profiles for small and large phytoplankton and dinoflagellate biomass over the year and throughout the estuary (Figure 6-27). Large phytoplankton, which are parameterised to represent large diatoms in the model have a sinking rate of 1.3m/d and so typically have a sub-surface peak in concentration.

In 2003 the model simulated an autumn dinoflagellate bloom in all areas of the estuary, with high levels of biomass in Ralphs Bay (station RBS) and the middle reaches (stations U5, U2, C). Over winter large phytoplankton dominated the modelled phytoplankton biomass in the middle and lower reaches of the estuary (stations U5, U2, C, RBS), whilst in spring there was a shift towards a more mixed population. In the upper and lower reaches of the estuary and Ralphs Bay (sites U1617, U12, C, RBS), dinoflagellates increased to dominate the modelled summer biomass.

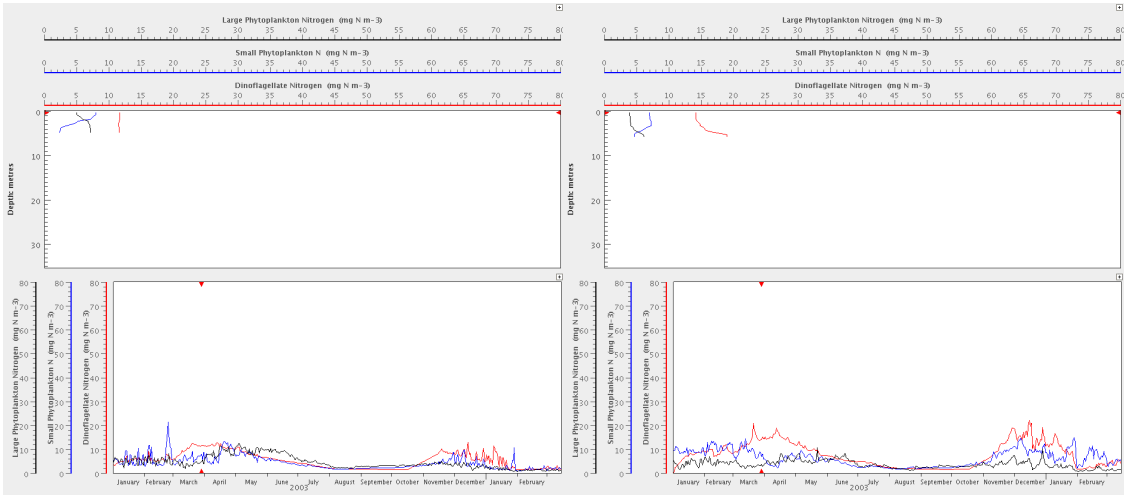

Site U1617 Site U12

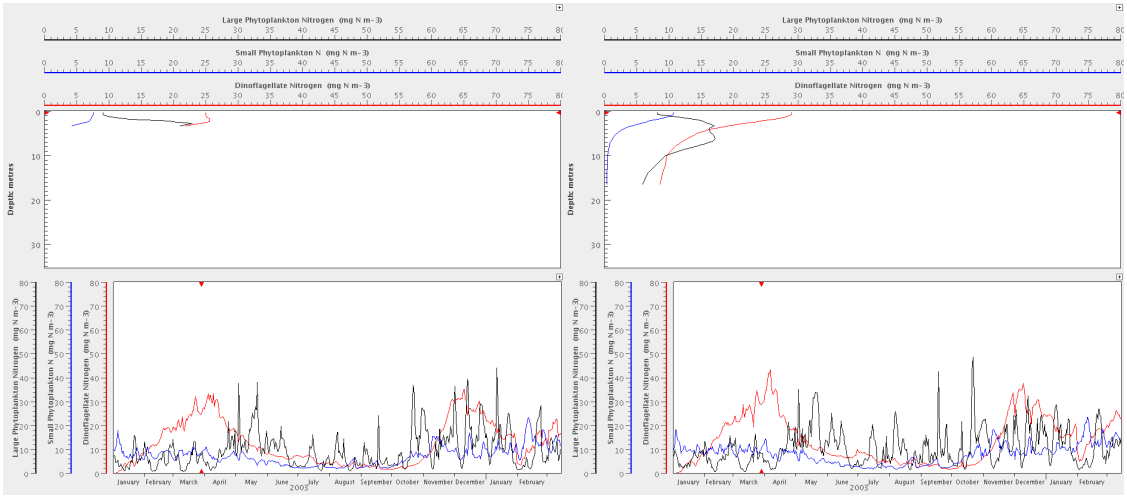

Site U5 Site U2

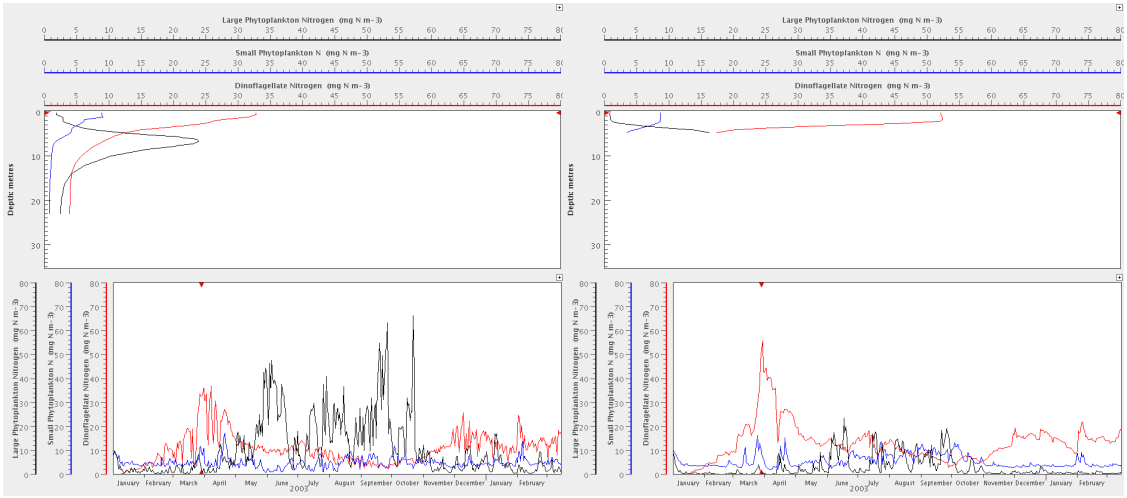

Site C Site RBN

Figure 6-27 Time series of surface concentrations of nitrogen biomass for 2003-4 and autumn depth profiles of small (blue) and large (black) phytoplankton and dinoflagellates (red) at sites U1617, U12, U5, U2, C and RBN.

6.4.2 Zooplankton Grazing

There were no observations of zooplankton grazing in the estuary in 2003-4 to validate these results, however, the simulated zooplankton dynamics are consistent with our understanding of zooplankton behaviour in the estuary. Zooplankton grazing showed a seasonal cycle in the model (Figure 6-28) with consistently high levels of small zooplankton grazing throughout the year which limited the biomass of small phytoplankton. Small zooplankton and small phytoplankton production was tightly coupled with the highest concentrations simulated in surface waters. Modelled grazing by small zooplankton was high in Ralphs Bay and the inner and upper reaches. In this model the red tide forming alga *Noctiluca* would appear in the category of small zooplankton not dinoflagellate as it is a heterotroph (i.e. eats phytoplankton). The timing of modelled small zooplankton blooms correlates well with the observed timing and location of *Noctiluca* blooms observed in the Estuary in other years (however there are no data to validate this result in 2003).

Grazing by large zooplankton was typically greater at depth coincident with the subsurface peak in large phytoplankton prey. Large zooplankton grazing modulates the seasonal autumn and spring blooms in large phytoplankton and dinoflagellate biomass, however the modelled zooplankton response may be underestimated in some parts of the estuary as elevated chlorophyll concentrations were found to persist longer than observed at some DEP sites (see Section 5.5).

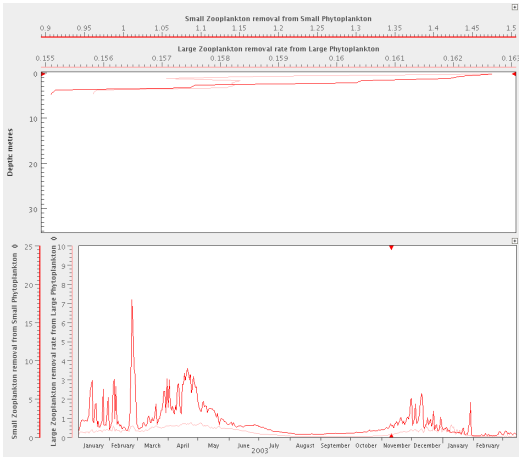

Site U1617

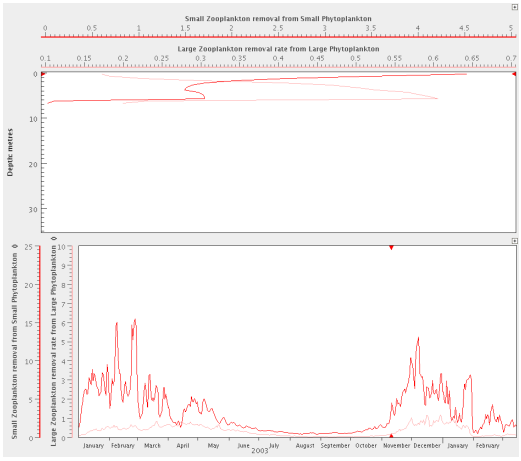

Site U12

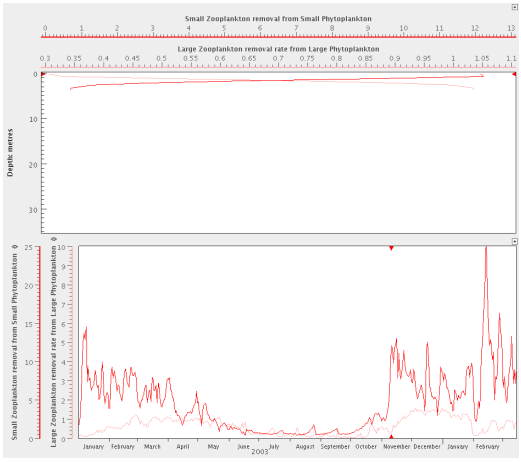

Site U5

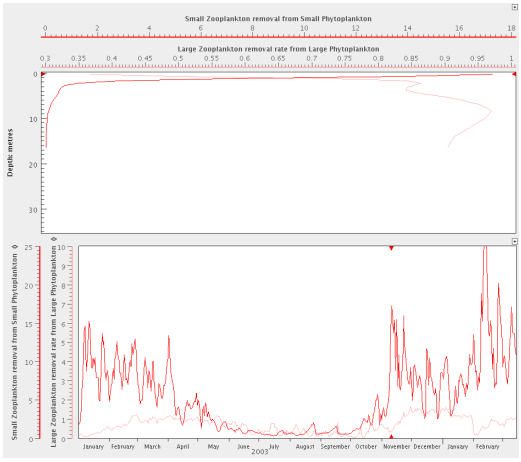

Site U2

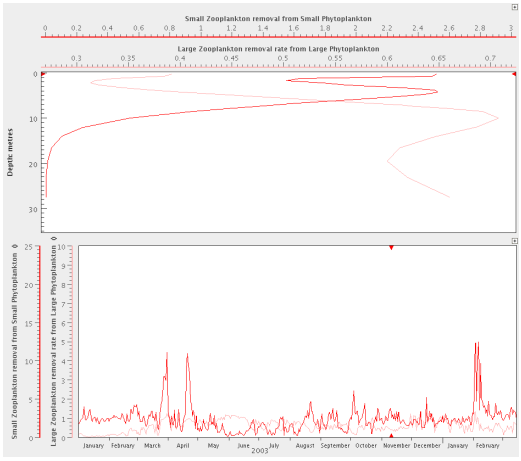

Site C

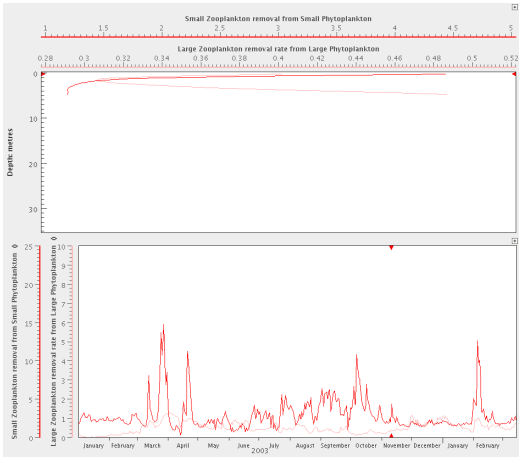

Site RBN

Figure 6-28 Time series of surface zooplankton grazing for 2003-4 and spring depth profile of small (red) and large (pink) zooplankton grazing (mg $Nm^{-3}d^{-1}$) at sites U1617, U12, U5, U2, C and RBN.

6.5 High Rainfall Plume Events

The model can be used to look at the general biogeochemical dynamics of the larger stormwater and sewage treatment plant plumes in the estuary. [For rigorous evaluation of outfall mixing zones a higher resolution model is required.] Figure 6-29 shows modelled surface nitrate concentrations during a period of high rainfall in Mar'03 with increasing freshwater coming down the Derwent River. Coastal plumes of elevated surface nitrate concentration are simulated adjacent to outfalls and storm water drain locations in the mid estuary, and are diluted and dispersed following the peak rainfall event (Figure 6-29); after 10 days the surface nitrate field has returned to more typical autumn concentrations.

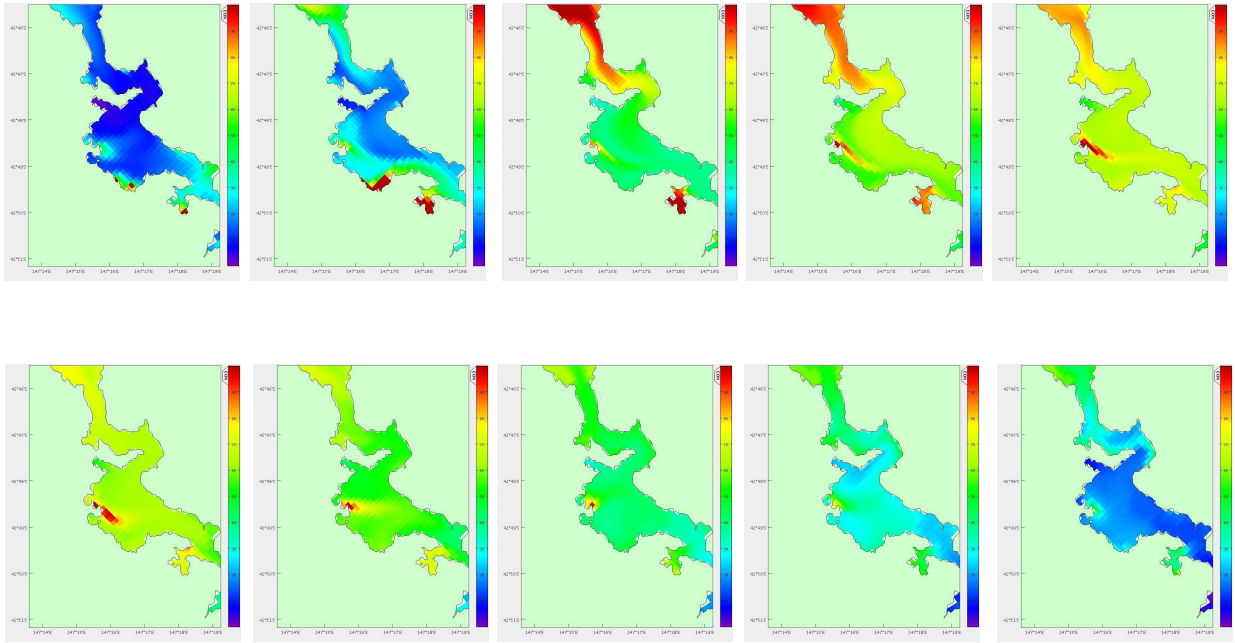

Figure 6-29 Consecutive daily snapshots of nitrate concentrations during a period of heavy rainfall causing high level of stormwater discharge and associated nutrients over a 10 day period during March 2003.

Modelled cross sections along a transect from Cameron Bay to the main channel of the estuary (Figure 6-30) show the vertical distribution of nitrate on consecutive days in March 2003 (Figure 6-31). Initially nitrate concentrations are elevated at depth adjacent to the shore. As discharge increases the plume extends to the surface and out across Elwick Bay. During following days the surface plume is dispersed and lower discharge volumes limit the nitrate plume to a sub-surface feature.

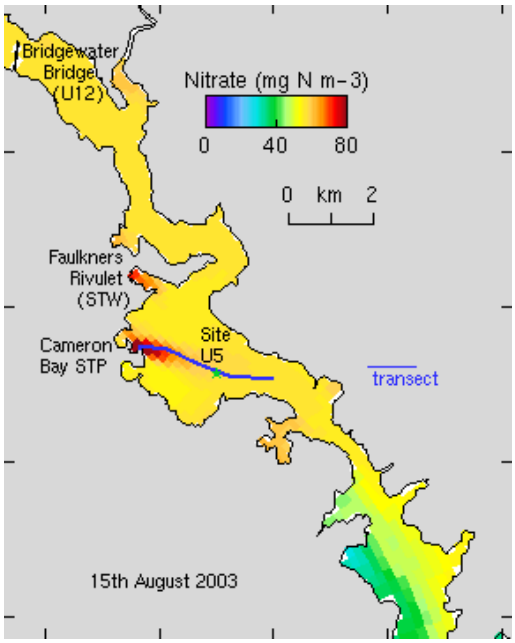

Figure 6-30 Transect from Cameron Bay used for Figure 6-31 cross section plots.

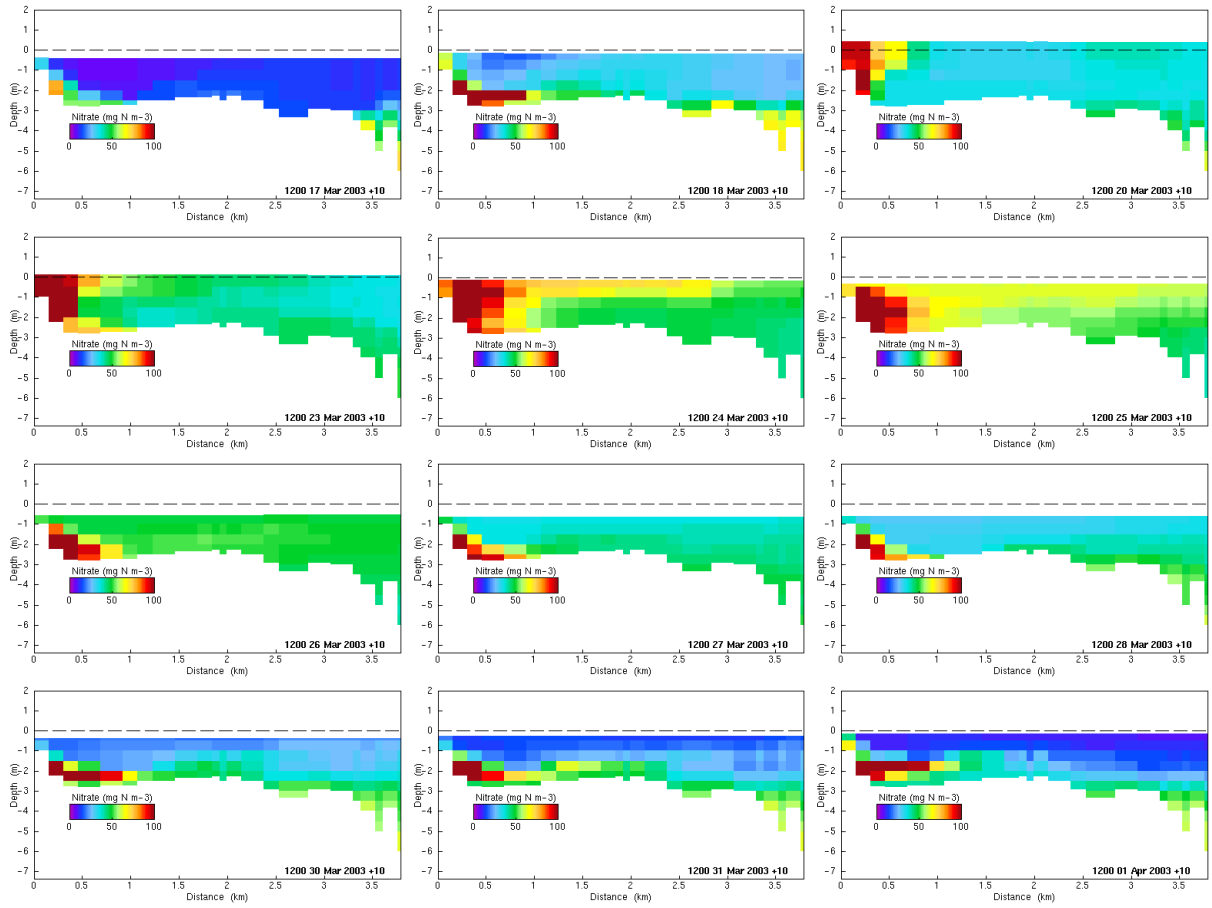

Figure 6-31 Daily cross sections across Elwick Bay of stormwater and sewage treatment plant nitrate plumes during March 2003. Transect location shown in Figure 6-30

6.6 Nitrogen Budget

As nitrogen is the nutrient of most limited supply for phytoplankton and macrophyte growth in the estuary a nitrogen budget was constructed to inform management of nutrient supply and export from the estuary. Nitrogen influx to the estuary was computed from point source loads of industrial, STP and stormwater nitrogen. The contribution from the Derwent River was determined by evaluating the flux of all nitrogen tracers across a section adjacent to the model boundary at New Norfolk. The flux across the marine boundary was estimated from the sum of day mean depth-integrated flux of all nitrogen tracers across a section adjacent to the marine boundary. Day mean fluxes were considered to avoid over-estimation of ventilation across the section due to small scale tidal excursions. A disadvantage of using depth-integrated flux is that on days with persistent depth-stratified reversal of flow the influx or export could be significantly larger, but the net flux of nutrients will be the same.

In 2003 the greatest influx of nitrogen to the estuary was the depth-integrated flux across the marine boundary 44%, followed by the Derwent river 29%. STPs inputs accounted for 18%, stormwater 6% and industry loads 3% of the total annual nitrogen load to the estuary. Export of nitrogen from the estuary was by denitrification (59%) and by the depth-integrated flux across the marine boundary (41%) (Figure 6-32, Figure 6-33). The budget suggests that in 2003 there was a net accumulation of nitrogen in the estuary of ~ 44 tN/y, however given the magnitude of fluxes through the estuary this value is minor. It should be noted that the model has limited capacity to bury or retain significant loads of nitrogen in the sediments as modelled refractory nitrogen is remineralised on a timescale of ~ 3 months. In localised areas of the upper and mid-estuary with high (and historically higher) organic loading, strongly anoxic sediment conditions could favour burial and retention of particulate nitrogen over much longer timescales.

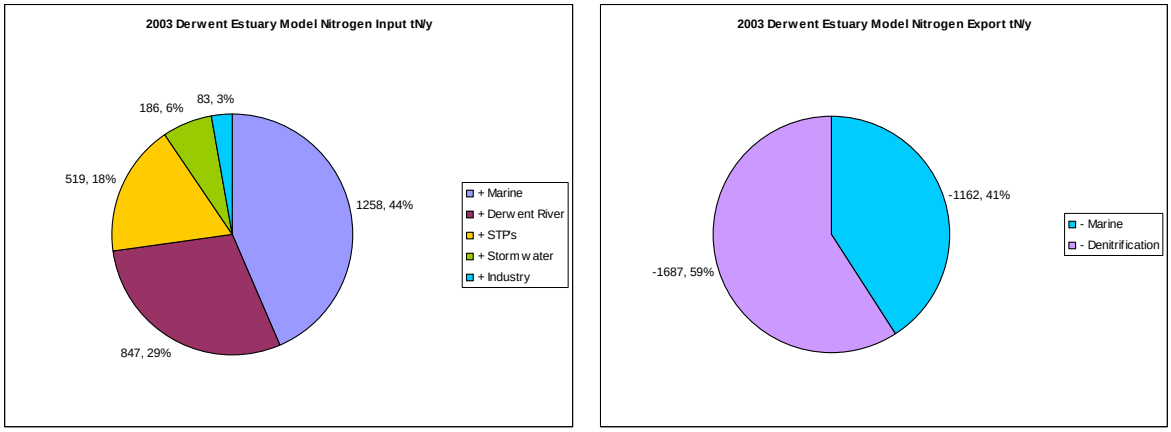

Figure 6-32 Nutrient fluxes into the estuary (left) and out of the estuary (right) in tN/y and % for each component.

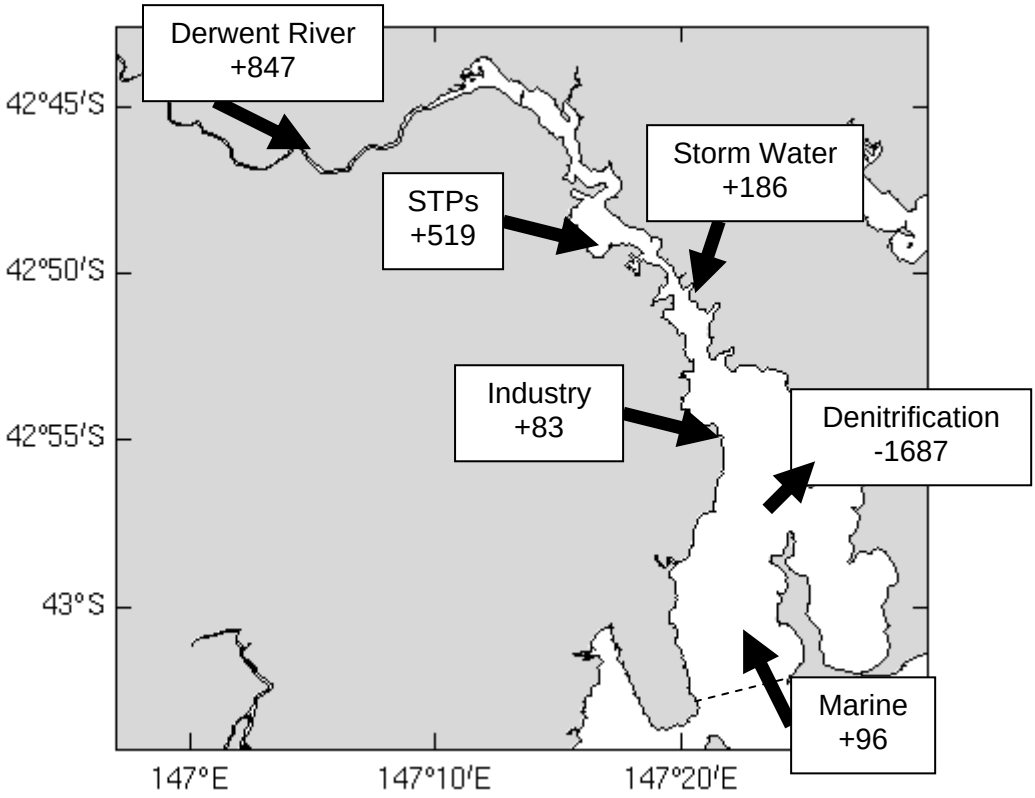

Figure 6-33 Modelled nitrogen budget for 2003 in tN/y

6.7 Chlorophyll Classification

Classification of coastal waters into oligotrophic, mesotrophic and eutrophic has been defined by Smith (1998) according to the concentration of annual mean chlorophyll in the near-surface layer. According to this classification, waters with annual mean chlorophyll concentration < 1 mg Chl m^{-3} are oligotrophic; those between 1-3 mg Chl m^{-3} are mesotrophic and waters with >3 mg Chl m^{-3} are considered to be eutrophic. Eutrophic systems often feature persistent elevated nutrient concentrations and depleted dissolved oxygen concentrations particularly in bottom waters. Many other systems have been devised to classify coastal water bodies, however the Smith (1998) is used in this report due to it's simplicity and transparency in communication.

In the Derwent estuary in 2003 modelled annual mean chlorophyll concentrations were calculated from 0-11 m of water depth or to the maximum depth in regions less than 11 m deep (Figure 6-34). Following Smith's (1998) classification 18.3 % of the modelled estuary was considered mesotrophic and 81.7 % eutrophic. There were no oligotrophic regions in the modelled estuary. Mesotrophic conditions were simulated in the lower reaches and the very south of Ralphs Bay where lower nutrient concentrations limited excessive accumulation of chlorophyll throughout the year. In the upper estuary mesotrophic conditions were found despite elevated nutrient concentrations due to light limitation of phytoplankton growth in this part of the estuary. Eutrophic conditions were simulated in the mid- and lower estuary and in the remainder of Ralphs Bay. In these locations ready access to nutrients and light allowed the simulation of high concentrations of chlorophyll and resulted in annual mean concentrations in excess of 3 mg Chl m^{-3}. In the mid-estuary and inner bays the model over

estimated the duration of the spring and autumn blooms compared to observations (see section 5.5); classification of these parts of the estuary, whilst likely still eutrophic, should be treated with caution.

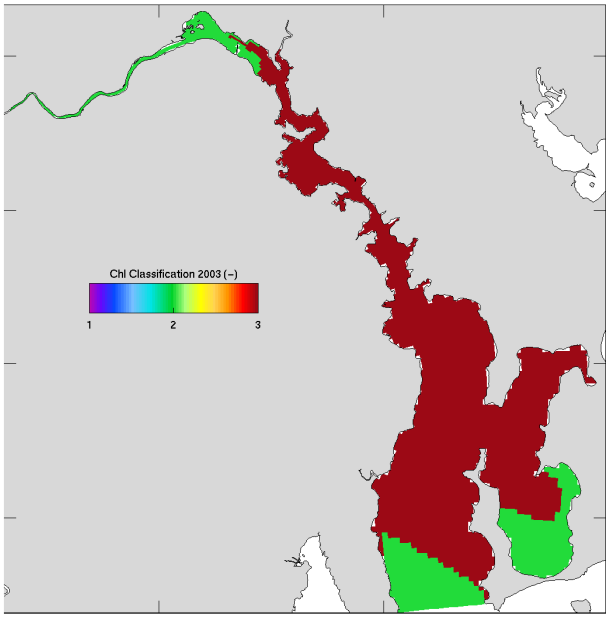

1 Oligotrophic (<1mg Chl m^{-3})	0.0 %
2 Mesotrophic (1-3mg Chl m^{-3})	18.3 %
3 Eutrophic (>3mg Chl m^{-3})	81.7 %

Figure 6-34 Regional classification (summarized in Table as % area) based on annual mean chlorophyll in near-surface (0-11m) layer and according to the classification of Smith (1998).

7. CONCLUSIONS

The objective of this project was to implement a high resolution 3D biogeochemical model of the estuary, calibrate the model against observations taken throughout the region and better characterise the cycling of carbon, nitrogen, phosphorus and dissolved oxygen in the estuary to inform managers. The calibrated biogeochemical model would also be available for scenario simulation of alternative management strategies and to reconstruct former conditions in the estuary prior to urbanisation.

A high resolution 3D biogeochemical model has been implemented and validated against observations for the Derwent Estuary. The model conserves mass and reproduces the observed seasonal cycles of nutrients (nitrate ammonia, DIP), phytoplankton, dissolved oxygen and dissolved organic carbon, at most stations throughout the estuary, very well. In the upper estuary the complex channel bathymetry is poorly resolved by the relatively coarse model grid and the hydrodynamics, sediment dynamics and biogeochemical cycles are less well constrained by the model. In Prince of Wales Bay, which has a very high nutrient load, the model did not reproduce the full range of observations, possibly due to sampling of local gradients in concentration and/or inadequate resolution of actual nutrient loads delivered to the Bay. The model also simulates the optical climate of the estuary, phytoplankton group succession, zooplankton dynamics and macrophyte growths as well as a number of sediment properties, including dissolved oxygen saturation and denitrification flux. Observations were not available to rigorously validate these components of the model however results are consistent with our understanding of the estuarine biogeochemical dynamics.

Results form the model can be used to describe the general biogeochemical dynamics of the estuary including the main channel and side bays. Where there are few or no coincident observations, model results should be treated only as a plausible hypothesis of the biogeochemical dynamics until validated against observations.

The biogeochemical model results illustrate the spatial and temporal dynamics of nitrogen, phosphorus, carbon and dissolved oxygen with unprecedented detail. A key feature of the estuary is the salt wedge salinity front which intersects the bed upstream of Elwick Bay. The model shows elevated nutrient, chlorophyll and depleted oxygen concentrations occur adjacent to the front, which delineates highly attenuating fresher water from more transparent saline water. Point source loads to the estuary appear to be retained and accumulate in the estuarine re-circulation resulting in a highly productive mid estuarine region. Modelled remineralisation of organic material, in deep water and sediment, draws down dissolved oxygen and facilitates coupled nitrification and denitrification of ammonia in the sediment. In shallow water light penetrates through the modelled water column to the epi-benthos, and supports macrophyte growth. The model suggests seagrass could grow in Ralphs Bay whilst macroalgae might dominate in Elwick bay and further upstream where elevated nutrient concentrations favour epiphytic growth [recent observations show a contrasting distribution of macrophytes likely resulting from historical succession and substrate conditions that have not been included in the model].

The simulated nitrogen budget for the estuary suggests that the estuary is in near steady state. Significant nitrogen fluxes into the estuary include marine, river and STP sources. Model results show that denitrification is the most important export term accounting for 59% of the total nitrogen export from the estuary. Recent observations of denitrification at sites in the estuary are of a similar order of magnitude to model results, however high small scale spatial and temporal variation in the observations confounds generalisation to larger scales.

Classification of the modelled estuary by annual mean chlorophyll concentration in near-surface waters concludes that 18.3 % of the region is mesotrophic (1-3 mg Chl m^{-3}) and 81.7 % of the region is eutrophic (>3 mg Chl m^{-3}). Mesotrophic regions include the upper reaches, where high attenuation limits phytoplankton growth, and the lower reaches and southern Ralphs Bay, where surface nutrients are depleted for much of the year. Eutrophic regions correspond to the mid- and lower estuary and the remainder of Ralphs Bay, where phytoplankton access to light and nutrients facilitates accumulation of biomass for extended periods of the year.

8. RECOMMENDATIONS FOR FUTURE WORK

Whilst it has been possible to validate some aspects of the pelagic biogeochemistry at a number of locations throughout the estuary, many components of this study have been difficult or impossible to verify with the limited range and type of observations routinely made. Recent developments in sensor technology allow some variables to be observed with very high spatial and temporal resolution for example from moored or underway systems and autonomous underwater vehicles. It would be useful for the future observing program to include greater diversity in the spatial and temporal scale of their observations to provide insights into the estuarine biogeochemistry and model validation data, over a range of scales.

In addition to the observations routinely made in the estuary some information on phyto- and zoo-plankton type or species, biomass and growth or grazing rate would allow these aspects of the model to be more rigorously constrained. Data on the main macrophyte species and estimates of biomass would be helpful and facilitate some development of the model to accommodate contrasting benthic substrate and levels of disturbance for the improved resolution of macrophyte beds.

This modelling study suggests a key process in the estuary maintaining the ‘health’ of the ecosystem is denitrification. For improved confidence in the model resolution of detrital

remineralisation, sediment oxygen dynamics and denitrification processes it would be valuable to complete a process study and compare the model algorithms and parameterisations against detailed observations of these processes. Information on the impact of local fauna bioturbation and bioirrigation on sediment biogeochemistry would also be helpful.

The current modelling study is limited to a specific time period where initialisation fields, boundary forcing, validation data, calibrated hydrodynamic and sediment models exist. This has limited the generalisation of results to other years with contrasting environmental forcing e.g. river flows or marine exchange. Future model development should focus of the implementation of an operational biogeochemical model which is routinely updated with the latest environmental conditions and most recent advances in science understanding.

9. REFERENCES

Baird, M. E. and Emsley S. M. 1999. Towards a mechanistic model of plankton population dynamics. Journal of Plankton Research, 21:85-126.

Butler, E. 2005 The tail of two rivers in Tasmania: The Derwent and Huon Estuaries. Handbook of Environmental Chemistry, 5: 1-49.

CSIRO Huon Estuary Study Team (2000) Huon Estuary Study – Environmental research for integrated catchment management and aquaculture. Fisheries Research and Development Corporation. Project Number 96/284, June 2000. CSIRO Division of Marine Research. Marine Laboratories, Hobart 285p

DPIWE 2003. Land Use Mapping at Catchment Scale. Department of Primary Industries, Water and Environment, Tasmania.

CSIRO Huon Estuary Study Team (2000) Huon Estuary Study – Environmental research for integrated catchment management and aquaculture. Fisheries Research and Development Corporation. Project Number 96/284, June 2000. CSIRO Division of Marine Research. Marine Laboratories, Hobart 285p

Edgar G.J., Barrett N.S., Graddon D.J. 1999 A classification of Tasmanian estuaries and assessment of their conservation significance using ecological and physical attributes, population and land use. Technical report series no 2. Tasmanian Aquaculture and Fisheries Institute, Hobart www.utas.edu.au/tafi/PDF_files/Tech_Report_2_Edgar_Barrett.pdf

Fogg, G. E. 1991. Tansley Review No. 30: The phytoplanktonic ways of life. New Phytology. 118:191-232.

Green, G., Coughanowr, C. 2003. State of the Derwent Estuary: a review of pollution sources, loads and environmental quality data from 1997-2003, Derwent Estuary Program, DPIWE, Tasmania.

Harris, G., Batley, G., Fox, D., Hall, D., Jernakoff, P., Molloy, R., Murray, A., Newell, B., Parslow, J., Skyring, G. & Walker, S. 1996. Port Phillip Bay Environmental Study Final Report. CSIRO, Canberra, Australia.

Herzfeld, M., Parslow, J., Margvelashvili, N., Andrewartha, J.R. and Sakov, P. 2005a. Numerical Hydrodynamic Modelling of the Derwent Estuary. CSIRO Marine and Atmospheric Research, Derwent Estuary Program, Final Report, 91 pp.

Herzfeld, M., Parslow, J., Sakov, P. Andrewartha, J.R. 2005b. Numerical hydrodynamic modelling of the D'Entrecasteaux Channel and Huon Estuary. Aquafin CRC Technical report, CSIRO, Hobart, Australia.

Hydro Tasmania Consulting 2008. Stage 1 Report: An Assessment of Surface Water Quality Monitoring in the NRM South Region, Tasmania. Hydro-electric Corporation, Hobart.

Margvelashvili, N. 2003. MECOSED: Model for estuarine and coastal sediment transport. CSIRO Report, 53 pp.

Margvelashvili, N., Herzfeld, M., Parslow, J., 2005. Numerical modelling of fine sediment and zinc transport in the Derwent Estuary. CSIRO Marine and Atmospheric Research, Derwent Estuary Program, Final Report, 51 pp.

Murray, A.G., Parslow, J.S. 1997. Port Phillip Bay integrated model: final report no. 44. Canberra, ACT: CSIRO Environmental Projects Office. Port Phillip Bay Environmental Study. (Technical report. CSIRO Port Phillip Bay Environmental Study), 201 pp.

Murray, A.G., Parslow, J.S. 1999. Modelling of nutrient impacts in Port Phillip Bay – a semi enclosed marine Australian ecosystem. Marine and Freshwater Research 50: 597–611.

Parslow, J.S, Margvelashvili, N., Palmer D., Revill, A.T., Robson, B., Sakov, P.V., Volkman, J.K., Watson, R.J., Webster, I.T. 2003. The response of the lower Ord River and estuary to management of catchment flows and sediment and nutrient loads. Final science report Ord–Bonaparte Program project 3.4/4.1/4.2. 111 pp.

Parslow, J., Herzfeld, M., Hunter, J.R., Andrewartha, J.R., Sakov P., Waring J. 2001. Mathematical Modelling of the Dispersal and Fate of CES Discharge from the Boyer Mill in the Upper Derwent Estuary. Final Report. CSIRO Marine Research, Hobart.

Robson, B., Webster, I., Margvelashvili, N., Herzfeld, M., 2006. Scenario modelling: simulating the downstream effects of changes in catchment land use. Cooperative Research Centre for Coastal Zone, Estuary and Water Way Management, Technical Report No.41, Indooroopilly, Australia, 34 pp.

Rykiel, E.J.Jr. 1996. Testing ecological models: the meaning of validation. Ecological Modelling 90:229-244.

SEAMAP www.utas.edu.au/tafi/seamap

Smith, V. H. 1998. Cultural eutrophication of inland, estuarine and coastal waters. In: Successes, Limitation and Frontiers in Ecosystem Science. Pace, M. L. and P. M. Groffman (eds.) pp. 7-49, Springer-Verlag, New York, New York.

Walker, S.J. 1997. A transport model of Port Phillip Bay. Port Phillip Bay Environment Study Technical Report no. 39, Melbourne.

Webster I.T., Parslow J.S., Grayson R.B., Molloy R.P., Andrewartha J., Sakov P., Tan K.S., Walker S.J., Wallace B.B. (2001) Gippsland Lakes environmental study: Assessing options for improving water quality and ecological function. (CSIRO, Glen Osmond, South Australia)

Wild-Allen, K., Parslow, J. Herzfeld, M., Sakov, P., Andrewartha, J. and Rosebrock, U. (2005). Biogeochemical modelling of the D'Entrecasteaux Channel and Huon Estuary. Aquafin CRC Technical Report, Hobart, Australia.

Wild-Allen, K., Skerratt, J., Rizwi, F., and Parslow, J. (2009). Derwent Estuary Biogeochemical Model: Management Scenario Report. CSIRO Marine and Atmospheric Research Report, Hobart, Australia.

10. APPENDICES

Appendix 10-1 Parameter file for Derwent Estuary biogeochemical model: final calibrated run is run40

Parameter0.name ZL_E
Parameter0.desc Growth eff large zooplankton
Parameter0.units none
Parameter0.value 0.38

Parameter1.name ZS_E
Parameter1.desc Growth efficiency, small zooplankton
Parameter1.units none
Parameter1.value 0.38

Parameter2.name SG_KN
Parameter2.desc Half-saturation of SG N uptake in SED
Parameter2.units mg N m^{-3}
Parameter2.value 15.0

Parameter3.name SG_KP
Parameter3.desc Half-saturation of SG P uptake in SED
Parameter3.units mg N m^{-3}
Parameter3.value 15.0

Parameter4.name PhyL_mL
Parameter4.desc Natural (linear) mortality rate, large phytoplankton (in sediment)
Parameter4.units d^{-1}
Parameter4.value 0.14

Parameter5.name PhyS_mL
Parameter5.desc Natural (linear) mortality rate, small phytoplankton (in sediment)
Parameter5.units d^{-1}
Parameter5.value 0.14

Parameter6.name MA_mL
Parameter6.desc Natural (linear) mortality rate, macroalgae
Parameter6.units d^{-1}
Parameter6.value 0.01

Parameter7.name SG_mL
Parameter7.desc Natural (linear) mortality rate, seagrass
Parameter7.units d^{-1}
Parameter7.value 0.00275

Parameter8.name MPB_mQ
Parameter8.desc Natural (quadratic) mortality rate, microphytobenthos
Parameter8.units d^{-1} (mg N m^{-3})$^{-1}$
Parameter8.value 0.0001

Parameter9.name ZL_mQ
Parameter9.desc Natural (quadratic) mortality rate, large zooplankton
Parameter9.units d^{-1} (mg N m^{-3})$^{-1}$
Parameter9.value 0.016

Parameter10.name ZS_mQ
Parameter10.desc Natural (quadratic) mortality rate, small zooplankton
Parameter10.units d^{-1} (mg N m^{-3})$^{-1}$
Parameter10.value 0.02

Parameter11.name ZL_FDG
Parameter11.desc Fraction of growth inefficiency lost to detritus, large zooplankton
Parameter11.units none
Parameter11.value 0.5

Parameter12.name ZL_FDM
Parameter12.desc Fraction of mortality lost to detritus, large zooplankton
Parameter12.units none
Parameter12.value 0.5

Parameter13.name ZS_FDG
Parameter13.desc Fraction of growth inefficiency lost to detritus, small zooplankton
Parameter13.units none
Parameter13.value 0.5

Parameter14.name ZS_FDM
Parameter14.desc Fraction of mortality lost to detritus, small zooplankton
Parameter14.units none
Parameter14.value 0.5

Parameter15.name F_LD_RD
Parameter15.desc Fraction of labile detritus converted to refractory detritus
Parameter15.units none
Parameter15.value 0.19

Parameter16.name F_LD_DOM
Parameter16.desc Fraction of labile detritus converted to dissolved organic matter
Parameter16.units none
Parameter16.value 0.01

Parameter17.name NtoCHL
Parameter17.desc Nitrogen:Chlorophyll A ratio in phytoplankton by weight
Parameter17.units m^{-1}
Parameter17.value 7

Parameter18.name k_w
Parameter18.desc Background light attenuation coefficient
Parameter18.units none
Parameter18.value 0.1

Parameter19.name k_DOR_N
Parameter19.desc DOR_N-specific light attenuation coefficient
Parameter19.units m^{-1} (mg N m^{-3})$^{-1}$
Parameter19.value 0.0009

Parameter20.name k_DetL
Parameter20.desc Detrital N-specific light attenuation coefficient
Parameter20.units m^{-1} ($mgNm^{-3}$)$^{-1}$
Parameter20.value 0.0038

Parameter21.name k_TSS
Parameter21.desc TSS-specific light attenuation coefficient
Parameter21.units m^{-1} (kg m^{-3})$^{-1}$
Parameter21.value 30.0
Parameter22.name k_C_fw

Parameter22.desc CDOM attentuation coefficient of freshwater
Parameter22.units m^{-1}
Parameter22.value 1.0

Parameter23.name k_SWR_PAR
Parameter23.desc fraction of incident solar radiation that is PAR
Parameter23.units none
Parameter23.value 0.43

Parameter24.name Q10
Parameter24.desc Temperature coefficient for rate parameters
Parameter24.units none
Parameter24.value 2.0

Parameter25.name PLumax
Parameter25.desc Maximum growth rate of PL at Tref
Parameter25.units d^{-1}
Parameter25.value 1.25

Parameter26.name PLrad
Parameter26.desc Radius of the large phytoplankton
Parameter26.units m
Parameter26.value 10e-06

Parameter27.name PLabsorb
Parameter27.desc Absorption coefficient of a PL cell
Parameter27.units m^{-1}
Parameter27.value 50000.

Parameter28.name PLSh
Parameter28.desc Sherwood number for the PS dimensionless
Parameter28.units none
Parameter28.value 1

Parameter29.name PLtable
Parameter29.desc Netcdf lookup table
Parameter29.units none
Parameter29.value /home/mgproja/fitz/data/biology/10plkINP.nc

Parameter30.name PLn
Parameter30.desc Number of limiting nutrients
Parameter30.units none
Parameter30.value 3

Parameter31.name PSumax
Parameter31.desc Maximum growth rate of PS at Tref
Parameter31.units d^{-1}
Parameter31.value 1.25

Parameter32.name PSrad
Parameter32.desc Radius of the large phytoplankton cells
Parameter32.units m
Parameter32.value 2.5e-06
Parameter33.name PSabsorb

Parameter33.desc Absorption coefficient of a PS cell
Parameter33.units m^{-1}
Parameter33.value 50000

Parameter34.name PSSh
Parameter34.desc Sherwood number for the PL dimensionless
Parameter34.units none
Parameter34.value 1

Parameter35.name PStable
Parameter35.desc Netcdf lookup table
Parameter35.units none
Parameter35.value /home/mgproja/fitz/data/biology/10plkINP.nc

Parameter36.name PSn
Parameter36.desc Number of limiting nutrients
Parameter36.units none
Parameter36.value 3

Parameter37.name MBumax
Parameter37.desc Maximum growth rate of MB at Tref
Parameter37.units d^{-1}
Parameter37.value 0.35

Parameter38.name MBrad
Parameter38.desc Radius of the large phytoplankton cells
Parameter38.units m
Parameter38.value 10e-06

Parameter39.name MBabsorb
Parameter39.desc Absorption coefficient of a MB cell
Parameter39.units m^{-1}
Parameter39.value 50000

Parameter40.name MBSh
Parameter40.desc Sherwood number for the PL dimensionless
Parameter40.units none
Parameter40.value 1

Parameter41.name MBtable
Parameter41.desc Netcdf lookup table
Parameter41.units none
Parameter41.value /home/mgproja/fitz/data/biology/10plkINP.nc

Parameter42.name MBn
Parameter42.desc Number of limiting nutrients
Parameter42.units none
Parameter42.value 3

Parameter43.name MAumax
Parameter43.desc Maximum growth rate of MA at Tref
Parameter43.units d^{-1}
Parameter43.value 0.02

Parameter44.name MAaA
Parameter44.desc Nitrogen specific absorption cross-section of MA
Parameter44.units m^2 mgN^{-1}
Parameter44.value 1e-03

Parameter45.name MAtable
Parameter45.desc Netcdf lookup table
Parameter45.units none
Parameter45.value /home/mgproja/fitz/data/biology/10benINP.nc

Parameter46.name MAn
Parameter46.desc Number of limiting nutrients
Parameter46.units none
Parameter46.value 3

Parameter47.name MAm
Parameter47.desc Stoichometry coefficient of Phosphorus
Parameter47.units none
Parameter47.value 2.4e-06

Parameter48.name SGumax
Parameter48.desc Maximum growth rate of SG at Tref
Parameter48.units d^{-1}
Parameter48.value 0.1

Parameter49.name SGaA
Parameter49.desc N specific absorp cross-section of SG
Parameter49.units m^2 mgN^{-1}
Parameter49.value 1e-05

Parameter50.name SGm
Parameter50.desc Stoichometry coefficient of Phosphorus
Parameter50.units none
Parameter50.value 2.4e-06

Parameter51.name ZSumax
Parameter51.desc Maximum growth rate of small zooplankton at Tref
Parameter51.units d^{-1}
Parameter51.value 3

Parameter52.name ZSrad
Parameter52.desc Radius of the small zoop cells
Parameter52.units m^{-1}
Parameter52.value 12.5e-06

Parameter53.name ZSswim
Parameter53.desc Swimming velocity small zooplankton
Parameter53.units m s^{-1}
Parameter53.value 2.0e-4

Parameter54.name ZSmeth
Parameter54.desc Grazing technique of small zooplankton
Parameter54.units none
Parameter54.value rect

Parameter55.name ZLumax
Parameter55.desc Maximum growth rate of large zooplankton at Tref
Parameter55.units d^{-1}
Parameter55.value 0.1

Parameter56.name ZLrad
Parameter56.desc Radius of the large zoop cells
Parameter56.units m^{-1}
Parameter56.value 500e-06

Parameter57.name ZLswim
Parameter57.desc swimming velocity for large zooplankton
Parameter57.units m s^{-1}
Parameter57.value 1.5e-3

Parameter58.name ZLmeth
Parameter58.desc Grazing technique of small zoo
Parameter58.units none
Parameter58.value rect

Parameter59.name TKEeps
Parameter59.desc TKE dissipation in water column
Parameter59.units m^2s^{-3}
Parameter59.value 1.0e-6

Parameter60.name cf
Parameter60.desc drag coefficient of the benthic surface
Parameter60.units none
Parameter60.value 0.005

Parameter61.name Ub
Parameter61.desc velocity at the top of the ben. bound. layer
Parameter61.units m s^{-1}
Parameter61.value 0.1

Parameter62.name ks
Parameter62.desc sand-grain roughness of the benthos
Parameter62.units m
Parameter62.value 0.1

Parameter63.name F_RD_DOM
Parameter63.desc fraction of refractory detritus that breaks down to DOM
Parameter63.units none
Parameter63.value 0.05

Parameter64.name r_floc
Parameter64.desc rate at which TSS flocculates above 10 PSU
Parameter64.units d^{-1}
Parameter64.value 0.01

Parameter65.name r_DetPL
Parameter65.desc Breakdown rate of labile detritus at 106:16:1
Parameter65.units d^{-1}
Parameter65.value 0.2

Parameter66.name r_DetBL
Parameter66.desc Breakdown rate of labile detritus at 550:30:1
Parameter66.units d^{-1}
Parameter66.value 0.1

Parameter67.name r_RD
Parameter67.desc Breakdown rate of refractory detritus
Parameter67.units d^{-1}
Parameter67.value 0.005

Parameter68.name r_DOM
Parameter68.desc Breakdown rate of dissolved organic matter
Parameter68.units d^{-1}
Parameter68.value 0.00176

Parameter69.name Tref
Parameter69.desc Reference temperature
Parameter69.units ºC
Parameter69.value 15.0

Parameter70.name Plank_resp

Parameter70.desc Respiration as a fraction of umax
Parameter70.units none
Parameter70.value 0.025

Parameter71.name Benth_resp
Parameter71.desc Respiration as a fraction of umax
Parameter71.units none
Parameter71.value 0.025

Parameter72.name DFumax
Parameter72.desc Maximum growth rate of dino at Tref
Parameter72.units d^{-1}
Parameter72.value 0.2

Parameter73.name DFrad
Parameter73.desc Radius of Dinoflagellate cells
Parameter73.units m
Parameter73.value 10.0e-6

Parameter74.name DFabsorb
Parameter74.desc Absorption coefficient of a dinoflagellate cell
Parameter74.units m^{-1}
Parameter74.value 30000.0

Parameter75.name DFSh
Parameter75.desc Sherwood number for Dinoflagellate
Parameter75.units none
Parameter75.value 1.0

Parameter76.name DFn
Parameter76.desc Number of limiting nutrients for Dinoflagellate
Parameter76.units none
Parameter76.value 3

Parameter77.name DFtable
Parameter77.desc Netcdf lookup table for Dinoflagellate
Parameter77.units none
Parameter77.value /home/mgproja/fitz/data/biology/10plkINP.nc

Parameter88.name DFCtoNvar
Parameter88.desc Maximal to minimal C:N ratio in Dinoflagellate
Parameter88.units none
Parameter88.value 1.5
Parameter88.adjust 0

Parameter89.name KO_aer
Parameter89.desc Oxygen half-saturation for aerobic respiration
Parameter89.units mg O m^{-3}
Parameter89.value 500.0

Parameter90.name r_nit_wc
Parameter90.desc Maximal nitrification rate in water column
Parameter90.units d^{-1}
Parameter90.value 0.1

Parameter91.name r_nit_sed
Parameter91.desc Maximal nitrification rate in water sediment
Parameter91.units d^{-1}
Parameter91.value 20.0

Parameter92.name KO_nit
Parameter92.desc Oxygen half-saturation for nitrification
Parameter92.units mg O m^{-3}
Parameter92.value 500.0

Parameter93.name Pads_r
Parameter93.desc Rate at which P reaches adsorbed/desorbed equilibrium
Parameter93.units d^{-1}
Parameter93.value 0.04

Parameter94.name Pads_Kwc
Parameter94.desc Freundlich Isothermic Const P adsorption to TSS in water column
Parameter94.units mg P kg TSS^{-1}
Parameter94.value 300.0

Parameter95.name Pads_Ksed
Parameter95.desc Freundlich Isothermic Const P adsorption to TSS in sediment
Parameter95.units mg P kg TSS^{-1}
Parameter95.value 74.0

Parameter96.name Pads_KO
Parameter96.desc Oxygen half-saturation for P adsorption
Parameter96.units mg O m^{-3}
Parameter96.value 2000.0

Parameter97.name Pads_exp
Parameter97.desc Exponent for Freundlich Isotherm
Parameter97.units none
Parameter97.value 1.0

Parameter98.name PD_mL
Parameter98.desc Linear mortality for dinoflagellate in sediment
Parameter98.units d^{-1}
Parameter98.value 0.14

Parameter99.name r_den
Parameter99.desc Maximum denitrification rate
Parameter99.units d^{-1}
Parameter99.value 40.0

Parameter100.name KO_den
Parameter100.desc Oxygen content at 50% denitrification rate
Parameter100.units mg O m^{-3}
Parameter100.value 10000.0

Parameter101.name r_floc_sed
Parameter101.desc Rate of the TSS floculation in sediment
Parameter101.units d^{-1}
Parameter101.value 0.001

Parameter102.name r_bury_TSS
Parameter102.desc Rate of the TSS burying
Parameter102.units d^{-1}
Parameter102.value 0.001

Parameter103.name r_immob_PIP
Parameter103.desc Rate of conversion of PIP to immobilised PIP
Parameter103.units d^{-1}
Parameter103.value 0.0012

Parameter104.name IDF
Parameter104.desc Saturation light intensity for dinoflagellates
Parameter104.units mol photons m^{-2} s^{-1}
Parameter104.value 1.0e-4

Parameter105.name Fmax_Nit_sed
Parameter105.desc Maximum nitrification efficiency
Parameter105.units
Parameter105.value 1.0

Parameter106.name EpiDiffCoeff
Parameter106.desc Diffusion Coefficient
Parameter106.units m^2s^{-1}
Parameter106.value 3e-9

Parameter107.name EpiDiffDz
Parameter107.desc Thickness of diffusive layer
Parameter107.units m
Parameter107.value 0.0065

Parameter108.name k_Mill
Parameter108.desc Mill Kd Proxy
Parameter108.units m^{-1}
Parameter108.value 10.

Parameter109.name r_LOC
Parameter109.desc remineralisation rate of Labile Organic C
Parameter109.units d^{-1}
Parameter109.value 0.4

Parameter110.name r_ads_LDOC
Parameter110.desc adsorption of LDOC onto LPOC
Parameter110.units d^{-1}
Parameter110.value 0.4

Parameter111.name F_Bact
Parameter111.desc max growth rate of bacteria
Parameter111.units d^{-1}
Parameter111.value 0.4

Parameter112.name KN_bact
Parameter112.desc N half saturation for bact growth
Parameter112.units mg N m^{-3}
Parameter112.value 3.0

Parameter113.name KP_bact
Parameter113.desc P half saturation for bact growth
Parameter113.units mg P m^{-3}
Parameter113.value 3.0

Appendix 10-2 Hobart Rainfall runoff - catchment modelling : Jason Whitehead et al. Derwent Estuary Program 2008

Daily water volume and pollutant loading to the Derwent Estuary, from sub-catchments surrounding the greater Hobart region were modelled using “Model for Urban Stormwater Improvement Conceptualisation” Version 3.0.1 software (MUSIC) (CRC Catchment Hydrology). The modelling work was undertaken by the Derwent Estuary Program to identify daily water volume, total nitrogen and total phosphorus released into the Derwent Estuary from the sub-catchments in the greater Hobart region.

Individual model scenario runs were established for each sub-catchment, at daily rainfall input and pollutant output frequency, for the time period 1 Jan 2003 to 31 March 2004 (inclusive). Those sub-catchments that included a large altitudinal variation were often sub-divided into upper and lower sub-catchments, as different rainfall conditions typically occur with altitude. Preparation of data from the modelling task included a number of steps:

Classification of greater Hobart region sub-catchments into different land use categories (Urban, Forested, Agricultural). For those areas designated urban it was necessary to define the portion of urban areas covered with impermeable surfaces. Imagery was used for this task. The *MUSIC* software uses algorithms for the pollutant modelling (see Duncan (1999)), which were retained at their default setting for this study. However, soil property data was added as a generalised estimate of Hobart soil conditions:

Forest and agricultural areas were made 100% pervious to water

Soil storage capacity = 30 mm

Initial soil storage (% of capacity) = 30

Field capacity = 20 mm

Infiltration capacity coefficient – a = 200

Infiltration capacity coefficient – b = 1

Ground water initial depth = 10 mm

Ground water daily recharge rate = 25%

Ground water base-flow rate = 5%

Ground water daily deep seepage rate = 0%

A subjective choice was required for the most appropriate rainfall stations to be used in the modelled scenarios. Manual daily rainfall stations from 18 sites around Hobart were chosen to provide the highest coverage of localised rainfall differences across the region. In most instances the rainfall station within or closest to the individual sub-catchments was used

The stormwater data and land us e information has been modified for a number of different CSIRO biogeochemical modelling scenarios as mentioned in the main body of this report.

There are some limitations with *MUSIC* for accurately calculating water flow to the Derwent Estuary:

The model does not enable calculation of the 'time of concentration' (e.g., the time it takes for water to travel from the place it has fallen as rain, to the point of arrival in the Derwent Estuary). However, the daily frequency of data output and relatively short travel distance within the Hobart regional sub-catchments negates this somewhat.

The flow is also based upon daily manual rainfall data, which is collect at 9 am but in the case of the model dates is recorded as the previous days rainfall total, creating some inaccuracy in the timing of pollutant loading to the estuary.

The model gives no consideration to the distance that water may have to travel (either over land, as groundwater or via streams) before being discharged to the Derwent. The simplified soil properties above reflect the shallow soils over much of the steeper topographic areas around Hobart; however, there is little allowance for water loss via infiltration to groundwater.

The flow outputs are most likely over-estimated as may be the increase in flow response following rainfall.

The nutrient values appear to overestimate observed values in the rivulets and this may be due to biological activity within the rivulets such as marsh/seagrass, weed etc.

Nevertheless, given the general lack of flow meter data from most rivulets in the Hobart region, the *MUSIC* models enables some generalised calculation of potential flow based on catchment size.

The *MUSIC* models have not been constructed to include water quality improvement arising from rivulets, of which there are many in the Hobart region. To enable some understanding of the improvement in water quality that may be offered by Hobart's rivulets the modelled TN and TP output was compared to actual measurements of TN & TP at 7 sites from 7 rivulets throughout the Hobart region over the period 1-Jan-2003 to 31-Dec-2003. The modelled results were typically higher that the observed results (TN (obs./model) = 0.48; TP (obs./model) = 0.37; TSS 0.001-2.1). At times there were anomalous spikes in the measured TN and TP that exceeded the modelled values, which may reflect activities in the catchments (e.g. fertiliser application etc). The difference between modelled and observed TN & TP may reflect the simplification of the model in that no rivulet amelioration to nutrient inputs is determined.

As a result of these findings, a multiplier has been applied to the original MUSIC output data (see body text) for those sub-catchments discharging to the Derwent via rivulets. Adjustment based on similarities to observed measurements from rivulets of similar urban/forested nature were also made to those catchments that do not discharge via major rivulets. CSIRO scientists have also differentiated the modelled TN and TP output data into various nutrients species as mentioned in the body of this report based on land-use information provided by the Derwent Estuary Program.

Duncan, H.P., (1999). *Urban stormwater quality: a statistical overview*. Report 99/3 Cooperative Research Centre for catchment hydrology

Appendix 10-3 Storm water loads– table continues on next page

Catchment kg/14.5 months	NO_3	NH_4	Dissolved Inorganic P	Labile Detrital N	Dissolved Organic N
albion	258	0	9	563	11
ashburton	3325	175	306	11272	444
barrossa	185	99	17	504	1
bedlam	103	5	8	332	29
beedhams	116	62	14	315	1
bellerive	175	94	10	476	2
blackmansbay	89	48	32	1045	8
blacksnake	281	15	39	958	32
blackstone	164	9	15	555	24
bonnet	90	0	5	199	0
bowen	216	11	24	723	39
browns	7595	0	633	12742	0
brdigewater	1321	0	132	4424	0
cartwright	305	0	15	670	7
cassidys	148	8	13	502	19
channel	140	0	5	308	2
connewarre	79	42	3	928	0
cornelian	20	11	1	238	0
dwnt_north	1672	0	220	5597	0
dwnt_south	9253	0	838	30969	9
dixons	119	0	5	261	3
droughty	622	0	106	1466	404
faulkners	2850	0	204	9526	0
folder	370	0	17	814	7
gagebrook	1321	0	132	4421	0
gibsons	253	0	152	674	11
geilston	582	50	88	1934	426
goodwood	195	105	8	325	0
gordons	152	82	9	413	1
granton	454	24	49	1521	77
hinsby	90	0	4	198	1
hobart	603	325	58	1649	0
howrah	216	116	13	590	2
humphrey	1158	0	64	3776	101
islet	607	0	29	2029	3
jaques	20	11	1	232	0
kingston	32	17	8	379	2
knopwood	128	69	7	350	0
lauderdale	1339	0	394	4483	0
lindisfarne	38	21	2	105	0
lipscombe	179	0	6	394	3
littlejohn	267	144	15	447	0

manning	422	0	18	930	9
mather	1837	0	852	5488	35
montagu	94	51	4	256	1
mortimer	1308	0	424	4378	2
natone	18	10	1	49	0
newtown	298	67	29	771	0
norfolk	955	0	87	3159	40
oldbeach	147	8	18	500	19
opossum	2280	120	194	7725	309
otago	583	31	64	1915	141
risdon	1859	148	99	3673	0
rokeby	2803	0	879	9384	0
rose	80	43	6	218	1
rosny	1171	102	91	2447	68
rusts	984	52	85	3424	45
sandybay	910	490	56	2489	0
shottower	41	0	2	90	1
skillion	53	28	3	237	0
springfield	1095	590	46	1829	0
sullivans	394	212	16	657	0
taronga	118	0	3	263	1
taroona	221	0	9	489	1
thistly	136	7	7	451	30
tinderbox	712	37	71	2430	78
tranmere	125	67	7	341	0
waimea	183	0	6	400	7
wayne	399	0	19	874	12
uni	289	155	12	789	0
Total (t/14.5 months)	**55**	**4**	**7**	**161**	**2**

Appendix 10-4 Tracer concentrations used to initialise sites

site	m depth	mg/m3 DOC	mg/m3 DetPL_N	mg/m3 DetR_N	kg/m3 TSS	mg/m3 NH4	mg/m3 NO3	mg/m3 PIPUF	mg/m3 DIP	mg/m3 PhyL_N	mg/m3 PhyS_N	mg/m3 PhyD_N	mg/m3 PhyD_C
u7	0.1	3000	0	0	0.003	2	2	27.75	5	13.55	8.62	8.62	48.98
u7	3.4	2700	0	0	0.001	2	2	43.75	5	--	--	--	--
u7	6.1	2500	62.53	62.53	0.004	2	2	30.49	8	--	--	--	--
u5	0.1	2900	80.42	80.42	0.003	2	2	10.42	4	10.78	6.86	6.86	38.96
u5	2.5	2900	30.42	30.42	0.003	2	2	41.22	2	--	--	--	--
rbs	0.1	2500	132.11	132.11	0.03	2	2	7.67	2	2.77	1.76	1.76	10.02
rbs	2.3	2400	32.11	32.11	0.008	2	2	36.27	2	--	--	--	--
u4	0.1	3200	0	0	0.002	2	2	37.14	3	12.32	7.84	7.84	44.53
u4	4.1	2900	20.48	20.48	0.005	2	2	38.48	2	--	--	--	--
u4	8.9	2700	0	0	0.01	2	2	48.14	7	--	--	--	--
rbn	0.1	2400	76.14	76.14	0.009	2	2	21.83	2	3.7	2.35	2.35	13.36
rbn	5.4	2400	26.14	26.14	0.016	3	2	35.63	2	--	--	--	--
pwb	0.1	2900	0	0	0.023	149	97	71	66	54.21	34.5	34.5	195.94
pwb	3.5	2800	0	0	0.004	2	8	63	9	--	--	--	--
rb	0.1	2500	30.12	30.12	0.012	2	2	29.72	3	3.08	1.96	1.96	11.13
rb	20.3	2300	30.12	30.12	0.009	3	2	38.72	15	--	--	--	--
u3	0.1	3100	0	0	0.007	2	2	51.1	3	9.24	5.88	5.88	33.4
u3	7.5	2500	0	0	0.011	2	2	66.1	8	--	--	--	--
u3	23.9	2500	0	0	0.036	17	5	69.1	25	--	--	--	--
e	0.1	2400	82.11	82.11	0.009	3	2	19.47	2	2.77	1.76	1.76	10.02
e	24.3	2400	32.11	32.11	0.011	14	4	35.27	25	--	--	--	--
ntbo5	0.1	2900	0	0	0.009	2	2	106.33	4	11.7	7.45	7.45	42.3
ntbo5	1	2800	0	0	0.009	2	2	108.33	3	--	--	--	--
ntbo9	0.1	2800	0	0	0.007	2	2	81.01	4	9.55	6.08	6.08	34.51
ntbo9	1.4	2900	0	0	0.002	2	2	95.01	3	--	--	--	--
ntbo9	5.54	2800	0	0	0.012	3	2	69.01	3	--	--	--	--
ntb13	0.1	2900	0	0	0.015	2	2	67.33	2	11.7	7.45	7.45	42.3
ntb13	1.38	3100	0	0	0.007	2	2	68.33	2	--	--	--	--
ntb13	5.22	2700	0	0	0.025	5	2	74.33	3	--	--	--	--
gb	0.1	3100	0	0	0.009	2	2	55.39	2	8.32	5.29	5.29	30.06
gb	0.95	3100	0	0	0.007	2	2	56.39	2	--	--	--	--
gb	3.5	2800	0	0	0.016	2	2	67.39	2	--	--	--	--

Appendix 10-5 Tracer concentrations used for model end boundaries (sites B1 B3 B5 and NN).

site	datetime	meters depth	Filt Phosphate as P ug/L PO4	Nitrite and Nitrate as N ug/L NOx	Total Organic Carbon mg/l TOC	Total suspended solids (0.45um) mg/L TSS	Dissolved Organic Carbon mg/l DOC	Large Phytoplankton Nitrogen (from chl ug/L) phyLG_N	Small Phytoplankton Nitrogen (from chl ug/L) phySm_N	Dinoflagellate Nitrogen (from chl ug/L) phy_Dm	Nitrogen (Total) as N ug/L TN	Ammonia and Ammonium as N ug/l NHx
B1	20/01/2003	0.1	2	2	2.6	15	2.5	1.5	1.0	1.0	294	2
B1	24/02/2003	0.1	2	2	3.9	8	3.2	2.8	1.3	2.2	368	18
B1	24/02/2003	18.5	2	2	3.1	3	3.1	--	--	--	343	2
B1	17/03/2003	0.1	11	2	3	1	2.8	1.3	1.7	3.3	254	11
B1	17/03/2003	19	8	2	2.9	1	2.9	--	--	--	265	7
B1	16/04/2003	0.1	9	4	3	5	3.0	5.5	5.5	4.3	288	8
B1	16/04/2003	19	10	15	2.7	4	2.6	--	--	--	327	20
B1	22/05/2003	0.1	6	4	2.6	1	2.6	17.5	8.8	8.8	285	5
B1	22/05/2003	17	13	34	2.4	8	2.2	--	--	--	334	21
B1	4/09/2003	0.1	10	53	1.4	4	--	2.7	1.6	1.1	247	23
B1	4/09/2003	19	13	51	0.4	7	--	--	--	--	260	27
B1	17/11/2003	0.1	4	2	1.4	6	--	4.0	3.4	7.4	193	2
B1	17/11/2003	21	12	22	1	6	--	--	--	--	218	22
B1	22/01/2004	0.1	4	2	0.5	7	--	1.3	0.8	1.5	300	7
B1	22/01/2004	20	4	2	0.4	4	--	--	--	--	287	8
B1	26/02/2004	0.1	2	2	0.7	11	--	2.3	1.7	2.3	362	2
B1	26/02/2004	17.5	3	2	0.2	13	--	--	--	--	367	2
B1	25/03/2004	0.1	4	2	1	1	--	2.4	1.9	2.0	271	3
B1	25/03/2004	18	6	4	1	1	--	--	--	--	281	4
B3	24/02/2003	0.1	2	2	3.3	9	3.2	2.5	1.2	2.0	326	2
B3	24/02/2003	16.7	5	3	3.2	37	2.8	--	--	--	341	7
B3	17/03/2003	0.1	9	2	3	3	2.9	1.1	1.5	3.0	243	5
B3	17/03/2003	18	9	2	2.8	1	2.8	--	--	--	247	7
B3	16/04/2003	0.1	11	3	2.7	5	2.7	8.2	8.2	6.5	281	8
B3	16/04/2003	18	11	17	2.6	10	2.6	--	--	--	279	21
B3	22/05/2003	0.1	6	5	2.7	2	2.6	15.4	7.7	7.7	228	7
B3	22/05/2003	16	10	23	2.8	2	2.6	--	--	--	261	19
B3	4/09/2003	0.1	14	62	1.7	5	1.6	2.9	1.7	1.2	268	26
B3	4/09/2003	19	12	54	1.3	5	1.3	--	--	--	238	24
B3	15/10/2003	0.1	2	2	1.7	6	1.8	14.4	9.6	6.0	329	2
B3	15/10/2003	17	3	2	1.7	4	1.8	--	--	--	330	2
B3	17/11/2003	0.1	5	2	1.3	3	1.3	4.3	3.7	8.1	173	2
B3	17/11/2003	17	9	10	1.2	4	1.2	--	--	--	237	10
B3	22/01/2004	0.1	5	2	0.5	5	0.6	1.3	0.8	1.5	296	7
B3	22/01/2004	19	3	2	1.6	5	1.6	--	--	--	294	5
B3	26/02/2004	0.1	3	2	0.8	15	0.7	2.8	2.1	2.8	346	2
B3	26/02/2004	17.5	11	10	0.3	8	0.5	--	--	--	377	16
B3	25/03/2004	0.1	6	2	0.7	1	0.5	3.2	2.5	2.7	262	3
B3	25/03/2004	18	3	2	0.6	1	0.4	--	--	--	276	3
B5	20/01/2003	0.1	2	2	2.6	11	2.5	2.2	1.4	1.4	269	4
B5	20/01/2003	11	3	2	2.7	13	2.5	--	--	--	282	2
B5	24/02/2003	0.1	2	2	3.2	14	3.2	3.1	1.5	2.5	321	2
B5	24/02/2003	11.1	6	2	3.1	9	3.1	--	--	--	340	2
B5	17/03/2003	0.1	9	2	3	1	3.0	1.3	1.7	3.3	260	4
B5	17/03/2003	11.5	12	2	3	1	3.0	--	--	--	260	8
B5	16/04/2003	0.1	11	2	2.7	6	2.6	8.2	8.2	6.5	252	9
B5	16/04/2003	11	11	8	2.8	5	2.6	--	--	--	288	16
B5	22/05/2003	0.1	8	20	2.5	1	2.5	9.1	4.6	4.6	249	14
B5	22/05/2003	12	11	24	2.5	4	2.5	--	--	--	277	19
B5	4/09/2003	0.1	14	63	1.6	5	--	4.2	2.4	1.8	296	28
B5	4/09/2003	11	12	57	1.4	3	--	--	--	--	258	24
B5	17/11/2003	0.1	5	2	1.3	2	--	3.6	3.1	6.7	175	3
B5	17/11/2003	10	5	2	1.3	1	--	--	--	--	168	2
B5	22/01/2004	0.1	5	2	0.5	5	--	1.4	0.8	1.6	301	4
B5	22/01/2004	12	4	2	0.5	5	--	--	--	--	288	6
B5	26/02/2004	0.1	3	2	0.3	5	--	1.8	1.3	1.8	--	2
B5	26/02/2004	12	4	2	0.7	6	--	--	--	--	361	2
B5	25/03/2004	0.1	6	2	0.9	1	--	3.5	2.7	2.9	234	2
B5	25/03/2004	12	6	2	1.1	1	--	--	--	--	267	4
NN	25/02/2003	0.5	2	4	3.1	15	3.0	5.9	2.8	4.7	2	145
NN	25/02/2003	7.5	7	14	3.9	19	3.7	--	--	--	20	265
NN	17/03/2003	0.3	2	10	2.9	1	2.8	4.1	5.5	10.8	4	156
NN	17/03/2003	7.9	2	10	2.5	1	2.5	--	--	--	3	158
NN	16/04/2003	0.3	2	14	5.5	6	5.5	13.4	13.4	10.6	6	246
NN	16/04/2003	6.3	3	14	5.5	6	5.5	--	--	--	6	232
NN	22/05/2003	0.4	3	48	11	14	11.0	13.7	6.8	6.8	16	483
NN	22/05/2003	6.9	3	48	11	13	11.0	--	--	--	16	485
NN	6/08/2003	0.4	4	52	3.9	1	3.9	2.6	1.7	1.7	12	247
NN	6/08/2003	6.9	4	53	4.4	1	4.4	--	--	--	13	211
NN	15/10/2003	0.5	2	36	4.3	2	4.1	3.7	2.5	1.5	6	213
NN	15/10/2003	3.2	2	35	4.1	1	4.1	--	--	--	6	223
NN	17/11/2003	0.5	2	17	4.1	1	--	4.5	3.9	8.4	8	188
NN	17/11/2003	7.6	8	45	--	2	--	--	--	--	61	279
NN	22/01/2004	0.5	2	3	1.6	3	1.6	1.3	0.8	1.5	3	150
NN	22/01/2004	5.5	10	24	1	5	0.8	--	--	--	41	279
NN	26/02/2004	0.5	2	20	3.7	3	3.6	1.6	1.2	1.6	5	212
NN	26/02/2004	6.6	2	25	3.4	3	3.5	--	--	--	7	211
NN	25/03/2004	0.5	2	16	2.3	1	2.2	2.0	1.6	1.7	5	201
NN	25/03/2004	7	12	44	1.1	1	0.8	--	--	--	36	348

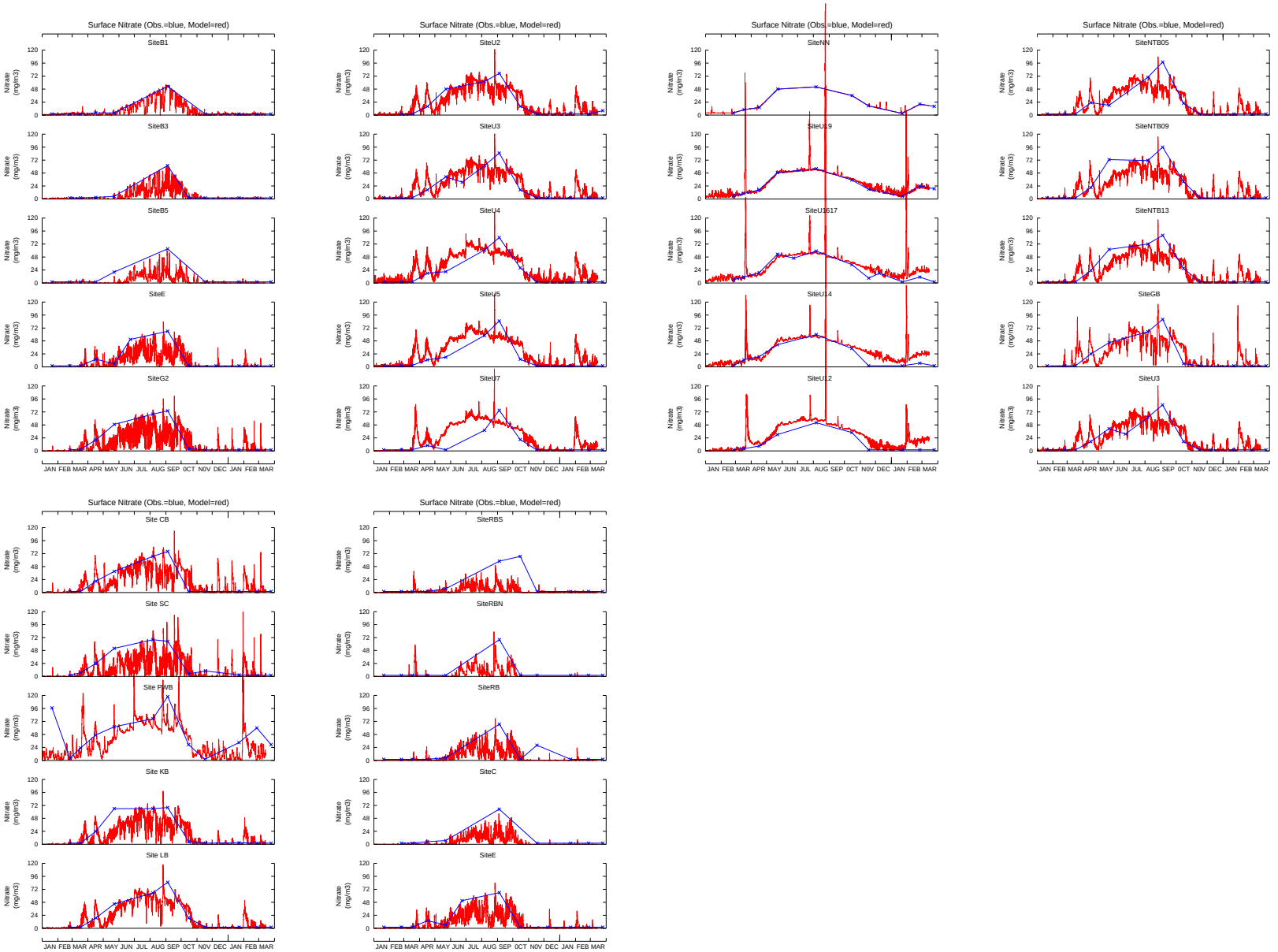

Appendix 10-6 Model calibration time series for observed (blue) and simulated (red) surface nitrate throughout the Derwent Estuary (Jan'03 – Mar'04).

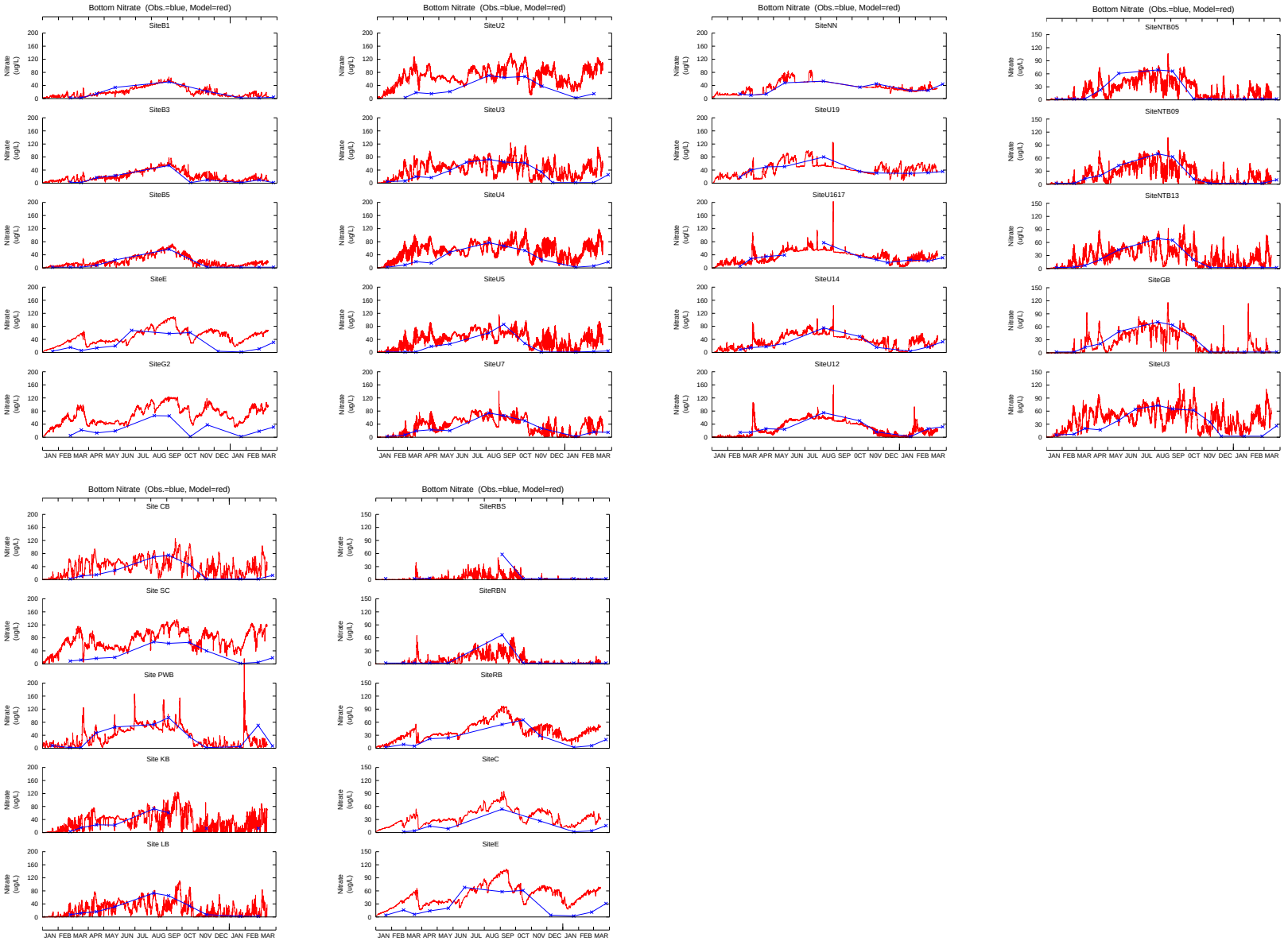

Appendix 10-7 Model calibration time series for observed (blue) and simulated (red) bottom water nitrate throughout the Derwent Estuary (Jan'03 – Mar'04).

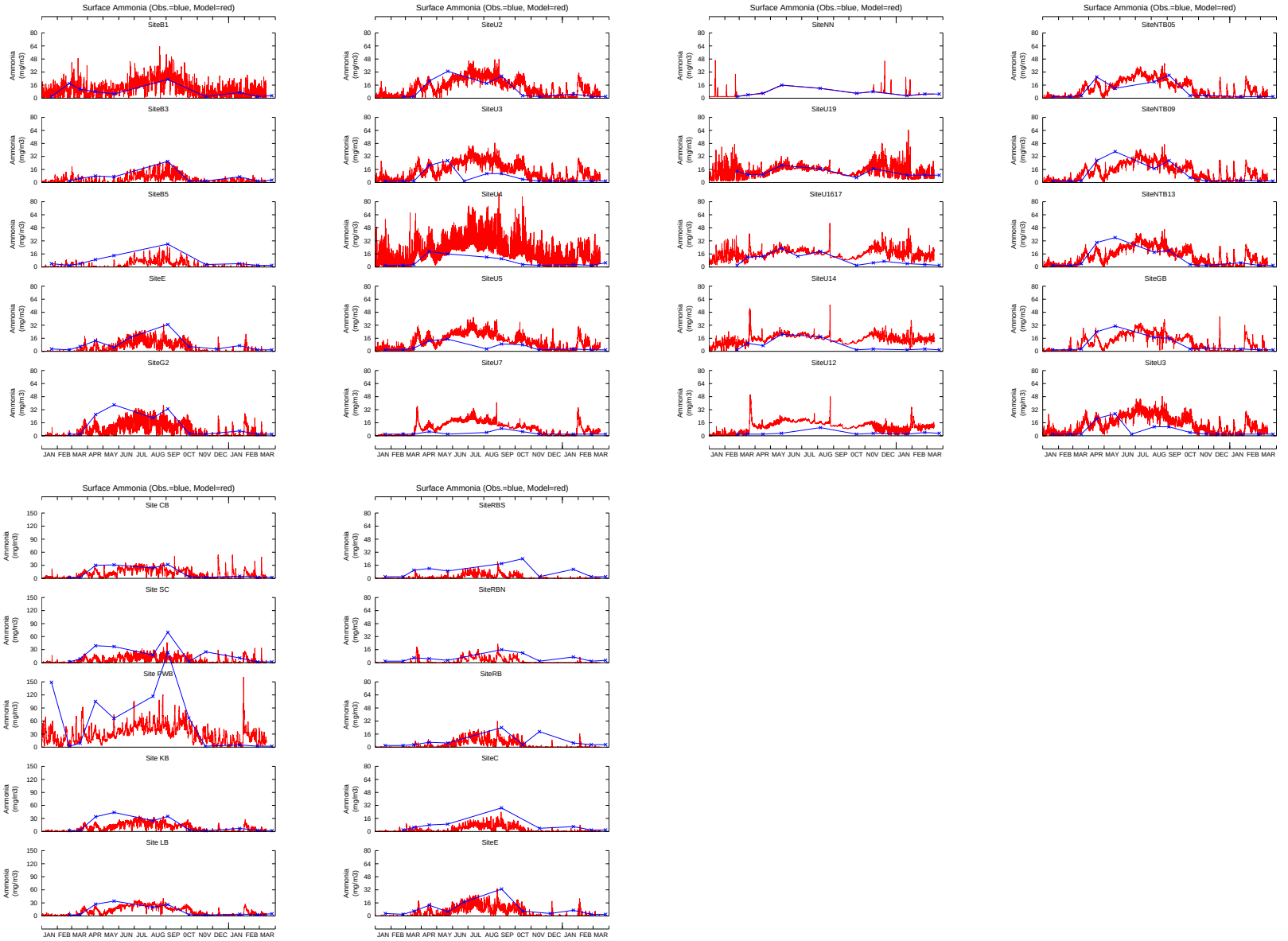

Appendix 10-8 Model calibration time series for observed (blue) and simulated (red) surface ammonia throughout the Derwent Estuary (Jan'03 – Mar'04).

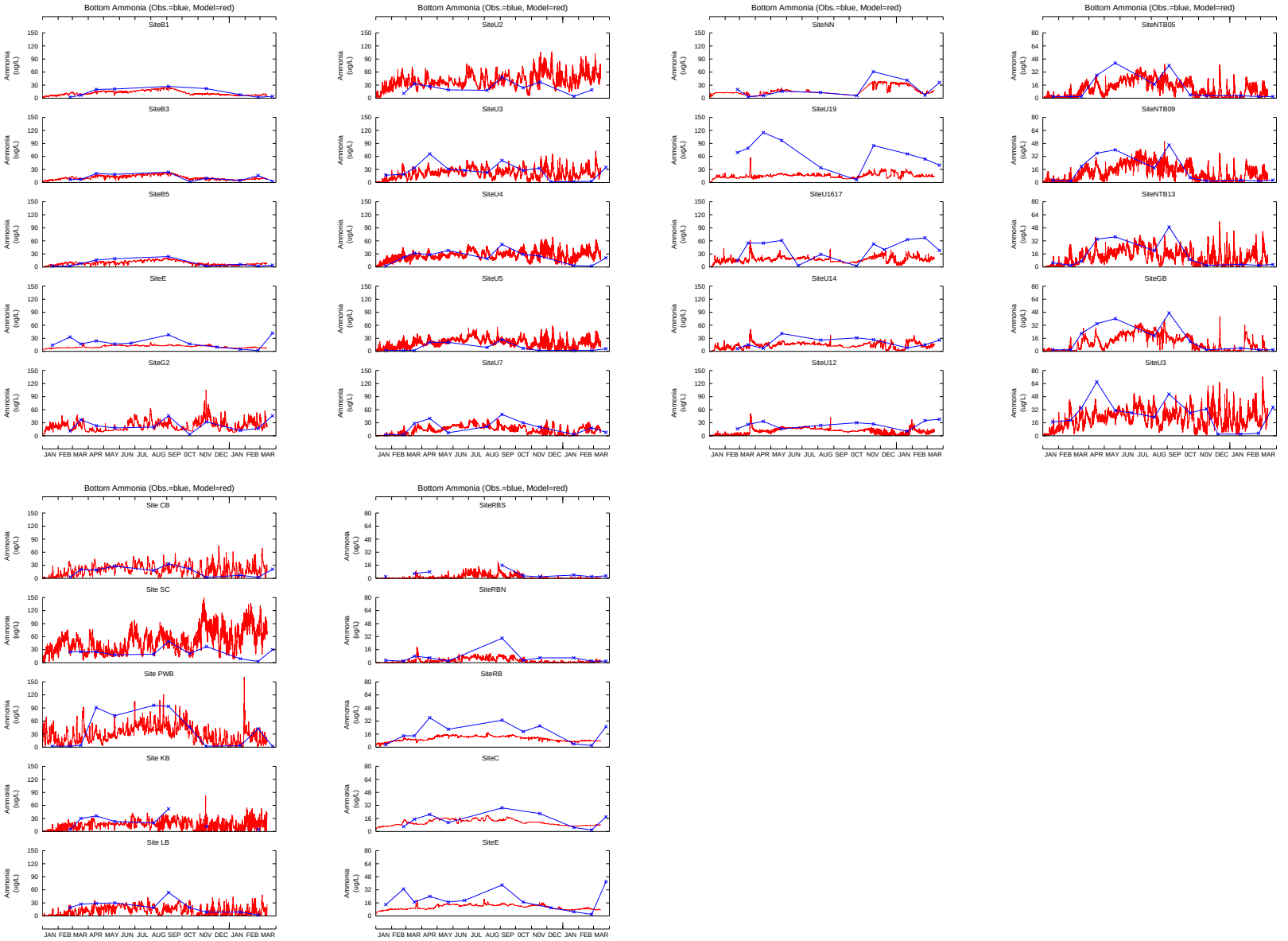

Appendix 10-9 Model calibration time series for observed (blue) and simulated (red) bottom water ammonia throughout the Derwent Estuary (Jan'03 – Mar'04).

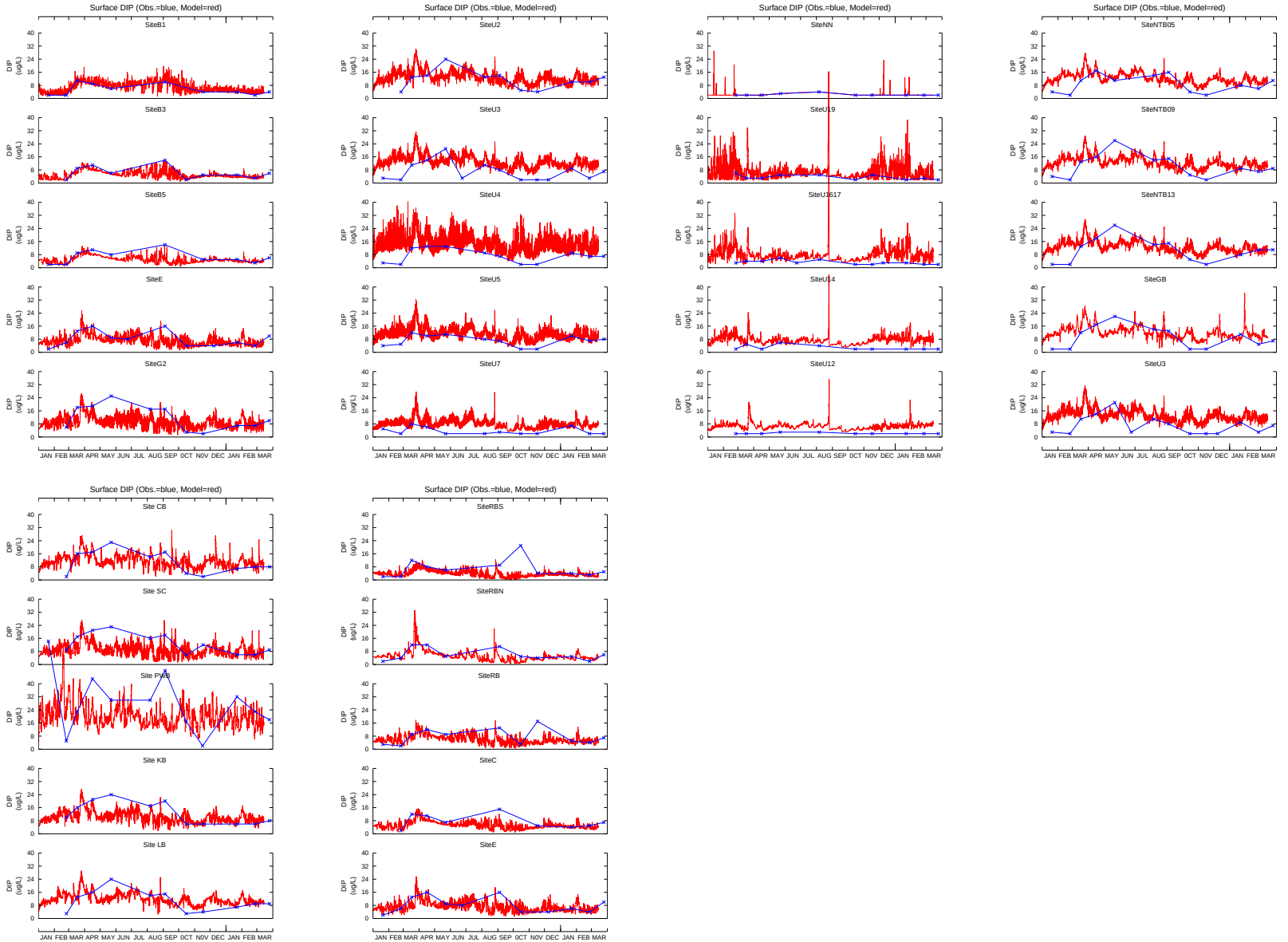

Appendix 10-10 Model calibration time series for observed (blue) and simulated (red) surface DIP throughout the Derwent Estuary (Jan'03 – Mar'04).

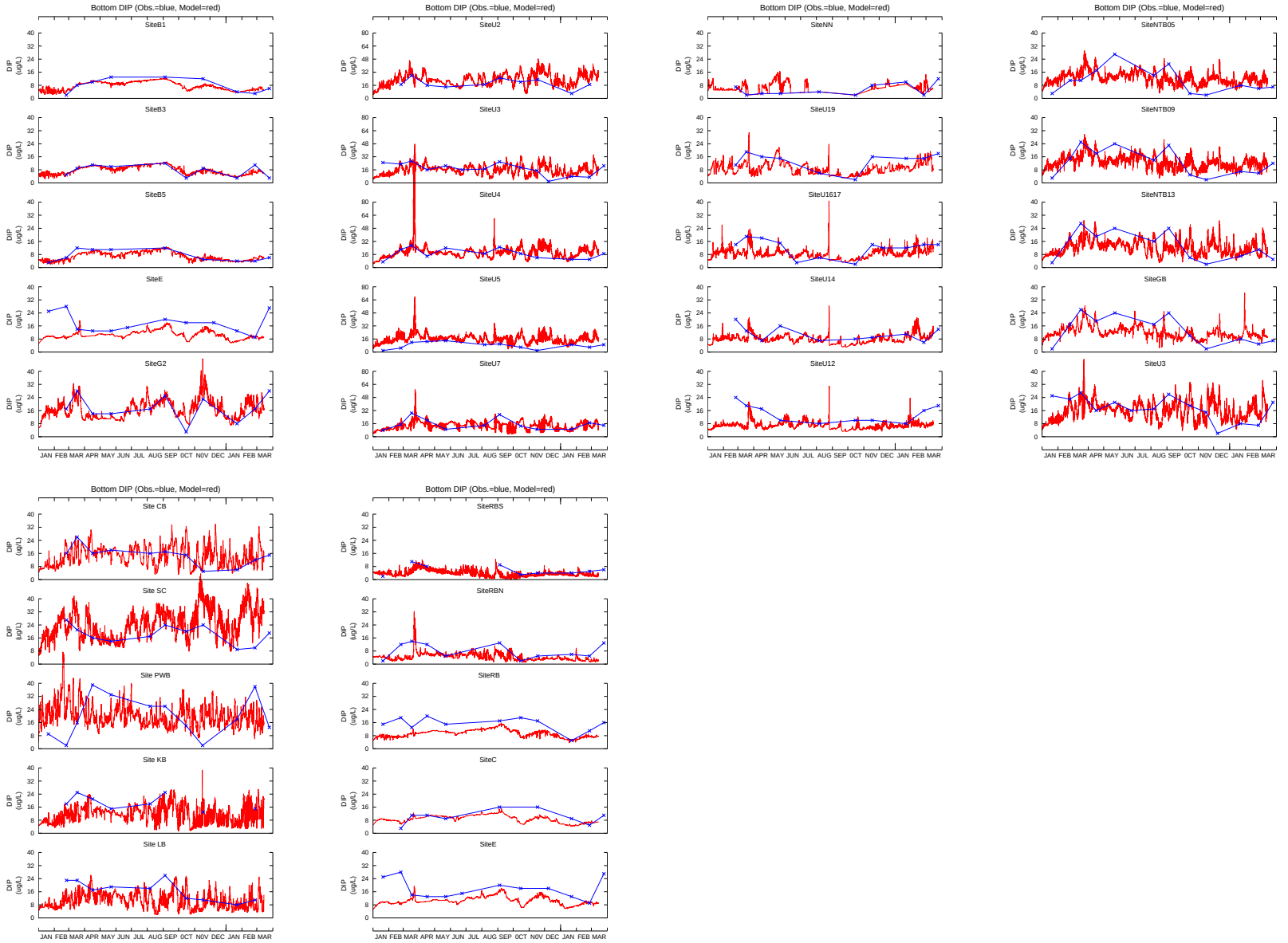

Appendix 10-11 Model calibration time series for observed (blue) and simulated (red) bottom water DIP throughout the Derwent Estuary (Jan'03 – Mar'04).

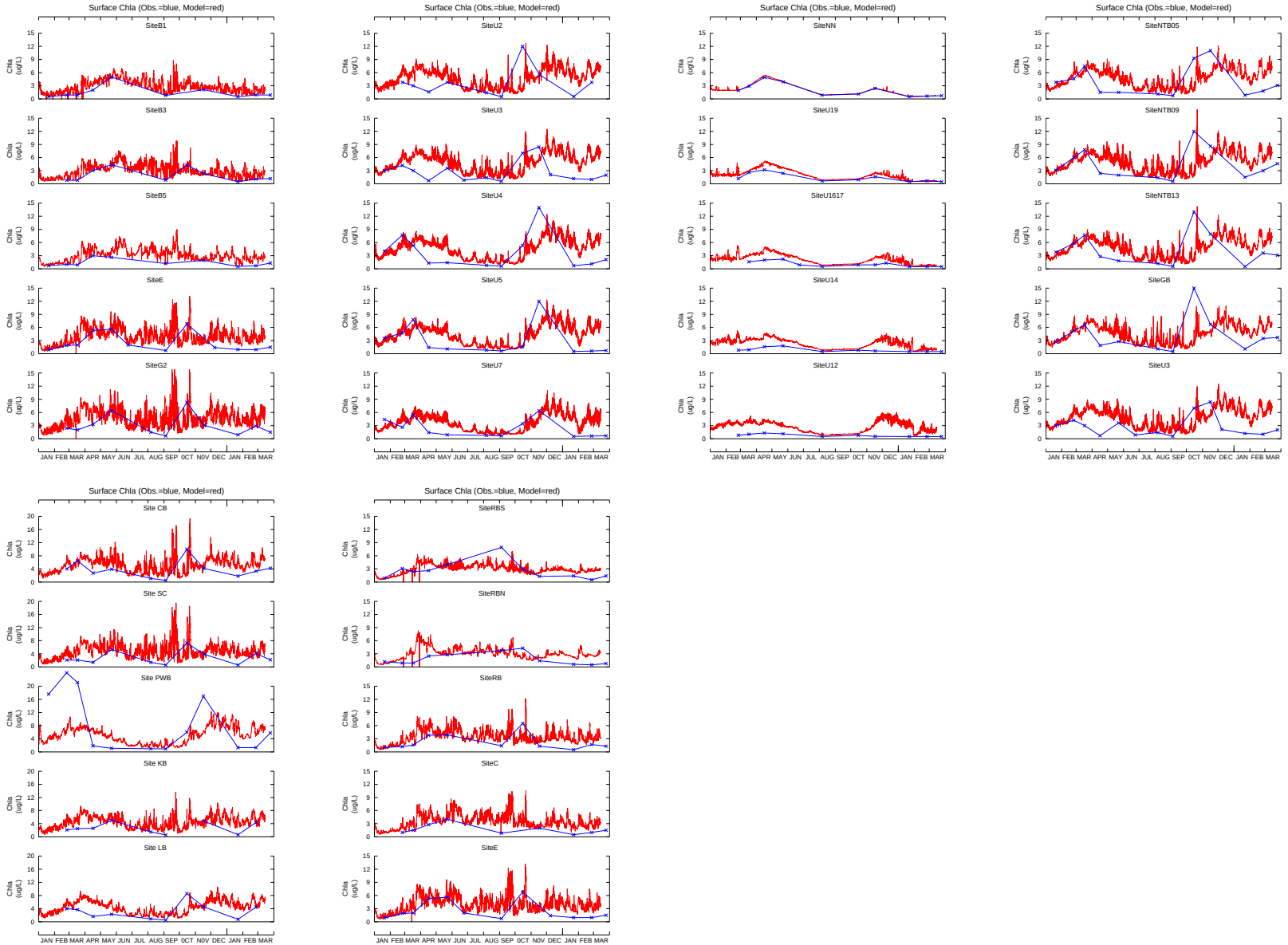

Appendix 10-12 Model calibration time series for observed (blue) and simulated (red) surface chlorophyll throughout the Derwent Estuary (Jan'03 – Mar'04).

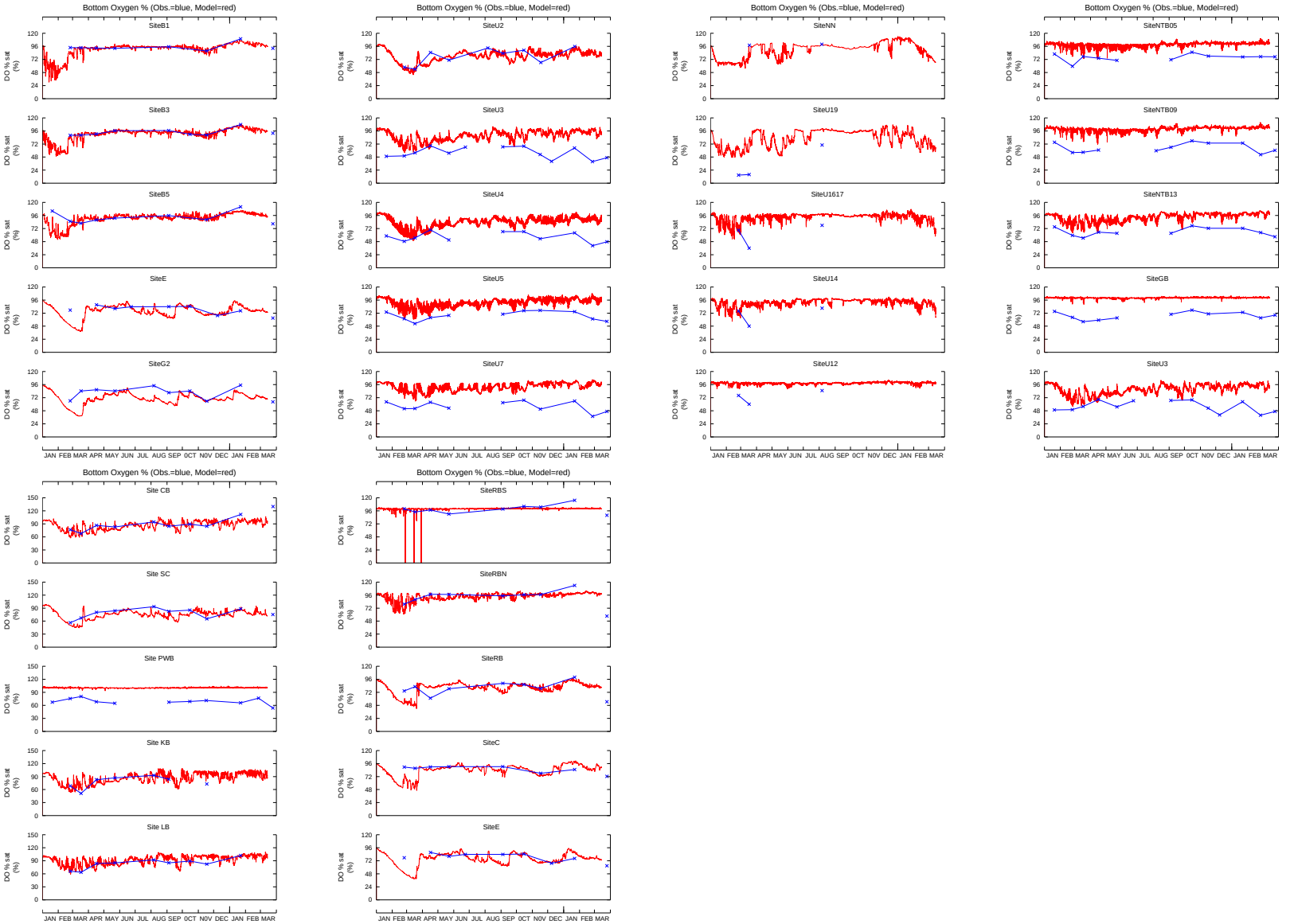

Appendix 10-13 Model calibration time series for observed (blue) and simulated (red) bottom water dissolved oxygen saturation throughout the Derwent Estuary (Jan'03 – Mar'04).

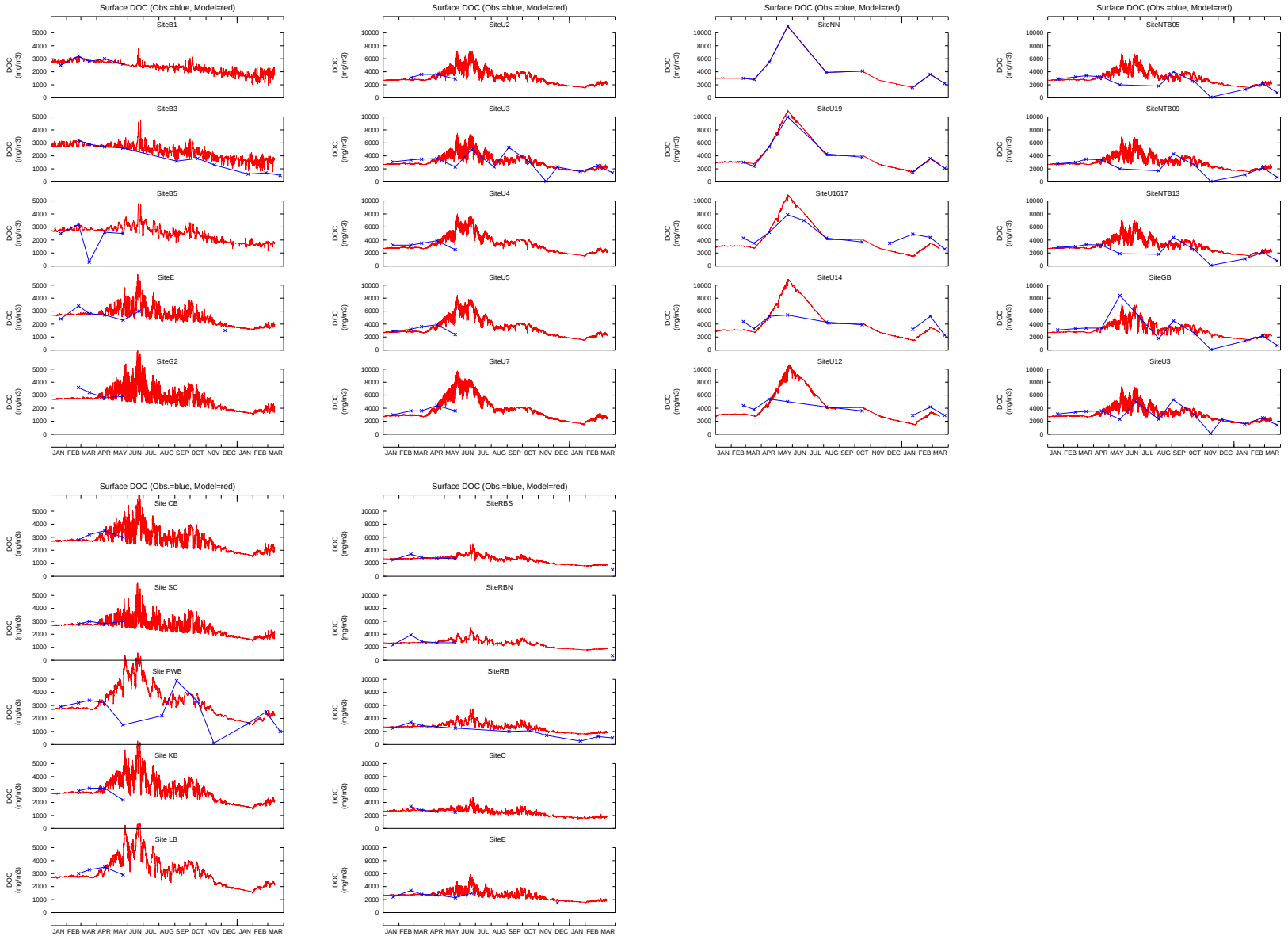

Appendix 10-14 Model calibration time series for observed (blue) and simulated (red) surface DOC throughout the Derwent Estuary (Jan'03 – Mar'04).

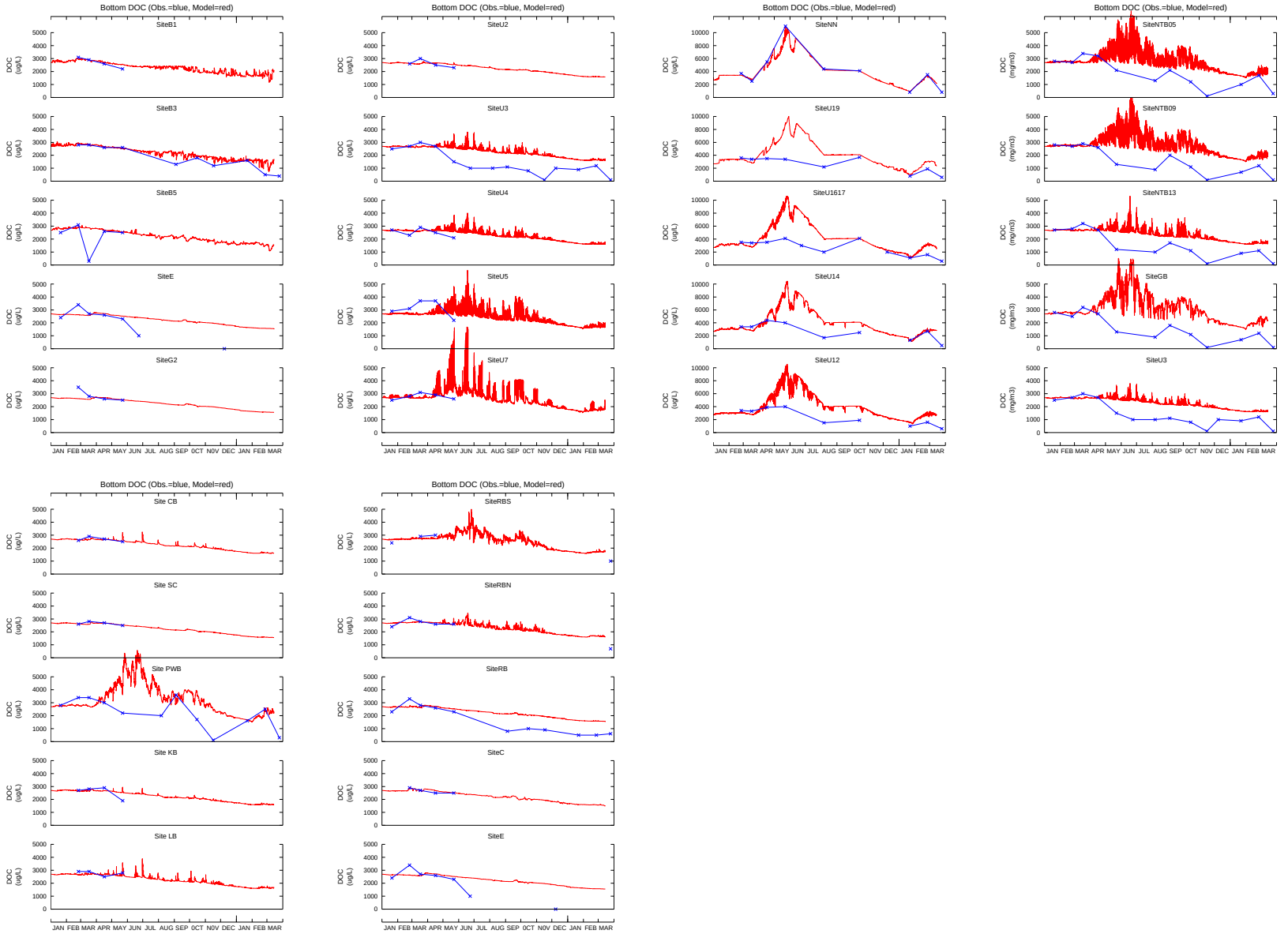

Appendix 10-15 Model calibration time series for observed (blue) and simulated (red) bottom water DOC throughout the Derwent Estuary (Jan'03 – Mar'04)